Vacuum stability of models with many scalars

José Eliel Camargo-Molina

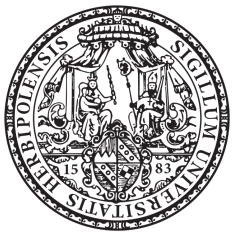

Würzburg 2015

Julius-Maximilians-
UNIVERSITÄT
WÜRZBURG

Vacuum stability of models with many scalars

Dissertation zur Erlangung des
naturwissenschaftlichen Doktorgrades
der Julius-Maximilians-Universität Würzburg

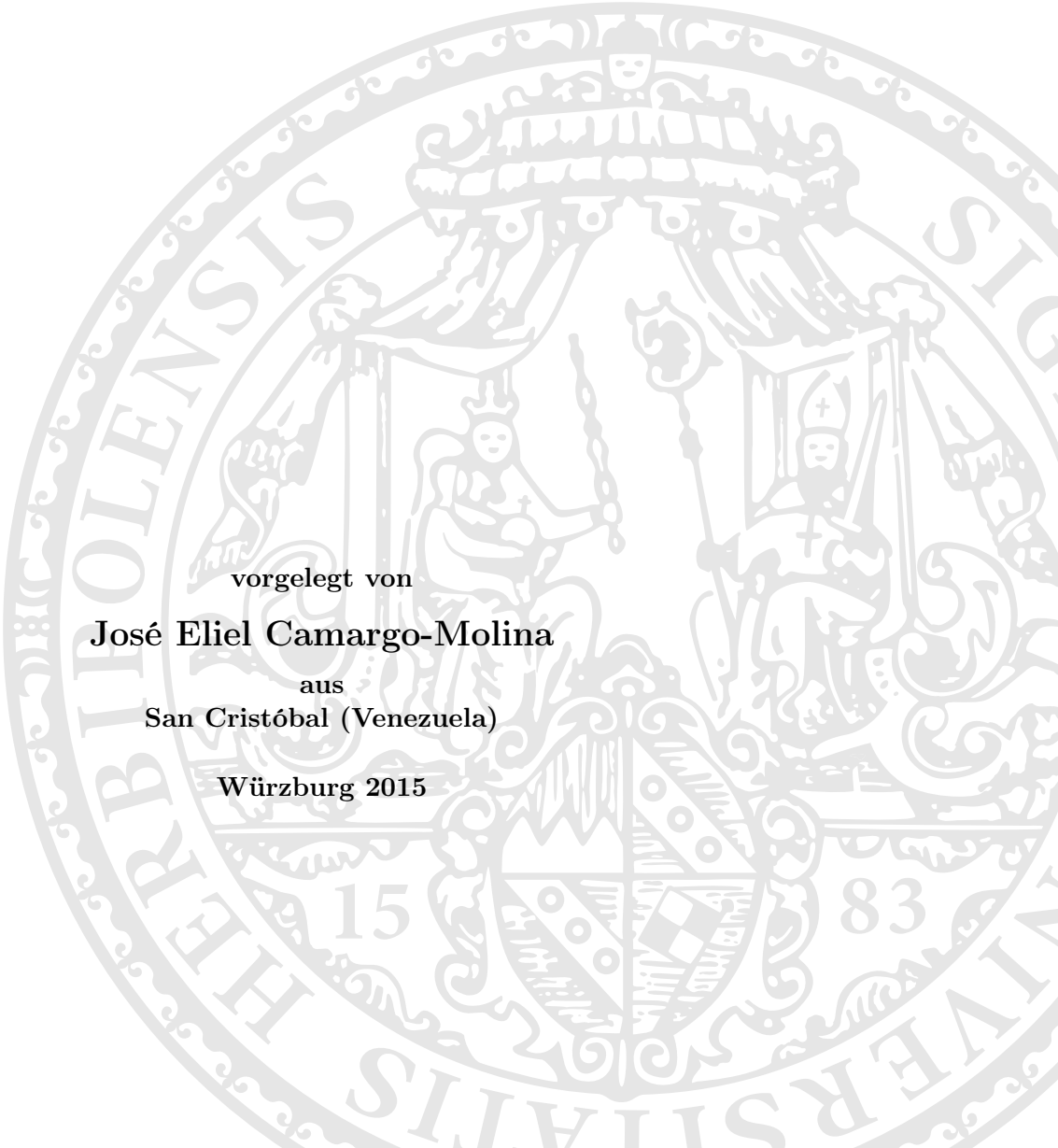

vorgelegt von

José Eliel Camargo-Molina

aus

San Cristóbal (Venezuela)

Würzburg 2015

Eingereicht am: 7. Januar 2015
bei der Fakultät für Physik und Astronomie

1. Gutachter: Prof. Dr. Werner Porod
2. Gutachter: Prof. Dr. Friedrich Röpke
3. Gutachter: _____
der Dissertation

Vorsitzende(r) : Prof. Dr. Matthias Kadler
1. Prüfer: Prof. Dr. Werner Porod
2. Prüfer: Prof. Dr. Thorsten Ohl
3. Prüfer: Prof. Dr. Raimund Ströhmer
im Promotionskolloquium

Tag des Promotionskolloquiums: 5. Mai 2015
Doktorurkunde ausgehändigt am: _____

LIST OF PUBLICATIONS

In connection to the present thesis, the following papers were published:

Peer-Reviewed publications

- J. E. Camargo-Molina, B. Garbrecht, B. O'Leary, W. Porod, and F. Staub, *Constraining the Natural MSSM through tunneling to color-breaking vacua at zero and non-zero temperature*, *Phys.Lett.* **B737** (2014) 156–161, [arXiv:1405.7376].

- J. E. Camargo-Molina, B. O'Leary, W. Porod, and F. Staub, *Stability of the CMSSM against sfermion VEVs*, *JHEP* **1312** (2013) 103, [arXiv:1309.7212].

- J. E. Camargo-Molina, B. O'Leary, W. Porod, and F. Staub, **Vevacious***: A Tool For Finding The Global Minima Of One-Loop Effective Potentials With Many Scalars*, *Eur.Phys.J.* **C73** (2013), no. 10 2588, [arXiv:1307.1477].

- J. E. Camargo-Molina, B. O'Leary, W. Porod, and F. Staub, *The Stability Of R-Parity In Supersymmetric Models Extended By* $U(1)_{B-L}$, *Phys.Rev.* **D88** (2013) 015033, [arXiv:1212.4146].

Conference proceedings

- J. E. Camargo-Molina, B. O'Leary, W. Porod, and F. Staub, *On the vacuum stability of SUSY models*, PoS EPS-HEP2013 (2014) 265, [arXiv:1310.1260].

ACKNOWLEDGEMENTS

These three years have been a great experience, both professionally and personally. I would like to thank all the people at the Institut für Physik und Astrophysik here in Würzburg. I always felt at home when at the office and I surely will miss arriving at Hubland every morning.
I would like to thank Ben O'Leary, who besides one of my collaborators has become a good friend. His constant disposition to discuss physics and answer my questions was always a good source for interesting revelations and my personal growth as a particle physicist. In the same way, I thank Lukas Mitzka, with whom I shared an office for these years. Not only did he always have an answer to many of my physics questions, but he helped me in too many practical issues, from transporting a bed through town to assisting me with the translation in german of the abstract for this thesis. Thanks Lukas, it was great sharing an office with you. Our rap battles were unforgettable. Thanks go to Florian Staub as well, his experience and advice was very valuable and our discussions were always very fruitful.
I would also like to thank Brigitte Wehner, who was always ready to save me from bureaucracy hell and with whom I had many interesting discussions regarding food, traveling and music. I can not forget to mention all my colleagues at TP2, especially those participating in the daily coffee breaks. They always brought entertainment and very interesting discussions regarding the most absurd subjects.
I would especially like to acknowledge Werner Porod, my supervisor. I am deeply grateful for his guidance, valuable career advice, patience and for always having time to sit down and discuss our work. I am very glad I got to be part of his research group for these years. I would also like to thank the DFG Graduiertenkolleg GRK1147 *Theoretische Astrophysik und Teilchenphysik*, for accepting me as a member and for providing funding for last two years of my studies.
Last but not least I would like to thank my girlfriend Marie and my family, their unconditional support was indispensable for making this happen.
In conclusion thanks to all of you, these years in Würzrbug will be a time I'll always remember fondly.

ZUSAMMENFASSUNG

Eine der populärsten Erweiterungen des SM ist die Supersymmetrie (SUSY). Dies ist eine Symmetrie, die Bosonen und Fermionen in Beziehung setzt und auch die einzige machbare Erweiterung der Raumzeitsymmetrien. SUSY kann einige offene Fragen des SM erklären und eröffnet die Möglichkeit einer Vereinheitlichung der Eichwechselwirkungen bei einer hohen Skala. Supersymmetrische Theorien erfordern das Hinzufügen neuer Teilchen, insbesondere eines zusätzlichen Higgs-Dubletts und zumindest eines Skalars für jedes Fermion im SM. So wie im SM das Higgs-Boson die $SU(2)_L$-Symmetrie bricht, können diese neuen Skalare jede Symmetrie, deren Ladung sie tragen, spontan brechen.
Angenommen, es gibt ein lokales Minimum des Potentials, das die korrekte Phänomenologie für einen Parameterraumpunkt eines Modells erzeugt: Durch die Suche nach anderen tieferen Minima mit Vakuumerwartungswerten, die gewünschte Symmetrien wie $SU(3)$ oder $U(1)_{EM}$ brechen, ist es möglich Parameterraumpunkte, in denen dies passiert, auszuschliessen. Das lokale Minimum mit der korrekten Phänomenologie kann immernoch metastabil sein, weshalb es auch notwendig ist, die Tunnelwahrscheinlichkeit zwischen zwei Minima zu berechnen.
In dieser Arbeit legen wir eine Prozedur vor und wenden sie an, um den Parameterraum von Modellen mit vielen Skalaren durch die Minimierung des effektiven Ein-Schleifen-Potentials und durch die Berechnung seiner Lebensdauer sowohl bei $T = 0$ und bei $T \neq 0$ einzuschränken. Nach einer kurzen Diskussion der Unzulänglichkeiten des SM und Einführung der Grundlagen von SUSY erläutern wir die Theorie und die die nötigen numerischen Methoden für eine erfolgreiche Analyse der Vakuumstabilitaet. Danach präsentieren wir `Vevacious`, ein öffentliches Programmpaket, in das wir unsere Prozedur implementiert haben.
Daraufhin analysieren wir drei interessante Beispiele. Für das Constrained MSSM (CMSSM) untersuchen wir die die Existenz von Minima, in denen die Farb- oder elektrische Ladung nicht erhalten ist (CCB-Minima), und wie dessen phänomenologisch relevante Region des Parameterraums dadurch bei $T = 0$ eingeschränkt wird. Wir zeigen, dass die Regionen, die die korrekte Higgsmasse und die richtige Relikt-Dichte für die Dunkle Materie reproduzieren, mit Regionen, die tiefere CCB-Minima aufweisen, überlappen.
Inspiriert durch die Ergebnisse für das CMSSM betrachten wir dann das Natural MSSM und prüfen die Parameterraumregion mit der korrekten Higgsmasse auf CCB-Minima bei $T \neq 0$.Wir finden, dass die Region des Parameterraums mit CCB-Minima deutlich mit denen mit einer korrekten Higgsmasse überlappt. Bei Berücksichtigung von thermalen Effekten hat ein Großteil der bei $T = 0$ langlebigen Punkte ein gewünschtes symmetriebrechendes Minimum mit einer sehr geringen Überlebenswahrscheinlichkeit bei $T \neq 0$. In beiden Studien finden wir, dass die analytischen Bedingungen, die bisher in der Literatur präsentiert wurden, nicht ausreichen, um Bereiche des Parameterraums mit CCB-Minima auszuweisen. Wir präsentieren einen Weg, unsere Prozedur für die Nutzung in Parameterraum-Fit-Studien zu beschleunigen. Zuletzt zeigen wir ein weiteres Beispiel. Für das BLSSM untersuchen wir die Verletzung der R-Parität durch Sneutrino-VEVs und in welchen Parameterraumbereichen dies geschieht. Wir stellen durch Vergleich mit unserer kompletten numerischen Analyse heraus, dass frühere Analysen in der Literatur darin fehlschlagen, diese Bereiche mit Erhaltung der R-Parität zu identifizieren.

ABSTRACT

One of the most popular extensions of the SM is Supersymmetry (SUSY). It is a symmetry relating fermions and bosons and also the only feasible extension to the symmetries of spacetime. With SUSY it is then possible to explain some of the open questions left by the SM while at the same time opening the possibility of gauge unification at a high scale. SUSY theories require the addition of new particles, in particular an extra Higgs doublet and at least as many new scalars as fermions in the SM. Much in the same way that the Higgs boson breaks $SU(2)_L$ symmetry, these new scalars can break any symmetry for which they carry a charge through spontaneous symmetry breaking.

Let us assume there is a local minimum of the potential that reproduces the correct phenomenology for a parameter point of a given model. By exploring whether there are other deeper minima with VEVs that break symmetries we want to conserve, like $SU(3)_C$ or $U(1)_{EM}$, it is possible to exclude regions of parameter space where that happens. The local minimum with the correct phenomenology might still be metastable, so it is also necessary to calculate the probability of tunneling between minima.

In this work we propose and apply a framework to constrain the parameter space of models with many scalars through the minimization of the one-loop effective potential and the calculation of tunneling times at zero and non zero temperature.After a brief discussion about the shortcomings of the SM and an introduction of the basics of SUSY, we introduce the theory and numerical methods needed for a successful vacuum stability analysis. We then present `Vevacious`, a public code where we have implemented our proposed framework. Afterwards we go on to analyze three interesting examples.

For the constrained MSSM (CMSSM) we explore the existence of charge- and color- breaking (CCB) minima and see how it constraints the phenomenological relevant region of its parameter space at $T = 0$. We show that the regions reproducing the correct Higgs mass and the correct relic density for dark matter all overlap with regions suffering from deeper CCB minima.

Inspired by the results for the CMSSM, we then consider the natural MSSM and check the region of parameter space consistent with the correct Higgs mass against CCB minima at $T \neq 0$. We find that regions of parameter space with CCB minima overlap significantly with that reproducing the correct Higgs mass. When thermal effects are considered the majority of such points are then found to have a desired symmetry breaking minimum with very low survival probability.

In both these studies we find that analytical conditions presented in the literature fail in discriminating regions of parameter space with CCB minima. We also present a way of adapting our framework so that it runs quickly enough for use with parameter fit studies.

Lastly we show a different example of using vacuum stability in a phenomenological study. For the BLSSM we investigate the violation of R-parity through sneutrino VEVs and where in parameter space does this happen. We find that previous analyses in literature fail to identify regions with R-parity conservation by comparing their results to our full numerical analysis.

CONTENTS

CHAPTER ONE

INTRODUCTION

It is an exciting time for particle physics. The recent discovery of a scalar particle with the properties of a Higgs boson at CERN has once again proved the incredible success of particle theory and is in itself an amazing experimental achievement. Not only was this particle the last missing piece of the puzzle but it also drives one of the most fundamental principles of particle theory: spontaneous symmetry breaking (SSB).

Particle theorists have always relied on the fundamental symmetries both of nature and theoretical models. Understanding the underlying symmetries of a problem allows us to understand many of its aspects with a great deal of simplification. Conserved quantities, one of the fundamental principles behind physical models, are also closely intertwined with the symmetries of nature. Thus a big part of particle theory has to do with the interplay between symmetries observed in experiments and models built with symmetry in mind. Sometimes experiments show us the way to go by making symmetries obvious and some other times theoreticians come up with successful models that relate disconnected pieces through not yet proven symmetries.

The process of SSB is driven by the fact that sometimes it costs less energy for particle fields to have a non-zero values in the vacuum. This value is called the vacuum expectation value or VEV. Although the theory describing the physics may have many symmetries built in, when one of the fields charged under any of the symmetries takes a constant value, the invariance under that symmetry breaks down. Sometimes it is useful to allow for symmetry breaking, as is the case with $SU(2)_L$ which does not allow for the standard model fermions to have masses.

Some other symmetries we have to keep in successful theories, as they are invariably seen to hold in experiments. This is the case of the symmetry associated with the conservation of electric charge, or the so-called color charge carried by quarks and gluons.

Although astonishingly successful the standard model has its shortcomings. It is rather certain that we need to develop a successful theory that goes beyond the standard model and offers explanations where the latter does not. We will go on in more detail about the open questions unanswered by the SM, but it suffices to say that a rather good possibility for answering some of these questions exists in supersymmetric models. By adding the only possible extra set of symmetries of spacetime, we introduce many new particles and relations between parameters that offer answers for some of these open questions. However, at the same time we also open the door for many candidate models that may or may not eventually be realized in nature. So it is

of great interest to find out whether a certain model can explain the universe we live in or if it contradicts any experimental result or fundamental principle.
The main purpose of this work is to propose a systematic way of testing theoretical models against the fact that there are symmetries we want to break and some other symmetries that a successful model should respect. If we consider SSB, this in turn translates to looking for a way of determining which fields will get VEVs.
Ideally we want scalar fields to get VEVs, as we definitely want to conserve the Lorentz invariance of our theory [1]. Along this work we will focus on SUSY models as they are good candidates for extensions of the SM and at the same time have many more scalar particles and therefore many more possibilities for breaking symmetries through VEVs. Finding whether a field will have a VEV or not has to do with minimizing the potential energy of the model. By finding where the lowest point of the potential lies in field space, we can then tell where the universe would like to be if such model was realized in nature. The problem becomes more interesting when we consider the fact that the field configuration at which the vacuum of our universe lies has not to be the lowest one. It is sufficient that it is a local minimum of the potential energy. The question is then how long will the universe stay there before eventually reaching the lowest point through tunneling, a process triggered by quantum and thermal effects in particle theories.
By answering these questions we can test whether a given model is compatible with the existence of a long-lived minimum with VEVs for the fields breaking the desired symmetries. In the following we will introduce a framework to perform such analyses and then apply it to three interesting examples. Along the way we will dive into the specifics of the problem of minimizing the potential and the technical details of how we achieve this practically.
In chapter 2 we will take a quick glimpse at the standard model, explain its shortcomings and justify the need to look for models that go beyond it. Then in chapter 3 we will introduce the basics of supersymmetric models, as well as the three specific models we will be treating along this work. In chapter 4 we will go through the problem of minimizing the potential in SUSY models both at zero and non-zero temperature and lay down the specifics on how to use vacuum stability as a phenomenological constraint. Lastly in 5 we will present the results coming from applying the proposed framework for three models: The CMSSM, the natural MSSM and the CBLSSM.

[1] It is also possible to let more complicated combinations of fields get VEVs, as long as they form a Lorentz invariant quantity. Fermionic and gluon condensates are examples of this fact [1] [2].

CHAPTER TWO

BEYOND THE STANDARD MODEL

As a preface to our study about the phenomenology of beyond standard model physics, it is important to understand why do we want to extend such a successful theory in the first place. Physics, as any other science, is driven by the attempt to describe what we can observe in nature. We want to find answers to questions posed by experiments through theoretical models that allow us to predict future results. The standard model, although extremely accurate in explaining what we have observed in collider experiments, fails to provide explanation for phenomena that could be explained through particle physics. The interesting question to explore is whether we can explain these observations by extending the SM. In this chapter we will first give a brief introduction to the standard model and the motivations behind model building in particle physics to then go through the open questions that can't be answered by the standard model alone. We will then explain why there is a necessity for theories that extend the SM and answer some of these questions.

2.1. A quick flight over the standard model of particle physics

Before we embark ourselves in the study of physics beyond the standard model, let us first discuss the basic pieces that make up the standard model itself. In this work we will be focusing in the spontaneous breaking of symmetries in SUSY models and scenarios where some of these symmetries might be broken or conserved. By laying down some of the basic principles behind the standard model we will at the same time set the mindset behind the construction of models that go beyond it, and we will familiarize ourselves with the mechanisms we will generalize in our studies.

The spontaneous symmetry breaking that is present in the standard model is an example of the more complicated processes we will be looking at when studying models with many scalar particles. This brief introduction will help us keep in mind that there are fundamental symmetries, like color and electric charge, that we want to preserve in any extension of the SM.

Before we go forward, we should introduce the protagonists of the story. The standard model contains all of the observed fundamental particles, there are three families of particles which differ only in their mass. Besides that, they seem to be identical copies. A tool to understand their properties lies in quantum numbers.

First we have the leptons, which carry lepton number and come in three families. The electron (e^-), muon (μ^-) and tau (τ) which all have electrical charge -1. Then we have the neutrinos, which come as well in three families the electron neutrino ν_e, the muon neutrino ν_μ and the tau neutrino ν_τ. As far as the standard model can tell they are massless, but experimentally they seem to have some but very little mass. Their names are no accident as they are related to the other leptons through flavor, another quantum number.
Then come the quarks, discovered later. They also come in three families but also in three different colors, red blue and green. Each family has two members: The up and down, the charm and strange with the last family comprised of the top and bottom quarks. They are the building blocks of hadrons, mesons and baryons. They are all fermions, with spin 1/2 and carry flavor and baryon quantum numbers.
Then we have the bosons. The gluon which mediates the strong force, the photon which mediates the electromagnetic force and next the W and Z bosons mediating the weak interaction. Last but not least we have the Higgs boson, which in contrast to all the other bosons that have spin 1, has spin 0. In the standard model it is the only of its kind and was the last particle to be discovered in July 2012.
Since the beginning of particle physics, scientists have been smashing particles together, watching closely nuclear decays and looking at the sky to understand better how all of this fundamental pieces make up the universe we live in. We've answered many questions with a level of success that amazes even experts that think about this stuff everyday.

2.1.1. Quantum Electrodynamics

A nice way to see the role symmetries play in particle physics and a remarkably simple theory is that of the interaction between electrons and photons. At the same time it is one of the building blocks of the standard model and a tool to understand some of the basic principles of quantum field theories (QFT). A quick introduction is a good warm up but also will lay down some of the main theoretical motivations for particle theorists in the search for new models. A more in depth review of the standard model escapes the scope of this work, but can be found at varying levels of detail in [3–5] among many others.
Simply enough, the Lagrangian of a free Dirac fermion (e.g. an electron) is

$$\mathcal{L}_0 \;=\; i\,\overline{\psi}(x)\gamma^\mu\partial_\mu\psi(x) \;-\; m\,\overline{\psi}(x)\psi(x)\,. \tag{2.1}$$

With a little bit of effort one can realize that this Lagrangian is invariant under phase transformations of the field $\psi(x) \to e^{i\theta}\psi(x)$. As in quantum mechanics, a phase transformation has no physical meaning.

However as $\psi(x)$ is a field that depends on the space-time coordinates, there is no reason for a phase rotation $\theta(x)$ not do so. In this case our simple Lagrangian $\mathcal{L}_0$ is not invariant anymore because $\partial_\mu\psi(x) \to e^{i\theta(x)}\left(\partial_\mu + i\,\partial_\mu\theta(x)\right)\psi(x)$. So as it stands $\mathcal{L}_0$ does not cut it. We need to come up with a Lagrangian that is invariant under local (space dependent) phase transformations. The easiest way to do this is by introducing some object transforming in such a way that it cancels exactly the extra bits coming form the transformation of $\psi(x)$. It is straightforward to see that the Lagrangian

$$\mathcal{L} \;=\; i\,\overline{\psi}(x)\gamma^\mu\partial_\mu\psi(x) \;-\; m\,\overline{\psi}(x)\psi(x) \;-\; eA_\mu(x)\,\overline{\psi}(x)\gamma^\mu\psi(x) \tag{2.2}$$

Is indeed invariant under local phase transformations if the newly added field A_μ transforms like

$$A_\mu(x) \to A_\mu(x) - \frac{1}{e}\,\partial_\mu\theta\,. \tag{2.3}$$

The notation here is no accident, as this is exactly how the vector potential transforms in classical electrodynamics under a gauge transformation. Indeed, local transformations that leave the Lagrangian invariant are precisely gauge transformations and the field A_μ represents the photon field interacting with the Dirac fermion. Phase transformations are transformations under the $U(1)$ group and by looking at the way $\psi(x)$ and A_μ transform under $U(1)$ we can see that they are in the fundamental and adjoint representation respectively. Because of this $U(1)$ is also the gauge group of QED. It is both useful and standard to define $D_\mu = [\partial_\mu + ieQA_\mu(x)]$ and rewrite 2.2 as

$$\mathcal{L} \;=\; i\,\overline{\psi}(x)\gamma^\mu D_\mu\psi(x) \;-\; m\,\overline{\psi}(x)\psi(x)\,. \tag{2.4}$$

The newly introduced field A_μ does not describe yet a physical photon. For this to be the case we have to give it the chance of propagating. For the field $\psi(x)$ this is described by the kinetic term $\overline{\psi}(x)\gamma^\mu\partial_\mu\psi(x)$. However, as A_μ carries a μ index, we need to be more careful. The answer, as one could expect, is to introduce the term

$$\mathcal{L}_{tot} = \mathcal{L} - \frac{1}{4}\,F_{\mu\nu}(x)\,F^{\mu\nu}(x) \quad \text{with} \quad F_{\mu\nu} \;\equiv\; \partial_\mu A_\nu - \partial_\nu A_\mu \tag{2.5}$$

This term is not only invariant under $U(1)$ transformations but also makes it so the Lagrangian reproduces Maxwell's equations. The Lagrangian of (2.5) gives rise to the theory of Quantum Electrodynamics, a very successful theory and the first step towards describing the standard model of particle physics.
We started out by looking for a Lagrangian with a specific local symmetry, this showed us the necessity of including new objects with definite transformation rules that turned out to be a fundamental part of the physics system at hand. This way of using symmetries as the guiding principle for our theories is a very valuable tool in particle physics.

2.1.2. $SU(3)_C \otimes SU(2)_L \otimes U(1)_Y$

We just looked at the Lagrangian of QED. We built it by requiring a local $U(1)$ invariance and introducing objects with specific transformation rules. The case of $U(1)$ is quite simple as it is an abelian group but it gives the general idea for constructing Lagrangians invariant under a given gauge group.
If we want to describe all the interactions in the same fashion we have to include the weak and strong forces into our framework with the same underlying spirit but with slight changes due to the different behaviour of the gauge group.
Let's start with the weak force. As it turns out one can define a quantum number that is conserved in weak interactions. It is called weak isospin or T with all left-handed fermions having $T = 1/2$ and it is possible to group left-handed fermions that behave equally under weak interactions in doublets with $T_3 = \pm 1/2$. Right handed fermions have $T = 0$ as they do not undergo weak interaction. This hints at the fact that we will need a local $SU(2)_L$ gauge symmetry as it is the simplest group with doublet representation so that we can pair left-handed fields with the same weak interaction.
In order to have hadrons and baryons as bound states of quarks while satisfying Fermi-Bose

statistics, we need to define a new quantum number: color. Quarks come in three different colors [1] and hadrons and baryons are then defined to be color singlet states. We can then think color as the corresponding charge of an $SU(3)_C$ gauge group therefore giving rise to the strong interaction. To write an invariant Lagrangian we will group quarks in triplet representations.

So to describe quarks, fermions and their interactions through mediators we have to write down a Lagrangian that has the corresponding local symmetries. In other words we need to have a theory with $SU(3)_C \otimes SU(2)_L \otimes U(1)_Y$ as the gauge group. In this sense, we need fields that are singlets under some of these three groups but can also transform non-trivially under the others. For this we have to introduce covariant derivatives and gauge bosons acting on the corresponding fields accounting for each local symmetry that we want in our Lagrangian.

There are a lot of nuances and it is not the purpose of this work to explain them in detail. To summarize, the main difference between including these forces and what we did in QED lies in the fact that the gauge group is not abelian this time. This implies that the generators of the symmetries are not simple phases and we have to introduce more complicated objects for $SU(2)_L$ and $SU(3)_C$.

This of course is very much in tune with the physics we observe, as in an abelian theory the gauge bosons are forced to be massless and the way they interact through the covariant derivative is much more simple. Let us however write down the result of this consideration and cast here the complete standard model.

First we arrange the lepton and quark particle fields in the following way (for simplicity we have suppressed family indexes so the reader has to think every particle comes threefold):

$$\begin{gathered} SU(2)_L \text{ space} \\ L = \begin{pmatrix} P_L\,\nu_l \\ P_L\,l^- \end{pmatrix}\ ,\ P_R\,l^-\ ,\ Q = \begin{pmatrix} P_L\,q_u \\ P_L\,q_d \end{pmatrix}\ ,\ P_R\,q_u\ ,\ P_R\,q_d \\ SU(3)_C \text{ space} \\ \begin{pmatrix} q_u^r \\ q_u^g \\ q_u^b \end{pmatrix}\ ,\begin{pmatrix} q_d^r \\ q_d^g \\ q_d^b \end{pmatrix}\ ,\ l^-\ ,\ \nu_l \end{gathered} \tag{2.6}$$

where $P_{L,R}$ are the chirality projection operators and the fields are written as Dirac spinors.

For simplicity let us start with the model including only the $SU(2)_L \otimes U(1)_Y$ part of the gauge group. As the reader might guess, we have to gauge bosons accounting for each group. For the $U(1)_Y$ part we'll add the B_μ boson as we did in QED. For the $SU(2)_L$ part we will have to add the W gauge bosons $\widetilde{W}_\mu(x) \equiv \frac{\sigma_i}{2} W_\mu^i(x)$. The Pauli matrices σ_i ensure that it is a $SU(2)_L$ field. To introduce the Lagrangian and covariant derivatives it will be convenient to use the two simplifying conventions:

$$\text{a)} \qquad \psi_1(x) = \begin{pmatrix} P_L\,q_u(x) \\ P_L\,q_d(x) \end{pmatrix}, \qquad \psi_2(x) = P_R\,q_u(x)\,, \qquad \psi_3(x) = P_R\,q_d(x) \tag{2.7}$$

[1] The specific number of colors can be inferred by studying for example $R_{e^+e^-} = \frac{\sigma(e^+e^- \to \text{hadrons})}{\sigma(e^+e^- \to \mu^+\mu^-)}$

$$\text{b)} \qquad \psi_1(x) \,=\, \begin{pmatrix} P_L\,\nu_l(x) \\ P_L\,l^-(x) \end{pmatrix}, \qquad \psi_2(x) \,=\, P_R\,\nu_l = 0\,, \qquad \psi_3(x) \,=\, P_R\,l^-(x) \tag{2.8}$$

Our discussion from now on will be valid for any assignment a) or b). The invariant Lagrangian will be:

$$\mathcal{L} \,=\, \sum_{j=1}^{3} i\,\overline{\psi}_j(x)\,\gamma^\mu\,D_\mu\psi_j(x) \,-\frac{1}{4}\,B_{\mu\nu}\,B^{\mu\nu} - \frac{1}{4}\,W^i_{\mu\nu}\,W_i^{\mu\nu}\,. \tag{2.9}$$

In the same fashion as with QED we introduce the covariant derivatives to ensure local invariance and field strength tensors to include the kinetic terms for the introduced gauge bosons.
The corresponding field strength tensors in this case are somewhat more complicated. They are explicitly:

$$B_{\mu\nu} \,\equiv\, \partial_\mu B_\nu - \partial_\nu B_\mu\,, \tag{2.10}$$

$$W^i_{\mu\nu} \,=\, \partial_\mu W^i_\nu - \partial_\nu W^i_\mu - g\,\epsilon^{ijk}\,W^j_\mu\,W^k_\nu\,. \tag{2.11}$$

The necessary covariant derivatives to satisfy local invariance are

$$\begin{aligned} D_\mu\psi_1(x) \;&\equiv\; \left[\partial_\mu + i\,g\,\widetilde{W}_\mu(x) + i\,g'\,y_1\,B_\mu(x)\right]\,\psi_1(x)\,, \\ D_\mu\psi_{2,3}(x) \;&\equiv\; \left[\partial_\mu + i\,g'\,y_{2,3}\,B_\mu(x)\right]\,\psi_{2,3}(x)\,, \end{aligned}$$

Note that the covariant derivatives act differently depending on the representation we have chosen for the fields. This of course reflects the fact that the D_μ are built precisely so that we can have local invariance under the gauge group. Fields in the singlet representation don't need the extra terms in the covariant derivative so they behave analogously to QED, whether ψ_1 does have an extra term accounting for the $SU(2)_L$ invariance.
Now we need to add the strong force to our model. Let us restrict ourselves to the assignment a) in the following. As expected, we will need then a new set of gauge bosons. In order to be able to promote a symmetry to be local we need as we have seen, the same number of gauge bosons as parameters needed to describe a transformation under the group under study. For $SU(3)$ this number is 8 thus we need to add 8 so-called gluons $G^\mu_a(x)$. With the help of $\frac{1}{2}\,\lambda^a$ ($a = 1, 2, \ldots, 8$), the generators of the $SU(3)$ algebra, we can write them as:

$$[G^\mu(x)]_{\alpha\beta} \,\equiv\, \left(\frac{\lambda^a}{2}\right)_{\alpha\beta} G^\mu_a(x)\,. \tag{2.12}$$

The covariant derivative for this case has to be modified as:

$$D^\mu\psi_1 \,\equiv\, \left[\partial^\mu + ig_s\,G^\mu(x) + i\,g\,\widetilde{W}_\mu(x) + i\,g'\,y_1\,B_\mu(x)\right]\,\psi_1 \tag{2.13}$$

$$D^\mu\psi_2 \,\equiv\, \left[\partial^\mu + ig_s\,G^\mu(x) + i\,g'\,y_2\,B_\mu(x)\right]\,\psi_2 \tag{2.14}$$

Finally the Lagrangian will be for the fields charged under $SU(3)$ (remember we have taken the a) assignment for this case):

$$\mathcal{L}_{SU(3)} \equiv \sum_i \bar{\psi}_i \, (i\gamma^\mu D_\mu) \, \psi_i - \frac{1}{4} G_a^{\mu\nu} G^a_{\mu\nu}. \tag{2.15}$$

with the corresponding field strength tensor

$$G_a^{\mu\nu}(x) \equiv \tfrac{\lambda^a}{2} \, \partial^\mu G_a^\nu - \partial^\nu G_a^\mu - g_s \, f^{abc} \, G_b^\mu \, G_c^\nu \, . \tag{2.16}$$

Note that the $SU(3)$ structure constants f^{abc} appear in the field strength tensor, bringing a new set of possible interactions with respect to the $U(1)$ case. It is the same for $SU(2)_L$ where the structure constants are easily written as the anti-symmetric tensor ϵ^{ijk} in equation (2.11).

2.1.3. $SU(2)_L \otimes U(1)_Y$ and The Brout-Englert-Higgs mechanism

There is a very important step before we can describe the physics of our world in terms of the standard model. Until now we have stated that our theory has a $SU(2)_L$ symmetry. Such symmetry forbids terms of the form $m\psi\overline{\psi} = m\psi_L\overline{\psi}_R + h.c$, as it clearly mixes right handed and left handed particles.

But without masses for fermions a description of matter as we know is not possible. The proposal of the Brout-Englert-Higgs [6][7] mechanism and then the electroweak model by Salam, Glashow and Weinberg [8] offered an elegant solution to this problem.

In a revolutionary turn of events, it was shown that the electromagnetic and weak force were closely related and that physics at the scales of our experiments where nothing but the remainder of the $SU(2)_L \otimes U(1)_Y$ symmetry breaking into $U(1)_{EM}$.

The precise mechanism of this breaking is known as the Brout-Englert-Higgs mechanism, or BEH for short, and it predicted the existence of the Higgs boson, a scalar particle responsible for the breaking of the symmetry through a vacuum expectation value (VEV).

It is important to devote some time to discuss the spontaneous breaking of symmetries through fields that attain VEVs, as it will be one of the main aspects of this work. Conceptually, what happens is that certain fields are allowed to have a non-zero value at the vacuum of a QFT. If the fields getting VEVs hold any quantum number associated with a symmetry, the fact that their VEVs are just numbers implies that at the vacuum such symmetry would be broken.

Such is the case with the Higgs field, but it can also be the case in theories with more complicated gauge groups that need to be broken. Conversely, the fact that we know certain symmetries remain in the physics we observe in experiments can be a guiding principle to drift away from models, or parameter points of such models, that would give VEVs to fields that hold quantum numbers we want to conserve.

Such is the case in SUSY where, as we will see, we have scalar particles carrying color and electric charge thus if we want to be realistic these fields should never get VEVs.

Let's see how such symmetry breaking process works in some detail. The first ingredient is a $SU(2)_L$ complex scalar doublet

$$\phi(x) \equiv \begin{pmatrix} \phi^{(+)}(x) \\ \phi^{(0)}(x) \end{pmatrix} . \tag{2.17}$$

For such a particle, the Lagrangian and the corresponding covariant derivative will be:

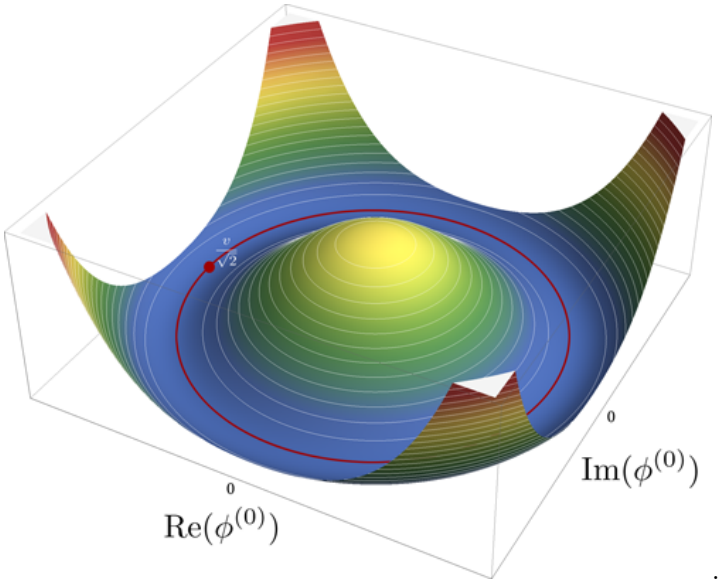

Figure 2.1.: Higgs potential. The circle of minimum potential where $SU(2)_L$ symmetry is broken is shown in red. The Higgs field VEV is attained at the global minimum below 0 in field space.

$$\mathcal{L}_S \;=\; (D_\mu\phi)^\dagger\, D^\mu\phi - m^2\phi^\dagger\phi - \frac{\lambda}{2}\left(\phi^\dagger\phi\right)^2 \qquad \text{with} \quad \lambda > 0\,,\; m^2 < 0\,, \tag{2.18}$$

$$D^\mu\phi \;=\; \left[\partial^\mu + i\,g\,\widetilde{W}^\mu + i\,g'\,y_\phi\,B^\mu\right]\,\phi\;. \tag{2.19}$$

By construction the Lagrangian is invariant under $SU(2)_L \otimes U(1)_Y$ transformations.

In order to see what happens next, it is very useful to cast the scalar field in a specific parametrization. We will take advantage of the local $SU(2)_L$ invariance to add an irrelevant (at this stage) $SU(2)_L$ transformation and write the field like

$$\phi(x) \;=\; \exp\left\{i\,\frac{\sigma_i}{2}\,\vartheta^i(x)\right\}\,\frac{1}{\sqrt{2}}\begin{pmatrix} 0 \\ \tilde{\phi}(x) \end{pmatrix}\,, \tag{2.20}$$

with real fields $\vartheta^i(x)$ and $\tilde{\phi}(x)$. This parametrization shows explicitly that $\vartheta^i(x)$ are not physical as they can be absorbed by a gauge transformation. The potential of the theory becomes now

$$m^2\phi^\dagger\phi + \frac{\lambda}{2}\left(\phi^\dagger\phi\right)^2 = m^2\tilde{\phi}(x)^2 + \frac{\lambda}{2}\tilde{\phi}(x)^4, \tag{2.21}$$

and is minimized by taking $(\langle 0|\,\tilde{\phi}\,|0\rangle)^2 = \frac{-m^2}{2\lambda} = (\frac{v}{\sqrt{2}})^2$. The clever thing about this parametrization is that the parameters of the $SU(2)_L$ transformation $\vartheta^i(x)$ are precisely the would-be massless Goldstone bosons associated with the broken symmetry. They will not get masses as they do not appear in the scalar potential.

Fixing $\vartheta^i(x)$ is equivalent to choosing a gauge. We will go to the so-called physical gauge and fix $\vartheta^i(x) = 0$, in that case we have that the potential is minimized by the VEV

$$\langle 0|\,\phi(x)\,|0\rangle \;=\; \frac{1}{\sqrt{2}}\begin{pmatrix} 0 \\ v \end{pmatrix}. \tag{2.22}$$

By doing this we have chosen $\langle 0|\,\phi^{(0)}\,|0\rangle = \frac{1}{\sqrt{2}}v$ to be real and set $\langle 0|\,\phi^{(+)}\,|0\rangle = 0$. At this stage the fact that $\phi^{(0)}$ has a non-zero VEV means that the Lagrangian is not manifestly $SU(2)_L$ invariant anymore and $SU(2)_L \otimes U(1)_Y$ symmetry gets spontaneously broken to $U(1)_{EM}$.
With $SU(2)_L$ broken, we would like to identify the neutral gauge bosons with the Z and the photon γ. The problem is that for example B_μ couples in the same way to electrons and neutrinos, so this can not work. However we can now take a combination of B_μ and W^3_μ:

$$\begin{pmatrix} W^3_\mu \\ B_\mu \end{pmatrix} \equiv \begin{pmatrix} \cos\theta_W & \sin\theta_W \\ -\sin\theta_W & \cos\theta_W \end{pmatrix}\begin{pmatrix} Z_\mu \\ A_\mu \end{pmatrix}, \tag{2.23}$$

with the mixing angle defined by $g\,\sin\theta_W \;=\; g'\,\cos\theta_W \;=\; e\,.$
Let us look at what happened to the gauge interaction part in (2.18). The covariant derivative (2.19) couples then $\tilde{\phi}$ to the gauge bosons of $SU(2)_L \otimes U(1)_Y$, by parametrizing $\tilde{\phi} = H + v$ we get:

$$(D_\mu\phi)^\dagger\, D^\mu\phi \xrightarrow{\vartheta^i(x)=0} \frac{1}{2}\,\partial_\mu H\partial^\mu H + (v+H)^2\,\left\{\frac{g^2}{4}\,W^\dagger_\mu W^\mu + \frac{g^2}{8\cos^2\theta_W}\,Z_\mu Z^\mu\right\}. \tag{2.24}$$

We started this process to get masses for fermions, but even before understanding how this would happen, the VEV has generated a quadratic term for the $W^\pm$ and the Z, in other words the gauge bosons now have masses $M_Z\,\cos\theta_W \;=\; M_W \;=\; \frac{1}{2}\,v\,g\,.$
Now that the Higgs field has acquired a VEV, the Yukawa interaction terms, which have the generic form $Y_i H\psi_i\bar{\psi}_i$ will generate mass terms for the fermions of our theory. Assuming we are in the base where the Yukawa coupligns are diagonal, we get that

$$\mathcal{L}_{mass} = -(H+\frac{v}{\sqrt{2}})(\,Y_u\,u\bar{u} + Y_d\,d\bar{d} + Y_l\,l\bar{l}\,) \tag{2.25}$$

$$= -Y_u\,H\,u\bar{u} - Y_d\,H\,d\bar{d} - Y_l\,H\,l\bar{l} - m_u\,u\bar{u} - m_d\,d\bar{d} - m_l\,l\bar{l} \tag{2.26}$$

Where $m_i = \frac{v}{\sqrt{2}}Y_i$ are the new mass terms generated by the process of electroweak symmetry breaking (EWSB).

2.2. Unexplained phenomena and BSM physics

The standard model of particle physics has rightfully been called the biggest theoretical success of our time. One of its most powerful features is the ability to predict experimental results to incredible levels of accuracy.
However it still fails to provide an explanation to several phenomena that are supported with hard experimental evidence. Baryon asymmetry, the nature of dark matter (which constitutes almost 30% of the total mass-energy in our universe) and neutrino masses are some examples.
Although some of these facts arise from different areas of physics, it may be possible to explain them through particle physics. It is therefore interesting to find theoretical models that answer this open questions by going beyond the standard model (BSM).

2.2.1. Baryon asymmetry

As far as we have been able to observe, there is an obvious imbalance of baryonic matter and antibaryonic matter in our universe. However there is no successful theoretical explanation for the reason of this asymmetry. Even though the initial conditions for the Big Bang can allow for some primordial baryon asymmetry, it would be diluted after inflation [9]. The idea that this asymmetry could be explained by particle physics came from Sakharov in 1967 [10], there it was stated that a model with baryon number and CP violating interactions could do the job. However the standard model lacks the necessary pieces and can not be a candidate to explain baryon asymmetry.

There are however different candidate mechanisms to explain this asymmetry though they all are extensions of the SM. The two more popular mechanisms are known as electroweak baryogenesis [11] and leptogenesis [12]. The first one cures the SM pitfalls by extending the scalar sector and adding new CP violating interactions. The second one adds right-handed neutrinos to the SM and is able to generate the asymmetry by converting the leptons coming form the decays of right-handed neutrinos into baryons through sphaleron processes.

2.2.2. Dark matter

Dark matter is a hypothesized type of matter that would account for observed effects of mass structures in astrophysical systems, with sizes ranging from galactic to cosmological scales, where no ordinary matter can be observed. Experiments observe effects that can only be explained either by a deviation from general relativity or by assuming the existence of a large amount of dark matter. It is assumed dark matter does not emit nor absorb radiation and it is therefore invisible to telescopes [13].

The latest measurements done by the Planck collaboration [14] put the fraction of dark matter in our universe around 30%. There are several experimental efforts that are on the lookout for direct [15] or indirect [16] measurements of dark matter. Although dark matter could be made of neutrinos, it would not explain the value for the relic density of dark matter measured from the cosmic microwave background.

2.2.3. Neutrino masses

In the standard model neutrinos are described as massless particles. However the process of neutrino oscillations, which mixes neutrino flavor states requires them to have mass [17].

Extending the SM to accommodate neutrino masses is rather straightforward. It can be achieved by adding an extra particle, a right-handed neutrino, and give Dirac masses to neutrinos in the same way the SM does to fermions. Because right-handed neutrinos would have to be singlets under the SM gauge group, they can also be added as Majorana particles, so that by being their own antiparticle, they can have their own a mass term. It is then possible to give masses to neutrinos through the see-saw mechanism: If we add both Dirac masses and Majorana masses (only for right-handed neutrinos), we can get very light left-handed neutrinos and a very heavy right-handed ones. This is very convenient as it could explain the fact that only left-handed neutrinos have been observed [18].

2.2.4. On the lookout for BSM

After the discovery of the Higgs boson at CERN in 2012, all the pieces of the standard model puzzle have been found. Its agreement with experiment continues to amaze and show us how robust its predictions can be. However, it is clear from our previous discussion that if we would like to explain the discussed phenomena with particle physics it is necessary to extend it.
A great deal of effort is put into finding ways of constraining models for new physics using new data coming from experiments. With some luck it could be possible to find direct signals of beyond standard model physics at the LHC as long as the scale of new physics is not too far away.
Although we are looking for new physics at experiments, we are also faced with the fact that after many years of searching for new particles, we have a plethora of interesting models that arise as candidates to answer these open questions. Any way of constraining new models and narrowing the possible alternatives is a big step forward.
In this sense, finding ways to systematically constraint either models or parameter ranges within them is one of the top priorities in the lookout for BSM physics. These constraints can come from different sources. They might come as tools to quickly match a model prediction to available data or new theoretical insights that might disprove the consistency of a model.
As the computing power available to the typical scientist grows, new windows for such constraints open. Calculations thought to be extremely complicated to do in vast parameter scans can be done now in a typical laptop computer and can be automated to a great degree. It is the purpose of this work to take advantage of these facts and present a systematic way for constraining the parameter space of several BSM models through the minimization of their scalar potential.
We will focus on SUSY models as they are one of the most popular extensions which offer answers to some of these open questions. As we will see, neutrino masses can be easily included in SUSY models and the many new particles offer several possibilities for dark matter candidates. It also offers the possibility for unification of all gauge forces at a high scale and it helps ameliorating some of the theoretical issues in the SM, like the hierarchy problem [19]. Let us then introduce in the following chapter how to include Supersymmetry in particle physics models.

CHAPTER THREE

SUPERSYMMETRY

One of the most popular extensions of the standard model is supersymmetry (SUSY). SUSY adds the only allowed extra symmetry of spacetime resulting in a relation between bosonic and fermionic particles. By including this extra symmetry new particles have to be introduced to construct a theory invariant under SUSY transformations, much in the same spirit than in the discussion about QED. Before we go into more detail, it will be convenient to lay down the notation we will be using through this chapter.

3.1. Indexes, dots and Grassmann variables

It will prove useful to work in two-component Weyl fermion notation. This, as we will see has to do with the fact that for SUSY the building blocks of matter can be written as multiplets comprised of two-component Weyl fermions.
In this basis we can write a four component Dirac spinor as

$$\Psi_D = \begin{pmatrix} \xi_\alpha \\ \chi^{\dagger\dot{\alpha}} \end{pmatrix}. \tag{3.1}$$

Note that left (right) handed spinors will have dotted (undotted) indexes. Indexes might be lowered or raised by using the epsilon tensor as

$$\xi_\alpha = \varepsilon_{\alpha\beta}\xi^\beta \qquad \chi^{\dagger\dot{\alpha}} = \varepsilon^{\dot{\alpha}\dot{\beta}}\chi^\dagger_{\dot{\beta}}. \tag{3.2}$$

The origin of this notation comes from the fact that for the Weyl representation the Lorentz group $SO(1,3)$ is decomposed into $SU(2)_L \otimes SU(2)_R$. The dot tracks to which $SU(2)$ subspace does the index belongs and the raising and lowering helps the tracking of invariants through the corresponding $SU(2)$ product. The fact that there is a dagger in the lower component is also a convenient way of writing everything in terms of left-handed fields as for a left-handed field χ, $\chi^\dagger$ behaves as a right handed one.
An important tool for laying down the superspace formalism and to understand SUSY transformations are Grassmann variables. These are just extra coordinates that anticommute with each

other and commute with spacetime coordinates. Adding these new coordinates to spacetime coordinates will span what is called superspace. They satisfy

$$\theta_i\theta_j = -\theta_j\theta_i, \qquad \theta_j x^\mu = x^\mu\theta_j, \qquad \theta_i^2 = 0. \tag{3.3}$$

A consequence of this is that the most general field with real coefficients in superspace with n Grassmann coordinates can be written as

$$F(x,\theta_1,...,\theta_n) = f^0 + f^i\theta_i + f^{ij}\theta_i\theta_j + ... + f^{12...n}\theta_1\theta_2...\theta_n. \tag{3.4}$$

We can also define differentiation and integration in superspace. The right derivative $\frac{\overrightarrow{d}}{d\theta_i}$ is defined to satisfy the following properties.

$$\frac{\overrightarrow{d}}{d\theta_j}\theta_i = \delta_{ij} \tag{3.5}$$

$$\frac{\overrightarrow{d}}{d\theta_j}(\theta_i\theta_j) = -\frac{\overrightarrow{d}}{d\theta_j}(\theta_j\theta_i) = -\theta_i \quad \text{for } i \neq j \tag{3.6}$$

The left derivative can be defined in the same fashion, however which one to use is a matter of convention. From now on when we write $\frac{d}{d\theta_i}$ (or $\frac{\partial}{\partial\theta_i}$), we will mean the right derivative.

Analogously, integration is defined as follows

$$\int (af(\theta_i) + bg(\theta_i))\, d\theta_i = a\int f(\theta_i)d\theta_i + b\int g(\theta i)d\theta_i, \tag{3.7}$$

$$\int d\theta_i = 0, \tag{3.8}$$

$$\int \theta_i d\theta_j = \delta_{ij}. \tag{3.9}$$

As with spacetime coordinates, we can also build spinor degrees of freedom with Grassmann variables in the exact same way. This will be necessary when describing SUSY in the superfield formalism. In this case we can build spinors with Grassmann variables in a straightforward way and superspace will be labeled with the coordinates

$$x^\mu,\ \theta^\alpha,\ \theta^\dagger_{\dot\alpha}. \tag{3.10}$$

Now every Grassmann coordinate will have two components. This means that integration over fermionic coordinates will have to be carried out for each component separately. In the following we will use the integration metrics

$$d^2\theta = -\frac{1}{4}d\theta^\alpha d\theta^\beta\epsilon_{\alpha\beta} \quad \text{and} \quad d^2\theta^\dagger = -\frac{1}{4}d\theta_{\dot\alpha}d\theta_{\dot\beta}\epsilon^{\dot\alpha\dot\beta} \tag{3.11}$$

When writing Lagrangians in superspace we will also need to define a covariant derivative for Grassmann variables. Requiring covariance under SUSY transformations, which we will introduce later, we get the following covariant derivatives:

$$
\begin{aligned}
D_\alpha &= \frac{\partial}{\partial\theta^\alpha} - i(\sigma^\mu\theta^\dagger)_\alpha\partial_\mu, & D^\alpha &= -\frac{\partial}{\partial\theta_\alpha} + i(\theta^\dagger\bar{\sigma}^\mu)^\alpha\partial_\mu, \\
D^{\dagger\dot{\alpha}} &= \frac{\partial}{\partial\theta^\dagger_{\dot{\alpha}}} - i(\bar{\sigma}^\mu\theta)^{\dot{\alpha}}\partial_\mu, & D^\dagger_{\dot{\alpha}} &= -\frac{\partial}{\partial\theta^{\dagger\dot{\alpha}}} + i(\theta\sigma^\mu)_{\dot{\alpha}}\partial_\mu.
\end{aligned} \tag{3.12}
$$

3.2. SUSY transformations

In 1967 Sidney Coleman and Jeffrey Mandula [20] proved, in the context of symmetries of the S-matrix, " the impossibility of combining space-time and internal symmetries in any but a trivial way". In other words, any symmetry Lie algebra for the S-matrix is always a direct product of the Poincaré group and an internal group. This is commonly known as the Coleman-Mandula no-go theorem. This means that besides the gauge symmetries and the Poincaré group, there can not be any other local symmetries in a consistent theory.

However in 1975 Rudolf Haag, Jan Łopuszański, and Martin Sohnius [21] proved that by allowing anti-commuting generators for the space-time symmetries it was possible to get around this and include an extra symmetry of spacetime. This extra symmetry has the fundamental property of creating an interplay between the internal symmetry and the spacetime symmetry of the theory as the symmetry generators interchange fermions and bosons and the anticommutator of two generators is a translation in spacetime. This extra symmetry is called a supersymmetry transformation and its generators satisfy

$$
\begin{aligned}
Q|\text{Boson}\rangle &= |\text{Fermion}\rangle, \\
Q|\text{Fermion}\rangle &= |\text{Boson}\rangle,
\end{aligned}
\qquad
\begin{aligned}
\{Q_\alpha, Q^\dagger_{\dot{\alpha}}\} &= 2\sigma^\mu_{\alpha\dot{\alpha}}P_\mu, \\
\{Q_\alpha, Q_\beta\} = \{Q^\dagger_{\dot{\alpha}}, Q^\dagger_{\dot{\beta}}\} &= 0, \\
[P^\mu, Q] = [P^\mu, Q^\dagger] &= 0.
\end{aligned} \tag{3.13}
$$

If we would like to explore the consequences of adding such symmetries to a physical model, the next logical step would be to think of a theory which is symmetric under the gauge group of the standard model, the Poincaré group and supersymmetry transformations coming from only one generator.

The first obvious and most famous consequence of adding this symmetry is that every particle in the SM would automatically have a SUSY partner, so that every Fermionic particle can be transformed by SUSY to its Bosonic partner and viceversa.

The first step is to introduce a set of Grassmann (anti-commuting) coordinates, which together with the spacetime coordinates will span what we will call superspace. This coordinates will commute with spacetime coordinates but anticommute with themselves and will carry a spinor index.

In the superspace formalism, where we work with Grassmann variables in addition to regular space coordinates, we can write SUSY transformations easily with the help of the differential operators:

$$\hat{Q}_\alpha = \frac{i}{\sqrt{2}}\frac{\partial}{\partial\theta^\alpha} - \frac{1}{\sqrt{2}}(\sigma^\mu\theta^\dagger)_\alpha\partial_\mu, \qquad \hat{Q}^\alpha = -\frac{i}{\sqrt{2}}\frac{\partial}{\partial\theta_\alpha} + \frac{1}{\sqrt{2}}(\theta^\dagger\overline{\sigma}^\mu)^\alpha\partial_\mu, \tag{3.14}$$

$$\hat{Q}^{\dagger\dot{\alpha}} = \frac{i}{\sqrt{2}}\frac{\partial}{\partial\theta^\dagger_{\dot{\alpha}}} - \frac{1}{\sqrt{2}}(\overline{\sigma}^\mu\theta)^{\dot{\alpha}}\partial_\mu, \qquad \hat{Q}^\dagger_{\dot{\alpha}} = -\frac{i}{\sqrt{2}}\frac{\partial}{\partial\theta^{\dagger\dot{\alpha}}} + \frac{1}{\sqrt{2}}(\theta\sigma^\mu)_{\dot{\alpha}}\partial_\mu. \tag{3.15}$$

A SUSY transformation, for infinitesimal parameters ϵ and $\epsilon^\dagger$, can be then written as

$$\delta_Q = \epsilon\hat{Q} + \epsilon^\dagger\hat{Q}^\dagger. \tag{3.16}$$

It is convenient to arrange single-particle states into irreducible representations of the supersymmetry algebra. By definition this supermultiplets will contain fields that can be expressed as linear combination of the SUSY generators acting on the others, so they will contain both fermionic and bosonic states with spins differing by $1/2$.
A general supermultiplet or representation of the SUSY algebra (with scalar coefficients), will look like

$$\mathcal{F}(x,\theta,\theta^\dagger) = a + \theta\xi + \theta^\dagger\chi^\dagger + \theta\theta b + \theta^\dagger\theta^\dagger c + \theta\sigma_\mu\theta^\dagger v_\mu + \theta^\dagger\theta^\dagger\theta\eta + \theta\theta\theta^\dagger\zeta^\dagger + \theta\theta\theta^\dagger\theta^\dagger d. \tag{3.17}$$

It is interesting now to see how this superfield would transform under a general SUSY transformation. It will be useful to know this when constructing SUSY invariant Lagrangians, as we will always try to look for terms that are invariant under such transformations. Explicitly, under a transformation (3.16), the components of the most general superfield will transform as:

$$\delta_Q\, a = \epsilon\xi + \epsilon^\dagger\chi^\dagger, \tag{3.18}$$

$$\delta_Q\, \xi_\alpha = 2\epsilon_\alpha b - (\sigma^\mu\epsilon^\dagger)_\alpha(v_\mu + i\partial_\mu a), \tag{3.19}$$

$$\delta_Q\, \chi^{\dagger\dot{\alpha}} = 2\epsilon^{\dagger\dot{\alpha}}c + (\overline{\sigma}^\mu\epsilon)^{\dot{\alpha}}(v_\mu - i\partial_\mu a), \tag{3.20}$$

$$\delta_Q\, b = \epsilon^\dagger\zeta^\dagger - \frac{i}{2}\epsilon^\dagger\overline{\sigma}^\mu\partial_\mu\xi, \tag{3.21}$$

$$\delta_Q\, c = \epsilon\eta - \frac{i}{2}\epsilon\sigma^\mu\partial_\mu\chi^\dagger, \tag{3.22}$$

$$\delta_Q\, v^\mu = \epsilon\sigma^\mu\zeta^\dagger - \epsilon^\dagger\overline{\sigma}^\mu\eta - \frac{i}{2}\epsilon\sigma^\nu\overline{\sigma}^\mu\partial_\nu\xi + \frac{i}{2}\epsilon^\dagger\overline{\sigma}^\nu\sigma^\mu\partial_\nu\chi^\dagger, \tag{3.23}$$

$$\delta_Q\, \eta_\alpha = 2\epsilon_\alpha d - i(\sigma^\mu\epsilon^\dagger)_\alpha\partial_\mu c - \frac{i}{2}(\sigma^\nu\overline{\sigma}^\mu\epsilon)_\alpha\partial_\mu v_\nu, \tag{3.24}$$

$$\delta_Q\, \zeta^{\dagger\dot{\alpha}} = 2\epsilon^{\dagger\dot{\alpha}}d - i(\overline{\sigma}^\mu\epsilon)^{\dot{\alpha}}\partial_\mu b + \frac{i}{2}(\overline{\sigma}^\nu\sigma^\mu\epsilon^\dagger)^{\dot{\alpha}}\partial_\mu v_\nu, \tag{3.25}$$

$$\delta_Q\, d = -\frac{i}{2}\epsilon^\dagger\overline{\sigma}^\mu\partial_\mu\eta - \frac{i}{2}\epsilon\sigma^\mu\partial_\mu\zeta^\dagger. \tag{3.26}$$

Something that will come handy later is the fact that the coefficient d of $\theta\theta\theta^\dagger\theta^\dagger$ transforms to a full derivative in the space coordinates.
However, as mentioned before, we are interested in irreducible representations that will help us describe the fields necessary to build a SUSY theory. There are several ways of constructing irreducible representations but we want to find those that can reproduce the physical fields of the standard model and their respective superpartners.
The first one, a chiral supermultiplet is constructed by requiring

$$D_{\dot{\alpha}}^{\dagger}\Phi = 0 \tag{3.27}$$

for the so-called left-chiral superfields and

$$D_{\alpha}\Phi^{*} = 0 \tag{3.28}$$

for right-chiral superfields. It can be shown that the result of constraining a general superfield (3.17) by equations (3.27) and (3.28) leaves us with

$$\begin{aligned}\Phi = \phi(x) + i\theta\sigma_{\mu}\theta^{\dagger}\partial_{\mu}\phi(x) + \frac{1}{4}\theta\theta\theta^{\dagger}\theta^{\dagger}\partial_{\mu}\partial^{\mu}\phi(x) + \sqrt{2}\theta\psi(x) \\ - \frac{i}{\sqrt{2}}\theta\theta\theta^{\dagger}\bar{\sigma}^{\mu}\partial_{\mu}\psi(x) + \theta\theta F(x),\end{aligned} \tag{3.29}$$

$$\begin{aligned}\Phi^{*} = \phi^{*}(x) - i\theta\sigma_{\mu}\theta^{\dagger}\partial_{\mu}\phi^{*}(x) + \frac{1}{4}\theta\theta\theta^{\dagger}\theta^{\dagger}\partial_{\mu}\partial^{\mu}\phi^{*}(x) + \sqrt{2}\theta^{\dagger}\psi^{\dagger}(x) \\ - \frac{i}{\sqrt{2}}\theta^{\dagger}\theta^{\dagger}\theta\sigma^{\mu}\partial_{\mu}\psi^{\dagger}(x) + \theta^{\dagger}\theta^{\dagger}F^{*}(x).\end{aligned} \tag{3.30}$$

It is sometimes convenient to do a superspace transformation to express chiral supermultiplets in a simple form. By doing $y^{\mu} = x^{\mu} + i\theta^{\dagger}\bar{\sigma}^{\mu}\theta$, $y^{\mu *} = x^{\mu} - i\theta^{\dagger}\bar{\sigma}^{\mu}\theta$, and working in the new coordinates $y^{\mu}, \theta, \theta^{\dagger}$ we can write (note that in this case $\theta^{\dagger}$ does not appear)

$$\Phi = \phi(y) + \sqrt{2}\theta\psi(y) + \theta\theta F(y), \tag{3.31}$$

$$\Phi^{*} = \phi^{*}(y^{*}) + \sqrt{2}\theta^{\dagger}\psi^{\dagger}(y^{*}) + \theta^{\dagger}\theta^{\dagger}F^{*}(y^{*}). \tag{3.32}$$

Chiral fields have eight degrees of freedom: a complex scalar field, a complex scalar auxiliary field and a left-handed spinor field. Now, to properly describe an interacting gauge theory we need gauge bosons, i.e. we will need another representation of the SUSY symmetry. The answer lies in another representation called vector superfields which we can construct through the constraint $V = V^{*}$. This adds the following constraints to the individual components of (3.17)

$$a = a^{*}, \quad d = d^{*}, \quad \chi^{\dagger} = \xi^{\dagger}, \quad v_{\mu} = v_{\mu}^{*}, \quad c = b^{*}, \quad \zeta^{\dagger} = \eta^{\dagger}. \tag{3.33}$$

In other words, vector superfields can be written as

$$\begin{aligned}V(x, \theta, \theta^{\dagger}) = +\theta\xi + \theta^{\dagger}\xi^{\dagger} + \theta\theta b + \theta^{\dagger}\theta^{\dagger}b^{*} + \theta\sigma_{\mu}\theta^{\dagger}A_{\mu} + \theta^{\dagger}\theta^{\dagger}\theta(\lambda - \frac{i}{2}\sigma^{\mu}\partial_{\mu}\xi^{\dagger}) \\ + \theta\theta\theta^{\dagger}(\lambda^{\dagger} - \frac{i}{2}\bar{\sigma}^{\mu}\partial_{\mu}\xi) + \theta\theta\theta^{\dagger}\theta^{\dagger}(\frac{1}{2}D + \frac{1}{4}\partial_{\mu}\partial^{\mu}a).\end{aligned} \tag{3.34}$$

Where we have redefined for convenience $\eta_{\alpha} = \lambda_{\alpha} - \frac{i}{2}(\sigma^{\mu}\partial_{\mu}\xi^{\dagger})_{\alpha}$, $v_{\mu} = A_{\mu}$ and $d = \frac{1}{2}D + \frac{1}{4}\partial_{\mu}\partial^{\mu}a$. It is clear from the previous equation that written this way, the vector superfield has a lot more degrees of freedom than what we are looking for. However it is possible to "gauge away" some of these fields by preforming a supergauge transformation. Explicitly we can do appropriate transformations to eliminate a, ξ and b and write the vector superfield as

$$V_{WZ} = \theta^\dagger \bar{\sigma}^\mu \theta A_\mu + \theta^\dagger \theta^\dagger \theta \lambda^\dagger + \frac{1}{2}\theta\theta\theta^\dagger\theta^\dagger D. \tag{3.35}$$

The superfield is now said to be in the Wes-Zumino gauge. In this form it is easy to see that a vector superfield has a gauge boson field A_μ, a spinor field λ and a auxiliary real scalar D as degrees of freedom.

3.3. Constructing a SUSY Lagrangian

Now that we have all the building blocks for our SUSY theory, we need to understand how to write down the Lagrangian out of the superfields we have described. Fortunately even though SUSY invariance introduces many new degrees of freedom, the extra symmetry also brings some simplification of the theoretical framework.
In this sense, the information needed to construct a SUSY Lagrangian can be enconded in two objects that will also come handy in constructing different SUSY models.

3.3.1. The Kähler potential

The first obvious object we can construct with superfields, which remains invariant under SUSY transformations is the integration of a superfield over all of superspace. This comes from the fact that as can be seen from equation (3.26), the component surviving the fermionic integration, the one with $\theta\theta\theta^\dagger\theta^\dagger$, transforms to a full derivative under SUSY transformations.
More generally any object that can be written as

$$\mathbb{S} = \int d^4x \int d^2\theta d^2\theta^\dagger \mathcal{S}(x, \theta, \theta^\dagger), \tag{3.36}$$

where $\mathcal{S}$ is a general superfield, is automatically invariant under SUSY transformations, therefore making it a good candidate for a SUSY Lagrangian. What happens is that after a SUSY transformation and the integration of the fermionic degrees of freedom the remaining integration over space will make any total derivative vanish.
If we would like to eventually construct Lagrangian terms from this type of contributions, we will need $\mathcal{S}$ to be a vector superfield, let's call it $\mathcal{V}$. This is due to the fact that we need the action to be real. A SUSY invariant term can be constructed by taking (expressing $\mathcal{V}$ in the Wess-Zumino gauge)

$$[\mathcal{V}]_D = \int d^2\theta d^2\theta^\dagger \mathcal{V}(x, \theta, \theta^\dagger) = \frac{1}{2}D. \tag{3.37}$$

The usual convention is to call this a D-term contribution. We need to construct SUSY invariant Lagrangian terms out of D-terms. It turns out that exploiting the fact that $\Phi^*\Phi$ is a vector superfield and by using the notation in (3.29) and (3.30) we find that

$$\mathcal{L}_{\Phi^*\Phi} = [\Phi^*\Phi]_D = \int d^2\theta d^2\theta^\dagger \Phi^*\Phi = -\partial^\mu\phi^*\partial_\mu\phi + i\psi^\dagger\bar{\sigma}^\mu\partial_\mu\psi + F^*F + \dots \tag{3.38}$$

Surprisingly enough these are the canonical kinetic terms for the fields in the supermultiplet Φ. The $\dots$ denote a total derivative part that as always will vanish upon integration over space. This is the simplest possible construction of the Kähler potential which is the object in which we will encode the kinetic part of our SUSY Lagrangians.

3.3.2. The superpotential

Another way of constructing SUSY invariant contributions arises from noticing that for a chiral superfield, the term proportional to $\theta\theta$ also transforms to a total derivative. This is easy to see by looking at equation (3.21) and noting that for chiral superfields $\zeta^\dagger = \frac{i}{\sqrt{2}}\bar{\sigma}^\mu\partial_\mu\psi(x)$.
In the same fashion as before, such terms will vanish under space integration. Using the notation in (3.31) we can construct a suitable SUSY invariant using

$$[\Phi]_F = \int d^2\theta\,\Phi\,\Big|_{\theta^\dagger=0} + \int d^2\theta^\dagger\,\Phi^*\,\Big|_{\theta=0} = F + F^*. \tag{3.39}$$

The usual convention is to name such type of invariants as F-term contributions.
Any holomorphic function of chiral fields is in turn a chiral field. This is quite handy as the F term contribution of a product of chiral fields will contain all the combinations of the components that conserve spin and are invariant under SUSY transformations. If I construct a holomorphic function of the fields (the factors of $\frac{1}{2}$ and $\frac{1}{6}$ are just handy conventions)

$$W = L^i\Phi_i + \frac{1}{2}M^{ij}\Phi_i\Phi_j + \frac{1}{6}y^{ijk}\Phi_i\Phi_j\Phi_k \tag{3.40}$$

in such a way that it respects the gauge invariance of the SM, then we've found a nice way of encoding the interactions of a suitable SUSY Lagrangian. This function is called the superpotential and it serves the purpose of encoding chiral field interactions. It is very popular with seasoned SUSY theorists, as it can be used to get a very quick glimpse at the interactions of any new model.
As W is a chiral field in itself we can construct SUSY invariant terms by taking its F-term contributions. With a bit of gymnastics one can show explicitly

$$[W]_F = \int d^2\theta W\,\Big|_{\theta^\dagger=0} + h.c. = -\left(\frac{1}{2}\frac{\partial^2 W}{\partial\Phi_i\partial_j}\psi_i\psi_j - \frac{\partial W}{\partial\Phi_i}F_i + h.c.\right). \tag{3.41}$$

An interesting fact which we have to keep in mind when building a superpotential is that the action of a QFT should be dimensionless. The terms coming to our action will be of the form

$$\int d^4x \int d^2\theta W\,\Big|_{\theta^\dagger=0} + h.c. \tag{3.42}$$

The integration measure over space d^4x has mass dimension -4, so the terms of the form $\int d^2\theta W$ should have mass dimension 4. Now, the integration measure in the fermionic coordinates satisfies $[d^2\theta] = 1$ [1], so there is no choice but $[W] = 4 - [d^2\theta] = 3$.

3.3.3. Vector superfields

So now that we have the interactions between chiral fields and their kinetic terms we still need to include the gauge vector multiplets . We can again use what we have learned to construct a SUSY invariant term that will encode the necessary terms. First we have to make the Kähler potential explicitly supergauge invariant. This can achieved by writing the kähler potential as

[1] This is easily seen by looking at a chiral superfield, which has mass dimension 1. This implies that $[\theta\theta\Psi] = 1$, thus Grassmann coordinates should have mass dimension $-\frac{1}{2}$. As we defined Berezin integration to satisfy $\int d\theta\theta = 1$, which is dimensionless, it follows $[d\theta] = \frac{1}{2}$ and then $[d^2\theta] = 1$

$$K = \sum k_{ij}\Phi_i^*(e^{2g_aT^aV^a})_i^j\Phi j, \tag{3.43}$$

where the V^a are the vector supermultiplets of our theory in the form of (3.34) and g_a, T^a the corresponding gauge coupling and generators. This in turn includes the interactions between gauge bosons, gauginos and matter. We only lack now the kinetic terms for our vector superfield. To do that we define the chiral superfield

$$\mathcal{W}_\alpha = -\frac{1}{4}D^\dagger D^\dagger e^{-2g_aT^aV^a}D_\alpha e^{2g_aT^aV^a} \tag{3.44}$$

and with it we can construct (assuming $\mathrm{Tr}[T^aT^b] = \kappa_a\delta_{ab}$)

$$\frac{1}{4\kappa_a g_a^2}\mathrm{Tr}[\mathcal{W}^\alpha\mathcal{W}_\alpha]. \tag{3.45}$$

The F term contributions coming from this chiral superfield will account for the kinetic terms of gauge bosons and gauginos. We are now ready to write a SUSY invariant Lagrangian that will have a chance at describing a physical theory including the standard model within it. So putting all our pieces together we can write our SUSY Lagrangian as

$$\mathcal{L} = \int d^2\theta \frac{1}{4\kappa_a g_a^2}\mathrm{Tr}[\mathcal{W}^\alpha\mathcal{W}_\alpha]\,\Big|_{\theta^\dagger=0} - \left(\frac{1}{2}\frac{\partial^2 W}{\partial\Phi_i\partial\Phi_j}\,\Big|_{\Phi_k=\phi_k}\psi_i\psi_j - \frac{\partial W}{\partial\Phi_i}\,\Big|_{\Phi_k=\phi_k}F_i + h.c\right) + \int d^2\theta d^2\theta^\dagger K. \tag{3.46}$$

We refer the reader to [22] and [19] for a more comprehensive treatment of these subjects.

3.4. Supersymmetry breaking

If SUSY would be conserved, all the members of a supermultiplet would have the same mass. This is certainly not the case as we have not observed any SUSY particles. So SUSY has to be a broken symmetry, but how is it broken? As we will see there are several ways to approach this problem and parametrize the breaking of SUSY without knowing the specifics of the SUSY breaking mechanism.

Even though we are trying to parametrize our ignorance, we still have to be a bit careful. We want to keep in mind the idea that the Lagrangian is SUSY invariant at high energies but somehow this symmetry gets broken spontaneously, much in the same way as with the BEH mechanism.

If we add new SUSY breaking interactions to the Lagrangian we would like them to preserve SUSY at higher scales, put simply we want them to be " small " compared to the SUSY part of our Lagrangian. In practice what this means is that we want terms that do not introduce divergences at high scales. This essentially means that we do not want to add terms with mass dimension > 4, as their respective couplings will grow with positive powers of the scale.

This is not the only thing we have to be careful about. The fact that fermions have scalar partners means that in a pure SUSY theory, quadratic divergences cancel and provide an elegant solution to the hierarchy problem i.e. SUSY explains why the Higgs mass is not so much bigger than the electroweak scale. Schematically, the quadratic divergent corrections to the Higgs mass coming from top and stop are such that

$$\partial m_h^2 \propto (\lambda - |y_t|^2)\Lambda^2, \tag{3.47}$$

where Λ is a cutoff scale and λ the quartic coupling of two stops to two Higgses. As we have seen, when adding Yukawa interactions in the superpotential, we are forced by SUSY to give quarks and squarks the same Yukawa coupling, therefore making $\lambda = |y_t|^2$. We would like to preserve this type of cancellations in our SUSY theory, even at lower scales, by preserving the relations between dimensionless couplings (like the Yukawa couplings). What this means is that we will only add soft SUSY breaking terms with combinations of fields with mass dimension $0 < d < 4$. Luckily this means we can still introduce terms that will get rid of the degeneracy in masses and push the SUSY masses high enough to have a phenomenologically consistent model.
A general soft SUSY breaking Lagrangian will then have the form

$$\mathcal{L}_{soft} = -\left(\frac{1}{2}M_a\,\lambda^a\lambda^a + \frac{1}{6}a^{ijk}\phi_i\phi_j\phi_k + \frac{1}{2}b^{ij}\phi_i\phi_j + t^i\phi_i + h.c\right) \tag{3.48}$$

$$-\,(m^2)^i_j\phi^{j*}\phi_i - \left(\frac{1}{2}c_i^{jk}\phi^{*i}\phi_j\phi_k + h.c\right). \tag{3.49}$$

It is worth noting several things at this point. First we have not added terms of the form $\mu\overline{\psi}\psi$ [2] as they will induce quadratic divergences [23]. Also, the terms t^i in the above equation are only allowed for gauge singlets, as our Lagrangian has to be always gauge invariant. Moreover the fact that excluding dimensionless couplings means we are free of quadratic divergences has a extra loophole. In the case of a model with a chiral supermultiplet which is a singlet under all gauge symmetries, the last term in (3.49) can lead to quadratic divergences. However this will not be an issue during this work as we will constrain ourselves to the MSSM and extensions which do not suffer from this problem.

3.4.1. The origin of SUSY breaking

We have already shown that for phenomenology studies it is sufficient to introduce by hand terms that break SUSY softly at the cost of introducing a large set of free parameters. we can try to improve this by assuming some mechanism for SUSY breaking.
For the purpose of this study we will focus in SUSY breaking models inspired by supergravity. Let us define what we mean by that. As we mentioned earlier, we would like to break SUSY spontaneously. If SUSY is unbroken in the vacuum state of a theory it follows that $H\,|0\rangle = 0$. This comes from the fact that the Hamiltonian can be written as $H = \frac{1}{4}(Q_1Q_1^\dagger + Q_1^\dagger Q_1 + Q_2Q_2^\dagger + Q_2^\dagger Q_2)$. Now, in the vacuum of the theory $\langle 0|\,H\,|0\rangle = \langle 0|\,V\,|0\rangle$ where V is the scalar potential of the theory

$$V = V_F + V_D \tag{3.50}$$

with V_F and V_D defined in (3.61)(3.63) respectively. Then we can conclude that as long as V_F or V_D acquire VEVs, we can be sure SUSY has been broken.
It turns out that the case where V_F gets a VEV is more attractive phenomenologically, as with the SUSY breaking induced by V_D it becomes difficult to give masses to all the MSSM particles (especially gauginos)[19]. We will therefore focus on what is called F-term SUSY breaking (where V_F gets a VEV).
Let us assume that gravity is mediated by a spin-2 particle, the graviton. By promoting SUSY to a local symmetry, thus making the ϵ parameters in equation (3.16) space dependent, it is

[2] For singlet fermion fields gauge invariance would not forbid such terms.

possible to unify the spacetime symmetries of general relativity with local SUSY transformations in a formalism called supergravity [24–26]. The gauge field for the local SUSY transformations will be the spin-3/2 superpartner of the graviton, the gravitino. Once SUSY is spontaneously broken the associated goldstone boson, the goldstino, gives mass to the gravitino in the same way the goldstone boson gives masses to the W and Z in the Higgs mechanism.
Because we need fields that are gauge singlets so that their F-term VEVs do not break gauge symmetries, we can see how we are forced to extend the MSSM. SUSY breaking is therefore thought to occur in a "hidden sector" of particles that have very small couplings to the visible sector (the MSSM).
We would of course need some kind of interaction between this hidden sector and the MSSM in order to generate the soft SUSY breaking terms through some kind of spontaneous breaking mechanism. One of most popular assumptions, and the one we will follow in the models we will try to constrain in this work, is that the interactions that mediate between both sectors are gravitational and include them in our SUSY model through the supergravity formalism [27, 28]. If F is the F-term contribution that breaks SUSY, then the generated soft terms should obey

$$m_{soft} \sim \frac{\langle 0| F |0\rangle}{M_p} \tag{3.51}$$

where M_p denotes the Planck mass $\sim 10^{18}\,\mathrm{GeV}$. This form comes from the fact that the soft masses should vanish when $\langle 0| F |0\rangle \to 0$ (if SUSY is restored) and should also vanish for $M_p \to \infty$ (where gravitational interactions become negligible). Taking X to be the field whose F-term contributions get a VEV, we have that the superpotential of the visible + hidden sector model will look like:

$$W = W_{MSSM} - \frac{1}{M_p}\left(\frac{1}{6}y^{Xijk}X\Phi_i\Phi_j\Phi_k + \frac{1}{2}\mu^{Xij}X\Phi_i\Phi_j\right) + \ldots, \tag{3.52}$$

$$K = \Phi^{*i}\Phi_i + \frac{1}{M_p}\left(n_i^j X + \overline{n}_i^j X^*\right)\Phi^{*i}\Phi_j - \frac{1}{{M_p}^2}k_i^j XX^*\Phi^{*i}\Phi_j + \ldots, \tag{3.53}$$

$$f_{ab} = \frac{\delta_{ab}}{g_a^2}\Big(1 - \frac{2}{M_p}f_a X + \ldots\Big). \tag{3.54}$$

For the MSSM, by letting X get a VEV, we get that the soft terms can be written as (following the notation in (3.49))

$$\begin{aligned} M_a &= \frac{F}{M_p}f_a, \\ a^{ijk} &= \frac{F}{M_p}(y^{Xijk} + n_p^i y^{pjk} + n_p^j y^{pik} + n_p^k y^{pij}), \\ b^{ij} &= \frac{F}{M_p}(\mu^{Xij} + n_p^i \mu^{pj} + n_p^j \mu^{pi}), \\ (m^2)_j^i &= \frac{|F|^2}{{M_p}^2}(k_j^i + n_p^i \overline{n}_j^p). \end{aligned} \tag{3.55}$$

Such prescription where we assume SUSY breaking is done through gravity mediation is known as mSUGRA SUSY breaking.

3.5. R-parity

In the SM baryon and lepton number (B and L respectively) are conserved through an accidental symmetry. If we write all the possible Lagrangian terms that are gauge invariant and renormalizable, we find that none of them break either B nor L [3]. Experimentally B and L violation is severely constrained besides a very small contribution to L violation coming from neutrino oscillations [17].
This conservation gets spoiled in SUSY as we have new particles, like squarks (sleptons), that carry baryon number (lepton number) but are of mass dimension 1, therefore allowing us to write gauge invariant and renormalizable terms that do not conserve B (L).
If we want conservation of B and L in a SUSY theory, we need a way of imposing it. By introducing a new discrete symmetry called R-parity it is possible to forbid B and L breaking terms in SUSY theories. It is a multiplicative symmetry defined by

$$\mathcal{P}_R = (-1)^{3B+L-2s}. \tag{3.56}$$

The rule for R-parity is that for any Lagrangian term, the total R-parity (the product of the R-parity of the fields involved) has to be equal to $+1$. Enforcing this symmetry is analogous to conservation of B and L. R-parity also has an interesting feature: it distinguishes the Higgs bosons and SM particles ($\mathcal{P}_R = 1$) from their superpartners or sparticles ($\mathcal{P}_R = -1$). The reason for this comes from the fact that in order to conserve B and L we need to have an even number of SUSY particles.
Another consequence of R-parity, more a corollary of the previous statement, is that the lightest SUSY particle or LSP, can not decay. The LSP being the lightest can only decay to SM particles but this would violate the rule of even sparticles in every interaction vertex. Having a stable light SUSY particle is phenomenologically attractive, as for example, such type of particle might be a good candidate for explaining dark matter.

3.6. Minimal supersymmetric standard model

If we want to study SUSY models, the first question we may ask ourselves is which are the minimum requirements to construct a model that is both supersymmetric and reduces itself to the standard model at lower energies. We already know that we have to add at least as much particles as there are in the standard model, however that is only part of the story. In this section we will describe the Minimal SUSY standard model (MSSM) which, as guessed by its name, extends the SM in the minimal way that is phenomenologically viable.

3.6.0.1. Particle content and superpotential

Before diving into the phenomenology of the MSSM and its extensions, let us describe it in some detail using the tools we have just developed in the previous sections. The two most important bits of information to understand a SUSY model are the particle content and the superpotential. It comes as no surprise that for the MSSM the particle content is the minimal we need to construct a consistent SUSY model. In table 3.1 you can find a list of fields coming into play and their respective spin and charges under the gauge group.

[3] There is a possibility for B violation in the standard model through non perturbative Bell Jackiw anomalies [29]. This is however not relevant for current experiments but interesting when considering baryogenesis.

As mentioned in section 3.3.2, the superpotential is required to be holomorphic. With one Higgs doublet $\phi = (h^0, H^+)^T$ we can write Yukawa interactions for up-type quarks $Y_u^{ij}\, u_i^c\, Q_j\, \phi$ but we can not do the same for the down-type quarks ($Y_d^{ij}\, d_i^c\ Q_j\, i\sigma_2\phi^\dagger$). The necessary superpotential term $Y_d^{ij}\, \hat{d}_i^c\, \hat{Q}_j\, i\sigma_2\hat{H}^*$ is not holomorphic. For the same reason it would not be possible to include a term $\mu\hat{H}\hat{H}^*$ in the superpotential, but we need to include Higgs boson self-interactions if we want to reproduce the standard model in some limit. The solution to this is to have two Higgs doublets, one with Yukawa couplings with up-type quarks (H_u) and another with down-type quarks and leptons (H_d).
Having noted that, we are now ready to put all the pieces together and write the superpotential of the MSSM:

$$W = Y_u^{ij}\, \hat{u}_i^c\, \hat{Q}_j\, \hat{H}_u\ - Y_d^{ij}\, \hat{d}_i^c\, \hat{Q}_j\, \hat{H}_d\ - Y_e^{ij}\, \hat{e}_i^c\, \hat{L}_j\, \hat{H}_d\ + \mu\, \hat{H}_u\, \hat{H}_d\,. \tag{3.57}$$

As the reader might note, this superpotential is explicitly R-parity-conserving. However, there is nothing stopping us from adding terms of the form

$$W_{RPV}^{\not L} = \frac{1}{2}\lambda^{ijk} L_i L_j e_k^c + \lambda'^{ijk} L_i Q_j d_k^c + \mu'^i L_i H_u \tag{3.58}$$

$$W_{RPV}^{\not B} = \frac{1}{2}\beta^{ijk} u_i^c d_j^c d_k^c. \tag{3.59}$$

In other words, we want the MSSM to conserve R-parity at this stage. One reason to impose R-parity conservation is that interactions arising from terms of the form (3.59) will induce proton decay, which we obviously would like to avoid. We would also like to be consistent with observations regarding baryon and lepton number violation.
The new scalars and the extra Higgs doublet make the scalar sector much more complicated and in turn much more interesting. One of the direct consequences is that the scalar potential, whose minimization drives the spontaneous breaking of symmetries, is not trivial to minimize even before adding quantum corrections. This is an issue that we will explore in detail throughout this work.
The perceptive reader might notice that we are lacking the last piece to completely describe the MSSM. We can not avoid to introduce a soft SUSY breaking Lagrangian in order to have a realistic SUSY model. For the MSSM this will include the minimum amount of terms necessary and therefore will look like:

$$\begin{aligned}
\mathcal{L}_{SSB} \;=\; & -\frac{1}{2}\left(M_3\tilde{g}\tilde{g} + M_2\tilde{W}\tilde{W} + M_1\tilde{B}\tilde{B} + h.c\right) \\
& -\left(T_u^{ij}\tilde{u}_i^c\, \tilde{Q}_j H_u - T_d^{ij}\tilde{d}_i^c\, \tilde{Q}_j H_d - T_e^{ij}\tilde{e}_i^c\, \tilde{L}_j H_d + h.c\right) \\
& -\tilde{Q}_i^\dagger\, (m_Q^2)^{ij}\, \tilde{Q}_j - \tilde{L}_i^\dagger\, (m_L^2)^{ij}\, \tilde{L}_j - \tilde{u}_i^c\, (m_U^2)^{ij}\, \tilde{u}_j^{c\dagger} - \tilde{d}_i^c\, (m_D^2)^{ij}\, \tilde{d}_j^{c\dagger} - \tilde{e}_i^c\, (m_E^2)^{ij}\, \tilde{e}_j^{c\dagger} \\
& - m_{H_u}^2 H_u^* H_u - m_{H_d}^2 H_d^* H_d - (B_\mu H_u H_d + h.c)\,.
\end{aligned} \tag{3.60}$$

The trilinear couplings T_i are often also written as $T_i = A_i \times Y_i$.
We now have all the pieces necessary to put together the minimal SUSY standard model. It is a model that offers the most simple way of including SUSY in a phenomenological theory and has

Superfield	Spin 0	Spin $\frac{1}{2}$	Generations	$U(1)_Y \otimes SU(2)_L \otimes SU(3)_C$
$\hat{Q}$	$\tilde{Q}$	Q	3	$(\frac{1}{6}, \mathbf{2}, \mathbf{3}, \frac{1}{6})$
$\hat{d}^c$	$\tilde{d}^c$	d^c	3	$(\frac{1}{3}, \mathbf{1}, \overline{\mathbf{3}}, -\frac{1}{6})$
$\hat{u}^c$	$\tilde{u}^c$	u^c	3	$(-\frac{2}{3}, \mathbf{1}, \overline{\mathbf{3}}, -\frac{1}{6})$
$\hat{L}$	$\tilde{L}$	L	3	$(-\frac{1}{2}, \mathbf{2}, \mathbf{1}, -\frac{1}{2})$
$\hat{e}^c$	$\tilde{e}^c$	e^c	3	$(1, \mathbf{1}, \mathbf{1}, \frac{1}{2})$
$\hat{\nu}^c$	$\tilde{\nu}^c$	ν^c	3	$(0, \mathbf{1}, \mathbf{1}, \frac{1}{2})$
$\hat{H}_d$	H_d	$\tilde{H}_d$	1	$(-\frac{1}{2}, \mathbf{2}, \mathbf{1}, 0)$
$\hat{H}_u$	H_u	$\tilde{H}_u$	1	$(\frac{1}{2}, \mathbf{2}, \mathbf{1}, 0)$

Table 3.1.: Chiral superfields and their quantum numbers in the MSSM.

served as a tool to understand many of the fundamental principles of SUSY in particle physics.

A lot of effort has been put into studying the phenomenological implications and possible ways of finding SUSY. Recently a significant effort has been put towards direct detection and thus the determination of the signals for different SUSY models in collider experiments like the LHC.

For the MSSM (and several of its extensions) we have a good idea of the ways it could show up at ATLAS or CMS, provided that the masses of the sparticles are not so far away from $2-3\,\text{TeV}$[4].

However by adding SUSY we have also introduced many new parameters that need to be either determined form experiment or scanned in the lookout for viable points in parameter space.

This is not necessarily a bad thing. By construction, perturbative QFT models have free parameters that have to be fixed by experiment before the theory can become predictive. Experiments have allowed us to determine the parameters of the standard model, but even for such successful theory determining all of its parameters was not possible until as recently as August 2012.

To understand how to find any sign of SUSY it is important to set some constraints for the parameters based on phenomenological reasons. As we parametrize SUSY breaking by the soft SUSY Lagrangian, we have some freedom in deciding how the SUSY spectrum looks. There are many ways of doing this. Some of them are motivated by assumptions for the specific SUSY breaking mechanism. Some other approaches, like the so-called natural MSSM, rely on concepts like naturalness and purely phenomenological motivations to guide us in the construction of a SUSY mass spectrum.

As we will see in section 5, it is also possible to constrain the parameter space of SUSY models through the analysis of their vacuum structure. This can also guide us in the search for viable parameter points and complement constraints coming from direct experimental measurements. In the following we will describe the models we will be treating along this work. They all build on the MSSM by introducing different motivations for the values of the free parameters and in the case of the BLSSM by extending the gauge group of the MSSM by an extra $U(1)_{B-L}$ symmetry as well.

[4]The reader might think that the center of mass energy is the relevant quantity. However in a hadron collider, the momentum gets distributed within the partons and the mass of produced particles is thus much lower

3.7. The scalar potential

By calculating the Lagrangian contributions coming purely from scalar degrees of freedom one can get the scalar potential of the theory.
The auxiliary fields F_i are not physical and one can remove them by solving their equations of motion $F_i = \frac{\partial W}{\partial \Phi_i}|_{\Phi_k=\phi_k}$. From equation (3.46) one sees that the pure scalar contributions coming from F-terms can be written as

$$V_F = |\frac{\partial W}{\partial \Phi_i}|^2 \Big|_{\Phi_k=\phi_k}. \tag{3.61}$$

The D-term contribution to the scalar potential coming from (3.43) is given by

$$V_D = -\left(\sum_a \sum_j D^a g(\phi^{*j} T^a \phi_j) + \frac{1}{2}\sum_a D^a D^a\right). \tag{3.62}$$

Solving the equations of motion for D^a one gets that $D^a = -g(\phi^* T^a \phi)$ and therefore:

$$V_D = \frac{1}{2}\sum_a \sum_{j,k} g^2 (\phi^{*j} T^a \phi_j)(\phi^{*k} T^a \phi_k) \tag{3.63}$$

Where a runs over the gauge groups. The scalar potential will also get contributions from the soft SUSY breaking terms in (3.60). This will be given by (For simplicity we have neglected flavor violation):

$$\begin{aligned} V_{\text{soft}} &= \sum_i m_i^2 |\phi_i|^2 + (B_\mu H_d H_u + \text{H.c.}) \\ &+ \sum_\alpha \left(A_{u_\alpha} Y_{u_\alpha} H_u \tilde{Q}_\alpha \tilde{u}^c_{R,\alpha} + A_{d_\alpha} Y_{d_\alpha} \tilde{Q}_\alpha H_d \tilde{d}^c_{R,\alpha} + A_{l_\alpha} Y_{l_\alpha} \tilde{L}_\alpha H_d \tilde{e}^c_{R,\alpha} + \text{H.c.}\right). \end{aligned} \tag{3.64}$$

The trilinear couplings $A_i Y_i$ are often also written as T_i. The scalar potential of the MSSM can therefore be written as

$$V^{MSSM} = V_F + V_D + V_{\text{soft}}. \tag{3.65}$$

It is important to point out, although obvious from equation (3.63), that the D-term contributions are always positive quantities even for negative values of the fields. This will be important to remember when analyzing the analytical conditions found in the literature for avoiding charge- and color-breaking minima in section 4.1.

3.8. Natural MSSM

Due to the fact that the soft SUSY breaking masses are free parameters of the theory, we have some freedom to choose the MSSM spectrum. However, we have to keep in mind that we need a phenomenologically viable model thus finding ways of restricting the possible spectra is important. One such way relies on the concept of naturalness. The naturalness requirement can

be understood by looking at the formula for the Z mass in the MSSM (valid for $\tan\beta > 8$) [5]:

$$\frac{1}{2}M_Z^2 = -\mu^2 + \frac{(m_{H_u}^2 + \Sigma_u)\tan^2\beta}{1-\tan^2\beta}\,, \tag{3.66}$$

where Σ_d, Σ_u are radiative corrections. From (3.66) we see that getting the correct value for M_Z relies on the interplay between μ, m_{H_u} and Σ_u. The naturalness criterion [30] states that these parameters should be in the order of the EWSB scale to avoid the need for substantial cancellation between the free parameters of the SUSY theory or "finetunning".
Moreover, the dominant contribution to Σ_u comes from stops. By noting that

$$\Sigma_u|_{stop} = -\frac{3y_t^2}{8\pi^2}(m_{Q_3}^2 + m_{U_3}^2 + |A_t|^2)\log\left(\frac{M_{SUSY}}{\text{TeV}}\right)\,, \tag{3.67}$$

and imposing that the amount of finetunning is less than 1% [31](quantified by the Barbieri-Giudice measure [32]), we can get a upper limit on the value of the stop masses and mixing:

$$(m_{Q_3}^2 + m_{U_3}^2 + |A_t|^2) \lesssim (3700\text{ GeV})^2 \log\left(\frac{M_{SUSY}}{\text{TeV}}\right)^{-1}\,. \tag{3.68}$$

The gluino contribution to Σ_u [31]

$$\Sigma_u|_{M_3} = -\frac{2y_t^2}{\pi^3}\alpha_s|M_3|^2\log^2\left(\frac{M_{SUSY}}{\text{TeV}}\right) \tag{3.69}$$

can also be sizable and in the same way than for stops it provides an upper bound, this time to the gluino mass:

$$|M_3| \lesssim 8500\text{ GeV}\cdot\log\left(\frac{M_{SUSY}}{\text{TeV}}\right)^{-1}\,. \tag{3.70}$$

By the same requirement on finetunning we get that $|\mu| \lesssim 645$ GeV . All the other SUSY particles can be very heavy. Although the amount of finetunning that is considered "natural" varies among the literature, the naturalness requirement gives an idea about how the spectrum of the natural MSSM looks like in broad terms. We have found that for the MSSM to be natural we need relatively light stops, moderately light gluinos and a not so large μ.
For the MSSM there is an extra fact to consider. In order to get the correct Higgs mass, loop contributions play a big role as at tree level $m_h^2 < m_Z|cos(2\beta)|$ [19]. These contributions would come mainly from stops and look like

$$\delta m_h^2 = \frac{3G_F}{\sqrt{2}\pi^2}m_t^4\left(\log\left(\frac{M_S^2}{m_t^2}\right) + \frac{X_t^2}{M_S^2}\left(1-\frac{X_t^2}{12M_S^2}\right)\right) \tag{3.71}$$

with M_S the average stop mass and $X_t = A_t - \mu\text{cot}(\beta)$. Getting the correct Higgs mass requires (in the case of $X_t = \sqrt{6}M_S^2$ where the contribution (3.71) is maximized) at least $m_{\tilde{t}}^2 \approx O(500 - 800\text{GeV})$ [33]. So there is an interplay between the amount of finetunning allowed and the prediction of the correct Higgs mass in the MSSM. This is an interesting fact that we will explore in the context of vacuum stability in section 5.2.

[5] similar relations hold in the general case [30]. However this simplifies the discussion without loss of generality.

3.9. Constrained Minimal supersymmetric standard model

One of the most popular SUSY models for phenomenological studies has been the so-called constrained MSSM or CMSSM. For this model we take the MSSM as our basic framework and add mSUGRA inspired unification of the soft SUSY breaking masses and trilinear couplings at a certain GUT scale, where gauge couplings also unify.

Following (3.55) we will assume that there is a common $f_a = f$ for the three gauginos, that $k_i^j = k\,\delta_i^j$ and $n_i^j = n\,\delta_i^j$ are the same for all scalars (with k and n real) , and that the other couplings are proportional to the corresponding superpotential parameters, so that $y^{Xijk} = \alpha y^{ijk}$ and $\mu^{Xij} = \beta\mu^{ij}$ (with universal real dimensionless constants α and β).This will give us

$$m_0^2 = m_{H_d}^2 = m_{H_u}^2 \tag{3.72}$$

$$m_0^2\mathbf{1} = m_D^2 = m_U^2 = m_Q^2 = m_E^2 = m_L^2, \tag{3.73}$$

$$M_{1/2} = M_1 = M_2 = M_3 = M_{\tilde{B}'}. \tag{3.74}$$

$$T_i = A_i Y_i = A_0 Y_i, \qquad i = e, d, u\ . \tag{3.75}$$

Thus for this model each point in parameter space is characterized by only 5 parameters:

$$M_0,\ M_{1/2},\ A_0,\ \tan\beta,\ \mathrm{sign}(\mu). \tag{3.76}$$

After values for these parameters are set at the GUT scale, it is then possible to obtain the SUSY spectrum at a lower scale through the MSSM renormalization group equations. This of course is very convenient for scans over parameter space, which might be one of the reasons why it is so popular. The CMSSM is a model with many assumptions but at the same time surprisingly predictive and rich in its phenomenology. Although thought to be one of the best bets for SUSY because of these reasons, it currently faces big challenges to accommodate present experimental results [34, 35].

Throughout this work we will build on other phenomenological studies on the CMSSM by bringing an extra source for constraints: Vacuum stability. It turns out that understanding when sfermions with electric and color charge get VEVs can further constraint the available parameter space for this model.

3.10. B-L extended Minimal supersymmetric standard model

The BLSSM is an extension of the MSSM by adding an extra $U(1)_{B-L}$ gauge group. It arises from the idea of including $B - L$ as conserved charge by promoting the associated $U(1)$ global symmetry to a local one.

There are several ways to extend the MSSM by $U(1)_{B-L}$. The BLSSM is the minimal extension which allows for a spontaneously broken $U(1)_{B-L}$ without necessarily breaking R-parity. This requires the addition of two SM gauge-singlet chiral superfields $(\hat{\eta}, \hat{\bar{\eta}})$ carrying $B - L$ which may develop VEVs thus breaking $U(1)_{B-L}$ without breaking R-parity. In order to have neutrino masses it is also necessary to introduce three generations of superfields containing right-handed neutrinos.

Superfield	Spin 0	Spin $\frac{1}{2}$	Generations	$U(1)_Y \otimes SU(2)_L \otimes SU(3)_C \otimes U(1)_{B-L}$
$\hat{Q}$	$\tilde{Q}$	Q	3	$(\frac{1}{6}, \mathbf{2}, \mathbf{3}, \frac{1}{6})$
$\hat{d}^c$	$\tilde{d}^c$	d^c	3	$(\frac{1}{3}, \mathbf{1}, \overline{\mathbf{3}}, -\frac{1}{6})$
$\hat{u}^c$	$\tilde{u}^c$	u^c	3	$(-\frac{2}{3}, \mathbf{1}, \overline{\mathbf{3}}, -\frac{1}{6})$
$\hat{L}$	$\tilde{L}$	L	3	$(-\frac{1}{2}, \mathbf{2}, \mathbf{1}, -\frac{1}{2})$
$\hat{e}^c$	$\tilde{e}^c$	e^c	3	$(1, \mathbf{1}, \mathbf{1}, \frac{1}{2})$
$\hat{\nu}^c$	$\tilde{\nu}^c$	ν^c	3	$(0, \mathbf{1}, \mathbf{1}, \frac{1}{2})$
$\hat{H}_d$	H_d	$\tilde{H}_d$	1	$(-\frac{1}{2}, \mathbf{2}, \mathbf{1}, 0)$
$\hat{H}_u$	H_u	$\tilde{H}_u$	1	$(\frac{1}{2}, \mathbf{2}, \mathbf{1}, 0)$
$\hat{\eta}$	η	$\tilde{\eta}$	1	$(0, \mathbf{1}, \mathbf{1}, -1)$
$\hat{\bar{\eta}}$	$\bar{\eta}$	$\tilde{\bar{\eta}}$	1	$(0, \mathbf{1}, \mathbf{1}, 1)$

Table 3.2.: Chiral superfields and their quantum numbers in the BLSSM. We include a factor of $\frac{1}{2}$ in the $U(1)_{B-L}$ charge with respect to the usual definitions of baryon and lepton number so that the bilepton fields have unit charges.

3.10.0.2. Particle content and superpotential

Although a straightforward extension of the MSSM, the BLSSM has a rich phenomenology. It introduces a Z' boson (with prospects for the LHC discussed in [36]), neutrinos with masses given through a type-I seesaw mechanism, several dark matter candidates with respect to the MSSM [37], and a rich Higgs boson sector [38].

In many of the previous studies of this model it is assumed that R-parity is conserved. This is just a consequence of the fact that it was constructed precisely so that even after breaking the $U(1)_{B-L}$ symmetry spontaneously R-parity would be conserved.

However, this fact relies on the strong assumption that it is only the new added gauge-singlet scalars $\tilde{\eta}, \tilde{\bar{\eta}}$ (with $\mathcal{P}_R = 1$) which get VEVs. This does not necessarily need to be the case, and it is this fact on which we will focus in our following considerations. We will be interested in the cases when the scalar partners of right-handed neutrinos get VEVs instead. If the sneutrinos develop VEVs, R-parity is automatically broken and the introduction of η and $\bar{\eta}$ is not justified anymore. Several aspects of the phenomenology of the spontaneous breaking of R-parity are discussed in [39, 40].

The issue of finding when sneutrinos break R-parity through VEVs will be explored in detail in chapter 5.4, where we will study how frequently and where in parameter space this happens.

The model consists of three generations of matter particles including right-handed neutrinos which can be embedded in $SO(10)$ 16-plets [41]. For convenience, we will refer to their scalar components as R-sneutrinos. Moreover, below the GUT scale the usual MSSM Higgs doublets are present, as well as the two fields η and $\bar{\eta}$.

Furthermore, the presence of η allows us to write terms that generate Majorana masses for the right-handed neutrinos when η gets a VEV. In order to write those terms η must carry twice the lepton number of (anti-)neutrinos. This leads us to interpret the $B - L$ charge of this field as its lepton number (likewise for $\bar{\eta}$), and call these fields bileptons. in Tab. 3.2 we summarize the quantum numbers of the chiral superfields under $U(1)_Y \times SU(2)_L \times SU(3)_C \times U(1)_{B-L}$.

The superpotential for the BLSSM is given by

$$\begin{aligned} W =& Y_u^{ij}\,\hat{u}_i^c\,\hat{Q}_j\,\hat{H}_u\, - Y_d^{ij}\,\hat{d}_i^c\,\hat{Q}_j\,\hat{H}_d\, - Y_e^{ij}\,\hat{e}_i^c\,\hat{L}_j\,\hat{H}_d\, + \mu\,\hat{H}_u\,\hat{H}_d \\ & \boldsymbol{+Y_\nu^{ij}\,\hat{\nu}_i^c\,\hat{L}_j\,\hat{H}_u\, - \mu'\,\hat{\eta}\,\hat{\bar{\eta}}\, + Y_x^{ij}\,\hat{\nu}_i^c\,\hat{\eta}\,\hat{\nu}_j^c}\,, \end{aligned} \tag{3.77}$$

where we show in bold the terms not present in the MSSM, and we have the additional soft SUSY-breaking terms:

$$\begin{aligned} \mathcal{L}_{SB} =& \mathcal{L}_{MSSM} - m_\eta^2|\eta|^2 - m_{\bar{\eta}}^2|\bar{\eta}|^2 - m_{\nu^c,ij}^2(\tilde{\nu}_i^c)^*\tilde{\nu}_j^c \\ & + \left(T_\nu^{ij}H_u\tilde{\nu}_i^c\tilde{L}_j + T_x^{ij}\eta\tilde{\nu}_i^c\tilde{\nu}_j^c - \lambda_{\tilde{B}}\lambda_{\tilde{B}'}M_{BB'} - \frac{1}{2}\lambda_{\tilde{B}'}\lambda_{\tilde{B}'}M_{B'} - \eta\bar{\eta}B_{\mu'} + c.c\right), \end{aligned} \tag{3.78}$$

with i, j being the generation indices. The extended gauge group breaks to $SU(3)_C \otimes U(1)_{EM}$ when the Higgs fields and bileptons receive vacuum expectation values (VEVs):

$$H_d^0 = \frac{1}{\sqrt{2}}\left(v_d + \sigma_d + i\phi_d\right), \qquad H_u^0 = \frac{1}{\sqrt{2}}\left(v_u + \sigma_u + i\phi_u\right), \tag{3.79}$$

$$\eta = \frac{1}{\sqrt{2}}\left(v_\eta + \sigma_\eta + i\phi_\eta\right), \qquad \bar{\eta} = \frac{1}{\sqrt{2}}\left(v_{\bar{\eta}} + \sigma_{\bar{\eta}} + i\phi_{\bar{\eta}}\right). \tag{3.80}$$

We define $\tan\beta' = v_\eta/v_{\bar{\eta}}$ as we do for the ratio of the MSSM VEVs ($\tan\beta = v_u/v_d$).
As we will explore later in detail, for certain parameter combinations a spontaneous breakdown of R-parity can also occur as sneutrinos can obtain non-vanishing VEVs [42]. We will denote the VEVs for the sneutrinos of the $SU(2)_L$ doublets $\tilde{L}_i$ by $v_{L,i}$ and those of the $SU(2)_L$ singlet sneutrinos $\tilde{\nu}_i^c$ by $v_{R,i}$, with $i = 1, 2, 3$.

3.10.0.3. GUT unification for the BLSSM

As we did for the MSSM, we will consider minimal supergravity inspired breaking of SUSY with GUT unification. Explicitly we implement the following unification prescription:

$$m_0^2 = m_{H_d}^2 = m_{H_u}^2 = m_\eta^2 = m_{\bar{\eta}}^2, \tag{3.81}$$

$$m_0^2\mathbf{1} = m_D^2 = m_U^2 = m_Q^2 = m_E^2 = m_L^2 = m_{\tilde{\nu}^c}^2, \tag{3.82}$$

$$M_{1/2} = M_1 = M_2 = M_3 = M_{\tilde{B}'}. \tag{3.83}$$

In the same way we assume the ordinary mSUGRA-inspired conditions for the trilinear soft SUSY-breaking couplings

$$T_i = A_0 Y_i, \qquad i = e, d, u, x, \nu\,. \tag{3.84}$$

We also assume that there are no off-diagonal gauge couplings or gaugino mass parameters at the GUT scale, allowing for the possibility of both $U(1)_{B-L}$ and $U(1)_Y$ to be a remnant of a larger product group broken at that scale [43].
We will also consider the mass of the Z', $\tan\beta'$ and the sign of μ' as inputs and use the following set of parameters to describe the constrained BLSSM:

$$M_0,\ M_{1/2},\ A_0,\ \tan\beta,\ \tan\beta',\ \mathrm{sign}(\mu),\ \mathrm{sign}(\mu'),\ m_{Z'},\ Y_x \text{ and } Y_\nu. \tag{3.85}$$

Y_ν is constrained by neutrino data and has to be very small in comparison to the other couplings in this model (as required by the embedded seesaw mechanism) so we will take $Y_\nu^{ij} = 10^{-5}\delta^{ij}$ as its precise structure will not affect our results in section 5.4. As Y_x can always be taken diagonal and we effectively have a total of 9 free parameters and 2 signs. In the following we will refer to this constrained version of the BLSSM as the CBLSSM. A complete review of its mass spectrum can be found in [43].

In general, picking a set of GUT-scale parameters is very unlikely to result in a potential with a phenomenologically acceptable minimum. The usual strategy adopted in spectrum generators like `SPheno` [44, 45] (and others, such as `ISAJET` [46], `SOFTSUSY` [47] and `SUSPECT` [48]) is to fix some for example $\mu, B_\mu, \mu', B_{\mu'}$ by demanding that the minimization conditions are satisfied for the VEVs given as input (they are given indirectly, by specifying $m_Z, \tan\beta, m_{Z'}, \tan\beta'$).

Unfortunately, this procedure only ensures that the input VEVs are an extremum of the scalar potential. There is no reason for these VEVs to be the global minimum and one should find all the possible solutions to the minimization conditions to be able to find it. This will be the starting point of our analysis in 5.4.

CHAPTER FOUR

VACUUM STABILITY OF SUSY MODELS

For SUSY models the main efforts for discovery have been centered around collider physics, where direct detection has been a realistic possibility since LEP II. In this sense most studies focus in the prediction of different signals emerging from the presence of SUSY particles in production and decay processes and in constraining the parameter space of different theories using the latest experimental results.

It is the main focus of this work to study a set of phenomenological constraints that aim to complement constraints coming from this type of studies. The vacuum structure of the potential for SUSY theories can provide complementary constraints by requiring a global minimum (or metastable local minimum) of the scalar potential in agreement with experimental facts.

A big part of the phenomenological success of the standard model relies on the spontaneous symmetry breaking mechanism triggered by the vacuum expectation value (VEV) of the scalar field of the theory, the Higgs boson. As we saw in section 2.1.3 this symmetry breaking works as the Higgs boson generates new $SU(2)_L$ breaking interactions by getting a VEV. In this particular case we want this symmetry to be broken in order to be able to write mass terms for particles we know from experiment are massive. However, let us consider for a moment that the Higgs Boson is not the only scalar of a theory. In this case, there is nothing forbidding these scalar particles to get VEVs and for any gauge group under which these particles are charged the corresponding symmetry will be broken. We know very well from experiments that we want to maintain certain gauge symmetries which to the best of our knowledge are unbroken. In this sense any theory that would make phenomenological sense will conserve $U(1)_{EM}$ (charge) and $SU(3)_C$ (color) gauge symmetries, so if we would like to add any scalar particles we have to be sure that this is the case and the fields allowed non zero VEVs are singlets under the gauge groups we want to conserve.

This is specially true with SUSY theories. As we saw in the section 3.6 even for the minimal SUSY theory we can think of we need to introduce not only an extra Higgs $SU(2)_L$ doublet (giving rise to charged Higgs scalar particles) but also a plethora of scalar fields, the partners of all the observed fermionic particles. This partners will be charged under $U(1)_{EM}$ or $U(1)_{EM} \otimes SU(3)_C$ and are not exempt of getting VEVs.

4.1. Previous attempts at avoiding color- and charge- breaking minima

The issue of short-lived DSB minima in SUSY models has been known for some time [49–56]. One of the main challenges of vacuum stability lies in the fact that beyond tree level, the problem becomes computationally expensive. Given the nature of the effective potential and the tunneling time calculation it is also very difficult to find general analytical rules to exclude a parameter point safely. However, thumb rules and analytical equations attacking the problem at tree level are simple enough that even when inaccurate they can be very convenient and gain some traction as a way of handling the vacuum stability problem.
In the following we will present a short overview of what we consider are the most popular ways of addressing vacuum stability in phenomenological studies and how some of these thumb rules and analytical conditions are derived. Later in this work we will put the conditions to test by comparing them to the numerical results of our framework in sections 5.1 and 5.2.
The scalar potential for the MSSM is given by equation (3.65). Let us assume for the moment that only a subset of the scalar particles can get VEVs. Then using the previous expression for V^{tree}, and allowing only $H_d = v_d/\sqrt{2}, H_u = v_u/\sqrt{2}, \tilde{\tau}_L = v_{L3}/\sqrt{2}, \tilde{\tau}_R = v_{E3}/\sqrt{2}$ to get VEVs we can explicitly write the tree level potential after setting all the other fields to zero as:

$$\begin{aligned} V^{\text{tree}}_{H_d,H_u,\tilde{\tau}_L,\tilde{\tau}_R}\Big|_{\phi_i=0} &= \frac{1}{32}\left(g_1^2(v_d^2 - v_u^2 + v_{L3}^2 - 2v_{E3}^2)^2 + g_2^2(v_d^2 - v_u^2 - v_{L3}^2)^2\right) \\ &+\frac{1}{4}Y_\tau^2\left(v_d^2 v_{L3}^2 + v_d^2 v_{E3}^2 + v_{L3}^2 v_{E3}^2\right) + \frac{Y_\tau}{\sqrt{2}} v_{L3} v_{E3}\left(A_\tau v_d - \mu v_u\right) \\ &-B_\mu v_d v_u + \frac{1}{2}\left(|\mu|^2(v_d^2 + v_u^2) + m_{H_d}^2 v_d^2 + m_{H_u}^2 v_u^2 + m_{\tilde{\tau}_L}^2 v_{L3}^2 + m_{\tilde{\tau}_R}^2 v_{E3}^2\right) \end{aligned} \tag{4.1}$$

Previous studies relied in manipulating the tree level potential and finding analytical conditions involving free parameters that would try to avoid dangerous directions, i.e parameter combinations that would give a potential with minima with unwanted VEVs. These conditions work in extreme cases as best, but at least offer some hindsight.
The most popular condition relies on assumptions made about the ratios of VEVs at color- and charge- breaking (CCB) minima. If one keeps the ratios of scalar fields constant to each other, it is possible to find specific directions in field configuration space that are at danger of CCB minima. Then that strong assumption will allow us to simplify the scalar potential and write it as a function of composite variables, which would thus be much more treatable.
Consider as an example that we take the stau and stop fields to be equal to the down-type Higgs so that $H_d = \tilde{\tau}_L = \tilde{\tau}_R$, and all other fields taken to be zero.
Along such directions we can write the potential as depending on a single variable, like the normalized magnitude of the VEVs.
D-term contributions to the potential can be thought to have a "stabilizing" effect which we can understand by noting as we did in section 3.7 that they are always positive. So if we are able to find certain directions in field space, where these D-term contributions vanish, we can try to avoid them and hope to also avoid potential unwanted minima. One can then solve the one-dimensional problem of minimizing the potential along these directions and compare it to the DSB minimum.
Let us write the potential projected along one of these directions:

$$V^{\text{tree}} = \frac{m^2}{2}v^2 - \frac{YA}{3}v^3 + \frac{Y^2}{4}v^4 \tag{4.2}$$

where v is the (scaled) length of the vector of field values. This is minimized either when $v = 0$ and $V^{\text{tree}} = 0$ or when [1]

$$v = v_{CCB} = \frac{A + \sqrt{A^2 - 4m^2}}{2Y} \tag{4.3}$$

We know that for the DSB minimum the tree level potential is < 0. Then if we can find a way of ensuring that at the CCB minimum the potential is always positive, we can find conditions on the parameters that would avoid that particular CCB vacuum from being the global minumum of V^{tree}.
Plugging v_{CCB} into V_{tree} and demanding a positive value independent of the sign of A and noting that the dependence on Y comes as an overall factor we get that

$$m^2 > \frac{2}{9}A^2. \tag{4.4}$$

This method for finding conditions gives rise to several particular cases, depending on which relations between the VEVs are assumed. Let us see some of the special cases.
One of the simplest directions along which the D-terms of eq. (4.1) vanish is the direction where H_u is taken to be 0, and $H_d = \tilde{\tau}_L = \tilde{\tau}_R = 3^{-1/4}v$, where the factor of $3^{-1/4}$ keeps the quartic term correctly normalized when casting the potential in the form of eq. (4.2). This in turn implies that in eq. (4.4) $m^2 = (m_{H_d}^2 + |\mu|^2 + m_{\tilde{\tau}_L}^2 + m_{\tilde{\tau}_R}^2)/\sqrt{3}$ and $A = 2^{-1/2}3^{1/4}A_\tau$.
This particular case has been widely used in the literature as a safeguard against CCB minima [49–52, 54]. The condition for stau VEVs looks like

$$A_\tau^2 < 3(m_{H_d}^2 + |\mu|^2 + m_{\tilde{\tau}_L}^2 + m_{\tilde{\tau}_R}^2) \tag{4.5}$$

and conversely the analogous condition for stop VEVs

$$A_t^2 < 3(m_{H_u}^2 + |\mu|^2 + m_{\tilde{t}_L}^2 + m_{\tilde{t}_R}^2)\,. \tag{4.6}$$

In [53] a slightly improved set of conditions were given. For the first generation they take a similar form as above:

$$A_u^2 < 3(m_{H_u}^2 + m_{\tilde{u}_L}^2 + m_{\tilde{u}_R}^2)\,. \tag{4.7}$$

As in this case there are no large Yukawa couplings involved, we can exchange the masses for the GUT scale parameters of the CMSSM [57]

$$(A_0 - 0.5M_{1/2})^2 < 9M_0^2 + 2.67M_{1/2}^2. \tag{4.8}$$

The only case where this condition might have a hope of working is when only VEVs for the first two generation sfermions are allowed. In this case the Yukawa couplings are much smaller than the gauge couplings and then the approximation made above makes sense. The moment we allow VEVs for the stops or staus when $\tan\beta$ is large the validity of the condition is not so sure anymore. However, it is worth examining how well such conditions do for the third generation, as in that case the expressions are considerably more complicated and a numerical approach is usually necessary to get reasonable results.

[1] The case $v_{CCB} = \frac{A-\sqrt{A^2-4m^2}}{2Y}$ is a maximum of the potential.

So when we refer to condition (4.7), we will assume it is valid for the the stops, explicitly written as

$$A_t^2 < 3(m_{H_u}^2 + m_{\tilde{t}_L}^2 + m_{\tilde{t}_R}^2). \tag{4.9}$$

An algorithm to isolate CCB minima of the tree level potential assuming vanishing (color) D-terms and either only stau or only stop VEVs was presented in [53]. The authors assumed that $\tan\beta = \frac{v_u}{v_d} > 1$ holds even at the CCB minimum, while we will show in the next chapters that this is not always the case. In fact we will see often that $\tan\beta < 1$ holds at the global minimum for points with stop VEVs.

Another different algorithm was presented in [58] for $\tan\beta \to \infty$. The algorithm only provides a conservative upper bound on $|A_t|$ so that there is no minimum of the tree level potential when H_u, $\tilde{t}_L$, and $\tilde{t}_R$ are allowed to have VEVs.

However, as we will see when we apply our framework, the limit of large $\tan\beta$ is characterized by *stau* VEVs without stop VEVs for the CMSSM, so we can already guess that the condition does not perform so well.

For simplicity, rather than implement the full numerical algorithm, we will study the condition

$$A_t^2 < (0.65 - 0.85)^2(3(m_{\tilde{t}_1}^2 + m_{\tilde{t}_2}^2 + 2m_t^2)) \tag{4.10}$$

where we have chosen 0.65 from the point where the CCB condition diverges from the tachyonic stop line in figure 1 of [58] to 0.85 as being close to the maximal allowed value from the optimal bound considered by them.

It is no surprise that these conditions do not perform well and are neither necessary nor sufficient to guarantee the absence of panic vacua, even before considering the one-loop effective potential [59, 60].

For conditions like (4.4) it is true that if satisfied, there will not be any deeper undesired minimum along that particular direction in field space. At the same time the fact that we are able to exclude minima along particular directions, does not exclude the fact that other deeper minima might appear in any other direction not protected by such type of conditions. Similarly there could be an undesired minimum along this direction that has a negative tree level potential value but not quite as negative as that of the DSB vacuum, thus forbidden by the condition but actually allowed.

The temporary hints for an enhanced di-photon decay rate of the Higgs Boson in 2012 revived the interest in charge-breaking minima. This was the case since in the MSSM the only way to explain such enhancement without affecting the other decay channels relies on very light staus [61, 62]. In this context, new checks for charge-breaking minima due to stau VEVs were either derived or revived [55, 56].

As an example of the new checks implemented around this time we have

$$\begin{aligned} \mu\tan\beta &< 213.5\sqrt{m_{\tilde{\tau}_L} m_{\tilde{\tau}_R}} - 17.0(m_{\tilde{\tau}_L} + m_{\tilde{\tau}_R}) + 4.52\times 10^{-2}\ \text{GeV}^{-1}(m_{\tilde{\tau}_L} - m_{\tilde{\tau}_R})^2 \\ &\quad -1.30\times 10^4\ \text{GeV} \end{aligned} \tag{4.11}$$

$$\begin{aligned} |(Y_\tau v_u \mu)/(\sqrt{2}m_\tau)| &< 56.9\sqrt{m_{\tilde{\tau}_L} m_{\tilde{\tau}_R}} + 57.1(m_{\tilde{\tau}_L} + 1.03 m_{\tilde{\tau}_R}) - 1.28\times 10^4\ \text{GeV} \\ &\quad + \frac{1.67\times 10^6\ \text{GeV}^2}{m_{\tilde{\tau}_L} + m_{\tilde{\tau}_R}} - 6.41\times 10^6\ \text{GeV}^3\left(\frac{1}{m_{\tilde{\tau}_L}^2} + \frac{0.983}{m_{\tilde{\tau}_R}^2}\right) \end{aligned} \tag{4.12}$$

where m_τ is the tau mass. The condition given by (4.11) was obtained by a numerical fit of the

result of a scan to an ansatz in [55]. In the same way, condition (4.12) also comes from a fit of the results of a scan to an ansatz in [56]. The former presentation of the conditions comes from combining the definition of $\tan\beta_{\text{eff}}$ from eq. (4) in [56] with their condition (10).
Its worth noting that (4.11) and (4.12) were derived for the case that $A_\tau = 0$. As it is known that in the CMSSM one needs large, negative A_0 to get the correct Higgs mass through stop loops, we can also foresee that these conditions won't be very successful for that model.
It is one of the purposes of this work to test analytic conditions against our proposed framework, so we will be plotting in section 5 the lines between points which satisfy these conditions on top of the results coming from our framework.

4.2. Vacuum Stability as a phenomenological constraint

The question arises as to how to determine in a more complete way which fields get VEVs. From our experience with the standard model we know that this means we have to minimize the scalar potential of our theory. Even in the standard model, where the problem is trivial at tree level, the issue of minimizing the potential gets trickier when we include quantum corrections. The desired vacuum of the SM (with desired we refer to the minimum reproducing the correct masses and broken symmetries) is at best metastable as the Higgs quartic coupling λ can become negative at higher energies [63].
But in the case of SUSY models, the issue is more complex. Although it is possible to find parameter points that include the desired vacuum as one of the vacua of the scalar potential, one needs to find all the other minima to be sure the desired one is the deepest. Even at tree level, the minimization of the scalar potential is not a trivial task if we include extra scalar fields. Although at first glance the problem of finding the minima might seem a very basic mathematical challenge, it is certainly not. The minimization conditions or tadpole equations are in general degree three polynomials, and there is no analytical way to solve a general set of n coupled polynomial equations (where n is the number of scalars in out theory) of degree bigger than two. Once the effective potential is considered the issue becomes much more involved and finding the global minimum of a theory is a very difficult task. Add to that the fact that even if our desired minimum is not the global one it can still be metastable and we are in front of a very interesting challenge.
One of the main purposes of this work is to present the framework necessary to tackle this issue and use the vacuum structure of a model as a complementary phenomenological constraint. For this we will need to find all the minima of the tree level potential, study the effect of quantum corrections and calculate tunneling times between the candidate vacua, at zero and non-zero temperature.
We will summon several mathematical and numerical techniques, which working together will provide us with the necessary tools to approach this issue consistently. The resulting framework has been implemented in the code `Vevacious`, which we will discuss further in this chapter.

4.3. Vacuum stability analysis framework

Let us assume first that the model we intend to work with always has at least one minimum that reproduces the correct physical picture. We will call this minimum the desired symmetry breaking minimum or DSB for short.

Other minima which break symmetries we want to conserve, e.g. charge or color, might appear with the situation becoming dangerous if one of them is situated at a lower point in the potential. We will call these type of minima panic vacua.
The main idea is already clear: We want to first determine whether panic vacua exist and if they do we would like to know the tunneling probability between the deepest panic vacua and the DSB. An unstable DSB would lead to the exclusion of that particular parameter point. But how would we do this practically? We will assume that there is a model with many scalars that we want to constrain, and we know how to write the tree level and effective potential at one-loop. In addition, we will also assume that through a spectrum calculator a set of parameter points has been found such that the DSB minimum is one of the solutions to the minimization conditions. Then to assess the stability of the DSB vacuum we will:

- Find all the solutions to the tree level minimization conditions, i.e the minima of the tree level scalar potential.
- Assess in a first step whether panic vacua exist i.e. undesired symmetry breaking minima deeper than the DSB minimum.
- Use the tree level minima as starting points for a numerical minimization of the one-loop effective potential.
- Calculate the tunneling probability at zero temperature between the DSB minimum and the most likely panic vacuum by a straight path between them.
- If the DSB is still stable, recalculate the tunneling probability at non zero temperature assuming a straight path between them.
- If the DSB is still stable, recalculate the tunneling probability at zero temperature through the optimal tunneling path between vacua.
- If the DSB is still stable, perform the above step but at non zero temperature.
- Classify the parameter point according to the stability of the DSB minimum.

The main idea of the previous procedure is to exclude a parameter point with the least amount of work possible. In this sense, computationally expensive procedures like non zero temperature calculations and finding the optimal path for tunneling are left for cases where simpler procedures have not been able to find a short-lived DSB minimum.
In the following we will lay down the specifics of each step and the tools used to carry it out. We will talk about the subtleties involved and the most interesting technical details. Let us start first with the solution to the problem of finding the minima of the tree level potential.

4.3.1. The Homotopy continuation method

As mentioned above, the first issue we encounter when studying the vacuum structure of a model is the minimization of its scalar potential at tree level. One could approach this problem with numerical minimization routines or reducing the problem by allowing some free parameters to be varied in order to achieve the desired vacuum. Neither of this techniques guarantees that we will know all the other minima of our theory or whether these will be deeper than our phenomenological choice.

It is always possible to study the phenomenology of a model for which a desired vacuum is one of the solutions of the tadpole equations, but the relevance of the results gets lost if that engineered vacuum is not the global one and has an unacceptably short tunneling time to an unphysical minimum.
In conclusion, if we want to proceed further we need a way of finding all the solutions of the tadpole equations for a given model and parameter point.
The homotopy continuation method [64, 65] has found use in several areas of physics [66–68], in particular to find string theory vacua [69, 70] and extrema of extended Higgs sectors [71], where the authors investigated a system of two Higgs doublets with up to five singlet scalars in a general tree level potential.
A computational implementation of this method, the numerical polyhedral homotopy continuation, is a powerful way to find all the roots of a system of polynomial equations quickly [72].
While the method is described in detail in [64, 65] here we present a rather crude introduction as it is one of the main tools used in our subsequent phenomenological analysis of the vacuum structure of SUSY models.
Given two functions $f(x), g(x) \in Y$ with $x \in X$, a homotopy is defined as a continuous function

$$\mathrm{Hom} : X \otimes [0,1] \to Y \tag{4.13}$$

with $[0,1] \in \mathbb{R}$, which satisfies $\mathrm{Hom}\,(x,0) = f(x)$ and $\mathrm{Hom}\,(x,1) = g(x)$. Which is to say that there is a continuous function which can parametrize the deformation of f into g with a parameter that goes from 0 to 1.
The usefulness of this type of functions relies in the mathematical fact that under a Homotopy transformation between polynomials $P(x_1,\ldots,x_n)$ and $Q(x_1,\ldots,x_n)$, the roots of P move smoothly to the roots of Q, provided that both polynomials have the same Bézout bound (upper bound on the number of roots). As the reader might already note, this process is not injective. However, provided that P has the maximum number of different roots, it is guaranteed that we will find all the roots of Q.
Let's be more precise. Suppose we have a system of polynomial equations

$$P(x_1,\ldots,x_n) = \begin{pmatrix} p_1(x_1,\ldots,x_n) \\ \vdots \\ p_m(x_1,\ldots,x_n) \end{pmatrix} = 0 \tag{4.14}$$

which we know how to solve and has the same number of roots as its Bézout bound. Now suppose we have another set of polynomial equations

$$Q(x_1,\ldots,x_n) = \begin{pmatrix} q_1(x_1,\ldots,x_n) \\ \vdots \\ q_m(x_1,\ldots,x_n) \end{pmatrix} = 0 \tag{4.15}$$

for which we have no solution, so we know none of its roots. Then we can construct a homotopy between both systems

$$\mathrm{Hom}\,(x_1,\ldots,x_n,t) = P(x_1,\ldots,x_n)(1-t) + \gamma\, t\, Q(x_1,\ldots,x_n), \tag{4.16}$$

where γ can be in general a complex number. This is the simplest homotopy possible, a

linear homotopy. By construction it satisfies that $\mathrm{Hom}\,(0, x_1, \ldots, x_n) = P(x_1, \ldots, x_n)$ and $\mathrm{Hom}\,(1, x_1, \ldots, x_n) = Q(x_1, \ldots, x_n)$.
Then it is guaranteed that the solutions of $H(t, x_1, \ldots, x_n) = 0$ will construct continuous paths in $\mathbb{C}$ connecting the known roots of P with the unknown roots of Q. The starting system P can be chosen for example as

$$P(x_1, \ldots, x_n) = \begin{pmatrix} (x_1^{r_1} - 1) \\ \vdots \\ (x_n^{r_m} - 1) \end{pmatrix} = 0 \tag{4.17}$$

with r_i the degree of q_i. This guarantees that we have $\sum_{i=1}^{m} r_i$ discrete solutions. Finding the roots of Q means tracing the paths, which can be done numerically with any reasonable path tracing algorithm like the Euler predictor or Newton corrector methods. In this way it is guaranteed as well that we will find all the roots of Q, without explicitly solving the system of equations: In a sense we have gotten the solution without solving the problem. This is a very robust method and its efficacy relies in the properties of the homotopy transformation. A detailed proof of the method can be found in [64]. It is important to note that the method works on the assumption that Q has a finite number of solutions. If we want to use this method to find the extrema of the tree level potential, we have to be sure that all gauge degrees of freedom have been taken away and only a discrete number of solutions remain.

4.3.2. One-loop effective potential

Now that we have a tool to find all the minima of the tree level potential, we have to understand the role played by higher order effects. The usual approach when trying to understand symmetry breaking mechanisms and the minimization of the potential often avoid going beyond the tree level potential of the given theory. This is a good pedagogical approximation and it shares many analogies with more familiar problems. However, quantum effects do play an important role in modifying the potential of the theory and it is necessary to understand how to account for these effects.
A good way of understanding the role of higher order effects is through the effective potential. In short, the effective potential is what we get when higher order contributions are allowed for the couplings between the scalar particles of the theory. Schematically and at one-loop it is what results from including diagrams of the form

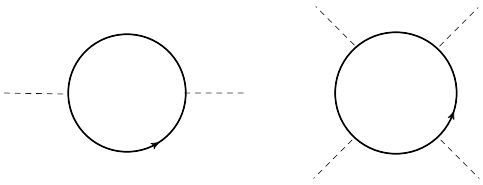

.

In order to calculate the effective potential at one-loop it is convenient to think in the path integral representation. For simplicity let's think about a scalar field theory. In that case the partition function (the generating functional of correlation functions) can be written as

$$Z = e^{iW(J)} = \int D\phi e^{i[S(\phi)+J\phi]} \quad \text{with} \quad J\phi = \int d^4x J(x)\phi(x). \tag{4.18}$$

This equation defines $W(J)$ which in turn yields all the connected green functions by the derivation with respect to $J(x)$ following

$$\langle G(x_1, x_2)\rangle = -\frac{\delta}{\delta J(x_1)}\frac{\delta}{\delta J(x_2)} iW(J)\bigg|_{J=0}. \tag{4.19}$$

We are interested in the vacuum of our theory. Let us first use the generating functional to get $\langle 0|\,\phi\,|0\rangle$ in the presence of the source J (not setting it yet to 0)

$$\langle 0|\,\phi\,|0\rangle = \phi_0 = \frac{\delta W(J)}{\delta J(x)} = \frac{1}{Z}\int D\phi e^{i[S(\phi)+J\phi]}\phi(x). \tag{4.20}$$

We would like to find the effective potential of our theory i.e. a quantity that is minimized at the vacuum of our theory. To do this we can now define a new functional $\Gamma(\phi_0)$ by a Legendre transformation

$$\Gamma(\phi_0) = W(J) - \int d^4x J(x)\phi_0(x), \tag{4.21}$$

where it is implied that J can be expressed as a function of ϕ_0 through equation (4.20). From (4.21) follows quite nicely that (this is the purpose of the Legendre transformation)

$$\frac{\delta\Gamma(\phi_0)}{\delta\phi_0(y)} = \int d^4x \frac{\delta J(x)}{\delta\phi_0(y)}\frac{\delta W(J)}{\delta J(x)} - \int d^4x \frac{\delta J(x)}{\delta\phi_0(y)}\phi_0(x) - J(y) = -J(y). \tag{4.22}$$

This leaves us with the "dual" relations $\frac{\delta\Gamma(\phi_0)}{\delta\phi_0(y)} = -J(y)$ and $\frac{\delta W(J)}{\delta J(x)} = \phi_0$. Now we are close to finding the explicit form of the effective potential. Without loss of generality we can parametrize Γ as

$$\Gamma(\phi_0) = \int d^4x[-P(\phi_0) + Q(\phi_0)(\partial\phi_0)^2 + R(\phi_0)(\partial\phi_0)^4 + ...]. \tag{4.23}$$

A very reasonable assumption is for ϕ_0 to not depend on x. This would make our vacuum translation invariant which is something we want. In this particular case we can write (4.21) and (4.23) in the following form

$$\Gamma(\phi_0) = \int d^4x[-P] \quad \rightarrow \quad \frac{\delta\Gamma(\phi_0)}{\delta\phi_0(y)} = -P'(\phi_0) = -J(y), \tag{4.24}$$

as in the path integral representation the sources J are mathematical tools and non-physical, we always want to set them to zero at the end. Doing this we find the familiar equation

$$-P'(\phi_0) = 0, \tag{4.25}$$

with ϕ_0 now being the VEV of ϕ in the absence of the source. So the vacuum of our theory is determined by finding the minima of P, much in the same way that for our classical theory we find the vacuum by minimizing the potential V. So P is nothing else than the effective potential and we will therefore call it V_{eff} from now on.
We will be interested in the first order quantum fluctuations of the potential, in other words we would like to work with the one-loop effective potential. The first step is to explicitly evaluate

$W[J]$. In general this is a very difficult task, but if we look at (4.18) but this time explicitly writing $\hbar$,

$$Z = e^{iW(J)} = \int D\phi e^{\frac{i}{\hbar}\int d^4x[\mathcal{L}(\phi)+J(x)\phi(x)]}, \tag{4.26}$$

it is easy to see that due to the smallness of $\hbar$ the exponential is dominated by small values of the integrand, so we can use the steepest descent approximation safely. First we expand around the minimum of the integrand, let's call it ϕ_s, so that $\phi = \phi_s + \tilde{\phi}$. This minimum ϕ_s is easy to find, as it is the solution to the Euler-Lagrange equations with an additional term for $J(x)$, that is

$$\partial^2\phi_s(x) + V'[\phi_s(x)] = J(x). \tag{4.27}$$

Using $\phi = \phi_s + \tilde{\phi}$ and expanding $W(J)$ we get

$$W(J) = S(\phi_s) + \int d^4x[J(x)\phi_s(x)] + \frac{i\hbar}{2}Tr\log(\partial^2 + V''(\phi_s)) + \mathcal{O}(\hbar^2). \tag{4.28}$$

The trace goes over the space of scalar fields on which the differential operator $(\partial^2 + V''(\phi))$ acts. From (4.28) we can note that at leading order $\phi_0 = \phi_s$, which is not really a big surprise as this is in fact how we define it when thinking in terms of the classical potential. Now assuming again that ϕ_0 does not depend on x, we can write

$$Tr\log(\partial^2 + V''(\phi_s)) = \int d^4x \int \frac{d^4k}{(2\pi)^4}\log[-k^2 + V''(\phi_s)]. \tag{4.29}$$

Putting all the pieces together we can write now the effective potential as:

$$V_{eff}(\phi) = V(\phi) - \frac{i\hbar}{2}\int d^4x \int \frac{d^4k}{(2\pi)^4}\log[\frac{k^2 - V''(\phi_s)}{k^2}] + \mathcal{O}(\hbar^2). \tag{4.30}$$

We have added an unphysical constant to make the logarithm dimensionless. As the attentive reader might notice, the spacetime integral in (4.30) diverges quadratically. This of course a sign that we have not renormalized the effective potential yet. The final result will depend of course on the specific theory at play and the renormalization conditions imposed. This expression is commonly referred as the Coleman-Weinberg potential [73] as it was first derived by the authors for the special case of QED with a ϕ^4 interaction. We show the explicit formulas for the MSSM and the BLSSM in the $\overline{DR}$ scheme in appendix A.

4.4. Tunneling out of the DSB vacuum at $T = 0$

In QFT the fact that we are in a local minimum of the potential does not guarantee its stability as in the classical case. If there are other minima that lie deeper along the potential, the possibility of tunneling due to quantum fluctuations opens. When treating the issue of undesired minima in the potential of theories with many scalars, this will play a big role.
While a local minimum reproducing the physics we observe might exist, it could be that a very high tunneling probability makes it unviable. Conversely, even if there are deeper unphysical minima, if the desired local minimum has a sufficiently long lifetime it can still be phenomenologically viable. So we need to answer the question as to how to determine the specifics of such process.

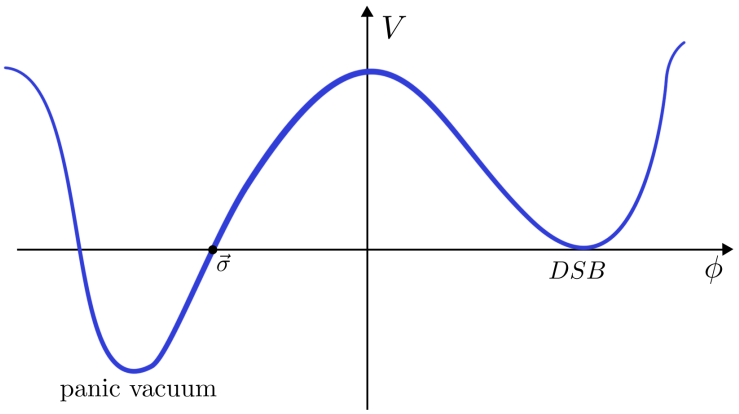

Figure 4.1.: A potential with two minima, a DSB with the wanted symmetry breaking and a deeper panic vacuum which we want to avoid.

Let us think first about the one-dimensional problem of a single scalar field with Lagrangian density

$$\mathcal{L} = \frac{1}{2}\partial_\mu \partial^\mu - V(\phi). \tag{4.31}$$

The explicit form of V is not relevant but let us assume it has two minima, a DSB minimum with the correct phenomenology and a deeper panic vacuum to which tunneling from the DSB is possible.
In the classical problem both minima are stable equilibrium points of the theory. However quantum effects can induce a tunneling making the transition possible. A schematic picture of how V looks is found in figure 4.1.
The way such tunneling would happen is in close analogy with the boiling of superheated fluids from which much of the jargon is usually borrowed [74, 75]. In this case the role of thermodynamic fluctuations will be played by quantum ones, but the picture is essentially the same. These fluctuations will cause bubbles of panic vacuum to appear, however once in a while a bubble will form with enough size so that it is energetically favorable for it to keep growing. Eventually this bubble would replace everything until the system has transitioned to the panic vacuum.
As the underlying process is essentially the same, we can very quickly understand that what we want to calculate is the probability of such bubble appearing per unit volume $\Gamma/\mathcal{V}$. In this case Γ stands for the vacuum decay width. The question is now how to calculate such expression. The complete problem is extremely complicated, however it is possible to get an answer in a semiclassical approach. Following closely the work in [74, 75] we have that

$$\Gamma/\mathcal{V} = Ae^{(-B/\hbar)}(1 + \mathcal{O}(\hbar)) = Ae^{-S_4}, \tag{4.32}$$

where B is the bounce action which we will define in the following and A is a quantity of energy dimension four, which is related to the ratio of eigenfunctions of the determinants of the action's second functional derivative.
The A factor is typically estimated on dimensional grounds as it is extremely difficult to compute. However the estimation is sufficient in most cases provided we have calculated the bounce action accurately. This is because changes in B have a stronger effect due to it being inside the

exponential. In practice one could take for example $A \approx Q^4$ where Q is the renormalization scale.

4.4.0.1. The bounce action: A semiclassical approximation

In the semiclassical approximation of a particle with a potential V with position vector $\vec{q}$ and Lagrangian

$$\mathcal{L} = \frac{1}{2}\dot{\vec{q}} \cdot \dot{\vec{q}} - V(\vec{q}), \tag{4.33}$$

one can see the tunneling as the particle penetrating the potential barrier and materializing at a scape point $\vec{\sigma}$ (shown in figure 4.1 for the one dimensional case) with zero kinetic energy, after which it just propagates classically. The width of this process will be in the form of (4.32) and B in this case will be expressed as [76]

$$B = 2\int_{DSB}^{\vec{\sigma}} ds\sqrt{2V}, \tag{4.34}$$

where $(ds)^2 = d\vec{q} \cdot d\vec{q}$. Usually there is a whole region of possible scape points $\vec{\sigma}$ thus we will perform the above integral along the path of minimum resistance (the one minimizing B) satisfying

$$\partial \int_{DSB}^{\vec{\sigma}} ds\sqrt{2V} = 0. \tag{4.35}$$

We can cast the problem in a more familiar way by noting that the variational problem (4.35) is solved by the equations

$$\frac{d^2\vec{q}}{d\tau^2} = \frac{\partial V}{\partial \vec{q}} \tag{4.36}$$

$$\text{with} \quad \frac{1}{2}\frac{d\vec{q}}{d\tau} \cdot \frac{1}{2}\frac{d\vec{q}}{d\tau} - V = 0. \tag{4.37}$$

We can then see that the problem is analogous to that of the solving the Euler Lagrange equation of the imaginary-time ($\tau = it$) version of Hamilton's principle applied to the " Euclidean " Lagrangian

$$\mathcal{L}_E = \frac{1}{2}\frac{d\vec{q}}{d\tau} \cdot \frac{d\vec{q}}{d\tau} + V. \tag{4.38}$$

Using equation (4.37) and noting that the DSB minimum can only be reached asymptotically as $\tau \to -\infty$, one can then arrive at the equation

$$\int_{DSB}^{\vec{\sigma}} ds\sqrt{2V} = \int_{-\infty}^{0} d\tau \mathcal{L}_E. \tag{4.39}$$

Moreover, noting the fact that the problem is symmetric under time reversal, we could also write the previous equation as

$$B = 2\int_{DSB}^{\vec{\sigma}} ds\sqrt{2V} = \int_{-\infty}^{\infty} d\tau \mathcal{L}_E. \tag{4.40}$$

So schematically we can think B to be a " bounce " as in this casting it is analogous to the particle going from the DSB to $\vec{\sigma}$ and back in the Euclidean problem.

4.4.0.2. Tunneling in QFT

It does not take a lot of effort to translate this procedure to the analogous problem in field theory. The equation of motion for the Euclidean Lagrangian in this case is given by

$$\frac{\partial V(\phi)}{\partial \phi} = \left(\frac{\partial^2}{\partial \tau^2} + \nabla^2\right)\phi \tag{4.41}$$

with the boundary conditions

$$\lim_{\tau \to \pm\infty} \phi(\tau, \vec{x}) = DSB, \qquad \frac{\partial \phi}{\partial \tau}(0, \vec{x}) = 0, \tag{4.42}$$

and the bounce action is given by

$$B = \int d\tau\, d^3x \left[\frac{1}{2}\left(\frac{\partial \phi}{\partial \tau}\right) + \frac{1}{2}\left(\vec{\nabla}\phi\right)^2 + V\right]. \tag{4.43}$$

If we are to follow the analogy with thermodynamics, then we can guess that the solutions will be expanding bubbles and therefore will exhibit $O(4)$ symmetry. If we assume that ϕ only depends on the radial coordinate ρ with $\rho^2 = |\vec{x}|^2 + \tau^2$ then we can rewrite the Euler-Lagrange equations as:

$$\frac{d^2\vec{\phi}}{d^2\rho} + \frac{3}{\rho}\frac{d\vec{\phi}}{d\rho} = \nabla V(\vec{\phi}). \tag{4.44}$$

It has been proven that any solution with $\phi \neq \phi(\rho)$ will always lead to a higher bounce action [77] so we can see how our guess is well founded. Assuming we have found a candidate path in field space parametrized by $\phi = \phi(t)$, these equations can be split in two parts, one parallel and one perpendicular to the path:

$$\frac{d^2t}{d\rho^2} + \frac{3}{\rho}\frac{dt}{d\rho} = \frac{\partial}{\partial t} V[\vec{\phi}(t)] \tag{4.45}$$

$$\frac{d^2\vec{\phi}}{dt^2}\left(\frac{dt}{d\rho}\right)^2 = \nabla_\perp V(\vec{\phi}). \tag{4.46}$$

The first of these equations can be solved by the so called overshoot undershoot method. There it is easier to think of the problem as that of a particle moving with potential $-V$ (along the path) and an extra particular friction term if we see ϕ as the spatial coordinate. Then the solution of the problem will be to find how to place the particle close from the panic vacuum so that it rolls down the potential and stops precisely at the DSB minimum (see figure 4.2).
We can then start by trying certain position close to the panic vacuum and see what happens. If the particle goes over the DSB minimum then we place the particle a bit below along the inverted potential. If the particle does not quite reach the DSB minimum we place it some distance above along the potential. Iterating this process we can then find the point where the particle will stop at the DSB minimum at $\rho = \infty$ to an arbitrary precision.

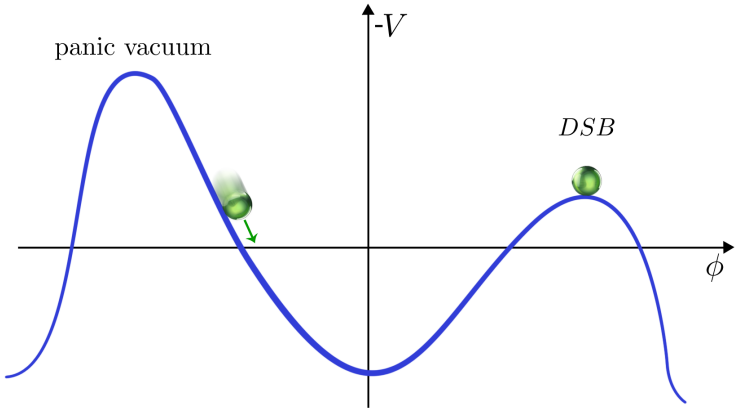

Figure 4.2.: The equations parallel to a chosen path in field space can be thought of as the classical equations of a particle rolling on the inverted potential when taking x as time and ϕ as the spatial variable. The solution will be the point from which the particle will roll and stop exactly at the DSB minimum.

Once we found the initial condition that satisfies this, by integrating (4.45) we can find $\phi(t(\rho))$, i.e. the field ϕ as a function of ρ. This will describe the candidate solution of the equations of motion for the critical bubble triggering the vacuum decay from the DSB minimum to the panic vacuum. If we have selected the appropriate path $\phi(t)$ for this, then $\phi(\rho)$ will also satisfy (4.46). Of course this is not the case for any arbitrary path chosen. The trick clearly is to find the right path. Continuing with the particle analogy, we can think the first equation as determining the forces parallel to chosen path and the second one as the one determining the normal force that the path exerts on the particle so that the particle moves along it, $N = \frac{d^2\vec{\phi}}{dx^2}\left(\frac{dx}{d\rho}\right)^2 - \nabla_\perp V(\vec{\phi})$. Then given an initial path that solves (4.45) but not (4.46) we can always deform it in the direction of N so that eventually the path with $N = 0$ is found. It is easier to start with a straight line and implement the previous procedure to find the path that solves the equations of motion, and therefore the path that minimizes the tunneling time between the minima. A schematic drawing of how such deformations will look like is shown in figure 4.3.
Unfortunately, this means that to calculate the tunneling time from the DSB to the panic vacuum, one needs to evaluate the potential along a continuous path through the field configuration space, and even though the extrema of the potential are gauge-invariant, the paths between them are not. However, it has been proved that at zero temperature, the gauge dependence at one-loop order cancels out [78].
At finite temperature, the situation is not so clear, though the Landau gauge may be most appropriate [79]. We will then perform finite temperature calculations in that gauge. Some studies have shown that for "reasonable" choices of gauge, the differences in finite-temperature tunneling times are small [80], it is however still possible to choose poor gauges that can even obscure the possibility of tunneling [81].

4.5. When the temperature is not zero

Usually when thinking about the physics around us we think about a Universe with temperature close to zero. This has not always been the case and to study the thermal history of the Universe

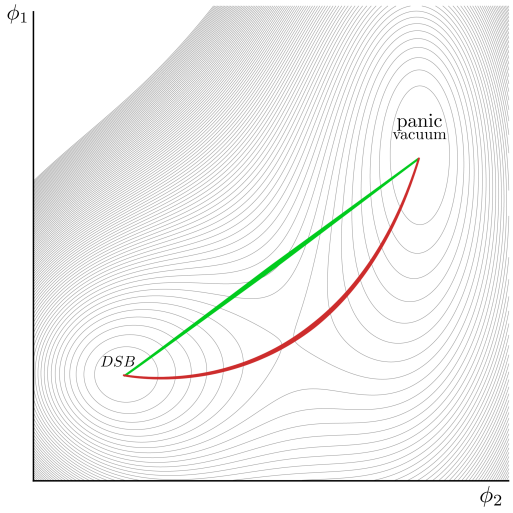

Figure 4.3.: The initial guess for a path in field space is just a straight line between vacua (green). The optimal path for tunneling (red curved) is found by deforming the first guess by the normal force applied on a particle moving under the inverted potential.

we have to obviously part from that assumption.

During the cooling of the Universe after the Big Bang, thermal effects played a big role. Tunneling could have been triggered not only by quantum fluctuations, but thermodynamic ones as well. The potential itself depends on temperature thus finding the optimal temperature at which tunneling might be triggered (with higher probability than at $T = 0$), has to do with the interplay between the modifications to the potential and the increase of thermodynamic fluctuations. Schematically the probability of tunneling between vacua can be reduced as walls between different minima get smaller at higher temperature and the relative depth between them also changes.

4.5.0.3. A glimpse at thermal QFT

As we just mentioned, finite temperature tunneling will not only be triggered by quantum fluctuations as when $T \neq 0$ thermodynamic effects start playing a role. In order to study the tunneling probability in such scenario one has to describe the process through thermal QFT.

First of all, the idea of including temperature in our analysis means that the expectation value of an operator in a thermal ensemble

$$\langle A \rangle = \frac{\mathrm{Tr}\left[\exp(-\beta H) A\right]}{\mathrm{Tr}\left[\exp(-\beta H)\right]}, \tag{4.47}$$

can be written as a calculation in an Euclidean QFT with periodicity in the imaginary time coordinate with period $\beta = \frac{1}{T}$.

Let us see this explicitly in the case of field theory. Consider the two point correlation function of a field ϕ at non-zero temperature

$$\begin{aligned}
\langle\phi(x,t)\,\phi(y,0)\rangle_\beta &= \frac{1}{Z}\mathrm{Tr}[e^{-\beta H}\phi(x,t)\,\phi(y,0)] && (4.48)\\
&= \frac{1}{Z}\mathrm{Tr}[\phi(x,t)e^{-\beta H}\,e^{\beta H}\phi(y,0)e^{-\beta H}] && (4.49)\\
&= \frac{1}{Z}\mathrm{Tr}[\phi(x,t)e^{-\beta H}\,\phi(y,-i\beta)] && (4.50)\\
&= \frac{1}{Z}\mathrm{Tr}[e^{-\beta H}\,\phi(y,-i\beta)\phi(x,t)] && (4.51)\\
&= \langle\phi(y,-i\beta)\,\phi(x,t)\rangle_\beta\,, && (4.52)
\end{aligned}$$

where we used the cyclic permutation invariance of the trace. One can see there that if we rewrite the above result in euclidean QFT with imaginary time $\tau = it$ we get

$$\langle\phi(x,\tau)\,\phi(y,0)\rangle_\beta = \langle\phi(y,\beta)\,\phi(x,\tau)\rangle_\beta\,. \tag{4.53}$$

This is called the Kubo-Martin-Schwinger relation (KMS for short). This relation imposes then that the fields obey the periodic condition

$$\phi(x,0) = \pm\phi(x,\beta), \tag{4.54}$$

with the sign depending on whether the fields correspond to fermionic or bosonic degrees of freedom.
At $T = 0$ we calculate the tunneling time assuming that the four-dimensional bounce action S_4 from equation (4.32) is the dominant contribution to the decay width of the false vacuum. However, for sufficiently high temperatures, the dominant contribution may come from solitons that are $O(3)$ cylindrical in Euclidean space rather than $O(4)$ spherical [82].
To see this consider the following: At T=0 the solution to (4.44) is manifestly O(4) symmetric as $\rho^2 = |\vec{x}|^2 + \tau^2$. If we now allow the temperature to be non-zero the solution will be forced to satisfy the periodicity condition in the τ direction. If r is the radius of the bubble solution at $T = 0$, for $T < 1/r$ the bubbles become a series of bubbles at a distance β from each other in the τ direction. If the temperature increases to $T \sim 1/r$ then the bubbles start to overlap. For temperatures $T \gg 1/r$ the bubbles merge into a $O(3)$ symmetric solution and the action S_4 has to be replaced with the action corresponding to the $O(3)$ symmetric solutions $\frac{1}{T}\,S_3$ as shown in figure 4.4. This comes from the fact that the new equation to solve at non zero temperature will be

$$\frac{d^2\vec{\phi}}{d^2\tilde{\rho}} + \frac{2}{\tilde{\rho}}\frac{d\vec{\phi}}{d\tilde{\rho}} = \nabla V(\vec{\phi}) \tag{4.55}$$

with $\tilde{\rho} = |\vec{x}|^2$.

4.5.0.4. Estimating survival probability of the DSB vacuum at $T \neq 0$

As we have seen, if the thermal contribution dominates, the expression for the decay width per unit volume $\Gamma/\mathcal{V}$ at a temperature T changes. For non-zero temperature we have to calculate now

$$\Gamma/\mathcal{V} = Ae^{-S_4} \rightarrow \Gamma(T)/\mathcal{V}(T) = A(T)e^{-S_3(T)/T}, \tag{4.56}$$

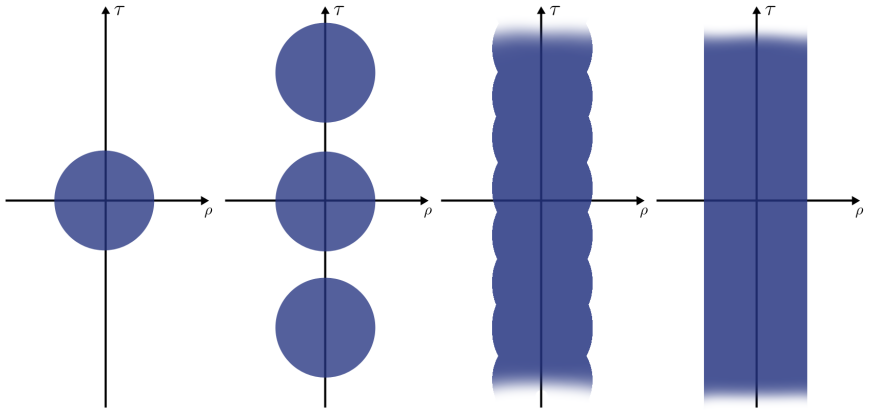

Figure 4.4.: I : Regions of non-vanishing solution for (4.44). II, III, and IV show regions of non-vanishing solution for (4.44) at $T < 1/r$, $T \sim 1/r$ and $T \gg 1/r$ respectively. The periodicity condition in the τ direction at non-zero temperature brings the $O(4)$ symmetric solutions to $O(3)$ symmetric ones. The x-axis represents the spacial components.

where $S_3(T)$ is now the bounce action integrated over three dimensions rather than four, with the integration over time simply replaced by division by temperature because of the constant value along the Euclidean time direction. The leading thermal corrections to the potential are at one loop, and given by [83]

$$\Delta V(T) = \sum T^4 J_{\pm}(m^2/T^2)/(2\pi^2) \tag{4.57}$$

where the sum is over all the degrees of freedom (i.e particles): bosons as sets of real scalars, fermions as sets of Weyl fermions, and

$$J_{\pm}(r) = \pm \int_0^{\infty} \mathrm{d}x\, x^2 \ln\left(1 \mp e^{-\sqrt{x^2+r}}\right) \tag{4.58}$$

with J_+ for a real bosonic degree of freedom and J_- for a Weyl fermion (We will use a slightly different convention as the one used in [83], for simplicity we will incorporate the negative sign into the definition of J_-). The thermal corrections will always lower the potential, although to a different degree depending on the value of m^2/T^2. This can be seen in figure 4.5 where we show the typical shape of $J_+(m^2/T^2)$ (the behavior of $J_-(m^2/T^2)$ is qualitatively similar).
The interesting quantity to look at in this case is the so-called survival probability, or the probability $P(T_i, T_f)$ of *NOT* tunneling between the time when the Universe is at temperature T_i and when it is at temperature $T_f < T_i$. We can write it explicitly as:

$$P(T_i, T_f) = \exp\left(-\int_{T_i}^{T_f} \frac{\mathrm{d}t}{\mathrm{d}T} \mathcal{V}(T) A(T) e^{-S_3(T)/T} \mathrm{d}T\right). \tag{4.59}$$

If we want to perform this calculation for a vast amount of parameter points we need to find a prescription to do so quickly. For these type of objects, even the numerical evaluation of the action is computationally expensive. While one could attempt the numerical integration of equation (4.59), it quickly becomes impractical for more than a handful of parameter points.

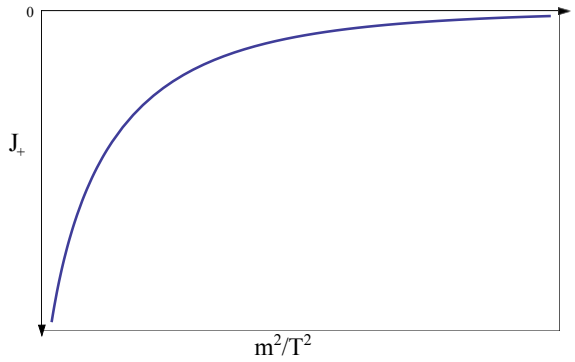

Figure 4.5.: Typical shape of $J_+(m^2/T^2)$. It shows that it asymptotically approaches zero as $m^2/T^2 \to \infty$ and also lowers the effective potential.

A solution we propose is to exclude parameter points based on an upper bound on the survival probability under some approximations in such way that $S_3(T)$ is to be evaluated only once. This is reasonable as the points we exclude will be definitely excluded, so the unwanted case of "false positives" (i.e falsely excluded points) is out of the question.

To achieve this let us first take the factor $A(T)$ to be T^4, as the evaluation of the eigenfunctions of the determinant is usually estimated on dimensional grounds due to its complication (the reasoning goes in the same direction as in the $T = 0$ case, however we use in this case T instead of Q). Any deviation would effectively contribute $\ln(AT^{-4})$ to $S_3(T)/T$, and as $S_3(T)/T$ is ~ 240 for survival probabilities that are not extremely close to zero or one, we can apply the same logic as in section 4.4.

The second set of assumptions we will make is that the Universe is radiation dominated during the evolution from T_i to T_f and that entropy is approximately conserved between T_i and today. Entropy conservation implies that $\mathcal{V}(T_0)/\mathcal{V}(T) = s(T)/s(T_0)$, where s is the entropy density and $T_0 = 2.73\,\mathrm{K}$ is the temperature of the Universe in the present. Moreover, during radiation domination we have [84]

$$H = \frac{\dot{a}}{a} = \frac{1}{M_{\mathrm{Planck}}}\sqrt{\frac{\pi^2 g_*(T)}{90}}T^2, \tag{4.60}$$

with M_{Planck} as the reduced Planck mass and $g_*(T)$ is the effective number of relativistic degrees of freedom at temperature T, H is the Hubble parameter and a is the scale factor of the FriedmannÐLemaîtreÐRobertsonÐWalker metric. Using the fact that in that regime we have $a \propto t^{1/2}$ leading to $H = 1/2t$ we then get

$$2t = \frac{1}{H} = M_{\mathrm{Planck}}\sqrt{\frac{90}{\pi^2 g_*(T)}}T^{-2}. \tag{4.61}$$

Taking then $\frac{\mathrm{d}}{\mathrm{d}T}$ and ignoring the T dependence of g_* (the effective degrees of freedom change slowly with temperature), we are left with

$$\mathrm{d}t/\mathrm{d}T = -M_{\mathrm{Planck}}\sqrt{\frac{90}{\pi^2 g_*(T)}}T^{-3}. \tag{4.62}$$

Using this result in (4.59) we get:

$$\frac{\mathrm{d}t}{\mathrm{d}T}\mathcal{V}(T) = -M_{\mathrm{Planck}}\sqrt{90/(\pi^2 g_*(T))}T^{-3}\mathcal{V}(T_0)\frac{s(T_0)}{s(T)}\,. \tag{4.63}$$

To further simplify our expression we then use the fact that for a Universe with 68.3% Dark Energy and 31.7% non-relativistic matter, the volume of the observable Universe using the co-moving horizon as boundary is

$$\mathcal{V}(T_0) = 141.4(H(T_0))^{-3} = (3.597\times 10^{42}/\ \mathrm{GeV})^3, \tag{4.64}$$

where $H(T_0) = 0.68\times 100\,\mathrm{km}(\mathrm{s\,Mpc})^{-1}$. By noting that the present value of relativistic degrees of freedom is $g_*(T_0) = 43/11$, we can also use the relationship

$$s(T_0)/s(T) = \frac{g_*(T_0)T_0^3}{g_*(T)T^3} = \frac{43}{11}\frac{T_0^3}{g_*(T)T^3}. \tag{4.65}$$

The question now is what value to take for $g_*(T)$. The tunneling is assumed to be dominated at a temperature where all degrees of freedom of the SM are taken to be relativistic, while non-SM particles are assumed to be still non-relativistic. This is a reasonable assumption as for temperatures above the SUSY scale, where the SUSY degrees of freedom become relativistic, the thermal contributions are likely to make the tunneling less probable. As thermal contributions to the masses are proportional to the temperature and always positive [83], if $T \simeq M_{SUSY}$ then the thermal contribution to the masses at the panic vacuum will be positive and $O(M_{SUSY})$ therefore diminishing the CCB minimum depth and making tunneling less likely. In this sense we would like to consider tunneling at $T < M_{SUSY}$, and in that case it would be sufficient to take the approximation that the only relevant relativistic degrees of freedom are coming from SM particles making $g_*(T) \equiv g_{*SM}(T) = 106.75$.

Putting it all together, we find that

$$\begin{aligned}&\int_{T_i}^{T_f}\frac{\mathrm{d}t}{\mathrm{d}T}\mathcal{V}(T)A(T)e^{-S_3(T)/T}\mathrm{d}T\\ &\simeq 1.581\times 10^{106}\ \mathrm{GeV}\int_{T_f}^{T_i}T^{-2}e^{-S_3(T)/T}\mathrm{d}T.\end{aligned} \tag{4.66}$$

As we pointed out, the evaluation of $S_3(T)$ is computationally expensive. One way of avoiding a continuous evaluation of the action is to make the reasonable assumption that it is a monotonically increasing function of T. As the magnitudes of the field values increase along the path from the DSB to the CCB vacuum, the field dependent masses that enter the effective potential increase (ignoring occasional cancellations). Thus thermal contributions will lower the effective potential *less* near the panic vacuum than near the DSB vacuum, hence *increasing* T leads to the absolute height of the energy barrier decreasing but the barrier height relative to the false vacuum, which is the important quantity, *increases*, and thus $S_3(T)$ increases. Using this assumption we get

$$\begin{aligned}\int_{T_f}^{T_i} T^{-2} e^{-S_3(T)/T} \mathrm{d}T &> \int_{T_f}^{T_i} T^{-2} e^{-S_3(T_i)/T} \mathrm{d}T \\ &= (e^{-S_3(T_i)/T_i} - e^{-S_3(T_i)/T_f})/S_3(T_i)\end{aligned} \tag{4.67}$$

$$\int_0^{T_i} T^{-2} e^{-S_3(T)/T} \mathrm{d}T > e^{-S_3(T_i)/T_i}/S_3(T_i). \tag{4.68}$$

Given this,

$$\begin{aligned}P(T_i = T, T_f = 0) &< \exp\big(-1.581 \times 10^{106}\ \mathrm{GeV} \\ &\qquad \times e^{-S_3(T)/T}/S_3(T)\big) \\ &= \exp\left(-\exp[244.53 - S_3(T)/T - \ln(S_3(T)/\ \mathrm{GeV})]\right)\end{aligned} \tag{4.69}$$

and all that remains is to find the optimal $T = T_{\mathrm{opt}}$ (the one that maximizes this quantity) to find an upper bound on the survival probability $P(T_i = T_{\mathrm{opt}}, T_f = 0)$ for the DSB vacuum. Hence if we can choose T_{opt} before attempting to calculate $S_3(T_{\mathrm{opt}})$, we only need to make one evaluation of $S_3(T_{\mathrm{opt}})$.
The evaluation of the three-dimensional bounce action along a straight path in "field space" from the false vacuum to the true vacuum, denoted $S_3^{\mathrm{straight}}(T)$, is much quicker to calculate than searching for the optimal path, so for each parameter point $S_3^{\mathrm{straight}}(T)$ can instead be calculated for a set of temperatures between the temperature at which the DSB vacuum evaporates and the critical temperature T_{crit} at which tunneling to the CCB minimum becomes impossible. $S_3^{\mathrm{straight}}(T)$ can then fitted as $(T_{\mathrm{crit}} - T)^{-2}$ times a polynomial in T, since the action should diverge as $(T_{\mathrm{crit}} - T)^{-2}$ as T approaches T_{crit} [85, 86]. This fitted function can then be numerically minimized to estimate the value of $T = T_{\mathrm{opt}}$ which minimizes $P(T_i = T_{\mathrm{opt}}, T_f = 0)$. This can then be used to evaluate the right-hand side of eq. (4.69), taken as the upper bound on the survival probability of the false vacuum.
The estimated optimal T_{opt} can be used to evaluate $S_3(T_{\mathrm{opt}})$ properly, along the correct tunneling path (by the procedure described in 4.4.0.2) between the CCB vacuum at temperature T_{opt} (which can be found by gradient-based minimization of the full one-loop thermal potential starting from the minimum at $T = 0$) and the "DSB vacuum at T_{opt}" (where gradient-based minimization starting from the position of the DSB vacuum at $T = 0$ will end up). Above the evaporation temperature, this should be the field origin, and indeed we will see this was the case for each parameter point in our analysis.

4.6. `Vevacious`

The software package `Vevacious` was developed to address the vacuum stability issue. It implements the framework we laid down in the previous sections by interfacing several tools with the specifics of our prescription. It requires a model file and a parameter point as inputs. It is written in C ++ and `Python` and it uses several available tools. The Homotopy continuation method is implemented using `HOM4PS2` [87], the numerical minimization uses the `Python` implementation of the `MINUIT` algorithm and the tunneling calculation at zero and non-zero temperature uses code

written originally for CosmoTransitions [88].
A careful description of Vevacious code escapes the purpose of this work. However the reader might consult the published manual [89] and access http://vevacious.hepforge.org/ where the latest version and a quick start guide might be downloaded. Nevertheless, we will lay down Vevacious's procedure and explain some of the details about the specific implementation of our prescription.

4.6.1. Objectives

The typical use would be as an extra phenomenological constraint in a parameter scan for a single model. The main effort has to be put in creating the model file, although it is possible to do it automatically with SARAH relatively straightforwardly. A set of popular model files is provided and the number of available ready-to-use models will increase with time.
Once the model file is given, the user can provide parameter points in the form of files in the *SUSY* Les Houches Accord (SLHA) format 1 [90] or 2 [91]. Even though the SLHA is used as the format, the model itself does not need to be supersymmetric, as long as the SLHA file contains appropriate BLOCKs.
Depending on the options, accuracy of the tunneling time and complication of the model, each point should be evaluated within a matter of seconds.
Once the model file and parameter point are provided, Vevacious determines the deepest panic vacuum in field space and gives a verdict on whether the input minimum is absolutely stable, or metastable. The user decides where to put the threshold for judging whether metastability is rated as long-lived or short-lived.
The main idea is to exclude a point as soon as we are able, so the path deformation and non-zero temperature procedures are considered after faster methods of exclusion have already been tried. So if a point is found by the first estimations to decay faster than the user given threshold the point is excluded and Vevacious finishes.

4.6.2. Outline

Here we lay down the steps taken by Vevacious, which are schematically shown in figure 4.6.

(1) An input file in the SLHA format is read to obtain the Lagrangian parameters defining the parameter point, required to evaluate the potential.

(2) *All* the extrema of the tree level potential are found using the homotopy continuation method to solve the tree level minimization conditions. The publicly available program HOM4PS2 [72] is used for this.

(3) The tree level extrema are used as starting points for gradient-based minimization of the one-loop effective potential. The MINUIT algorithms [92] are used here through PyMinuit [93], its Python incarnation. By default, PyMinuit is restricted to field configurations where each field is only allowed to get VEVs less than or equal to one hundred times the renormalization scale specified in the SLHA file. This can be modified as it was considered better to allow the user to decide whether the results of Vevacious are within a trustworthy region or not.

(4) The minima are then sorted and depending on the settings it calculates the tunneling time from the DSB vacuum to the panic vacuum. The bounce action is then calculated with

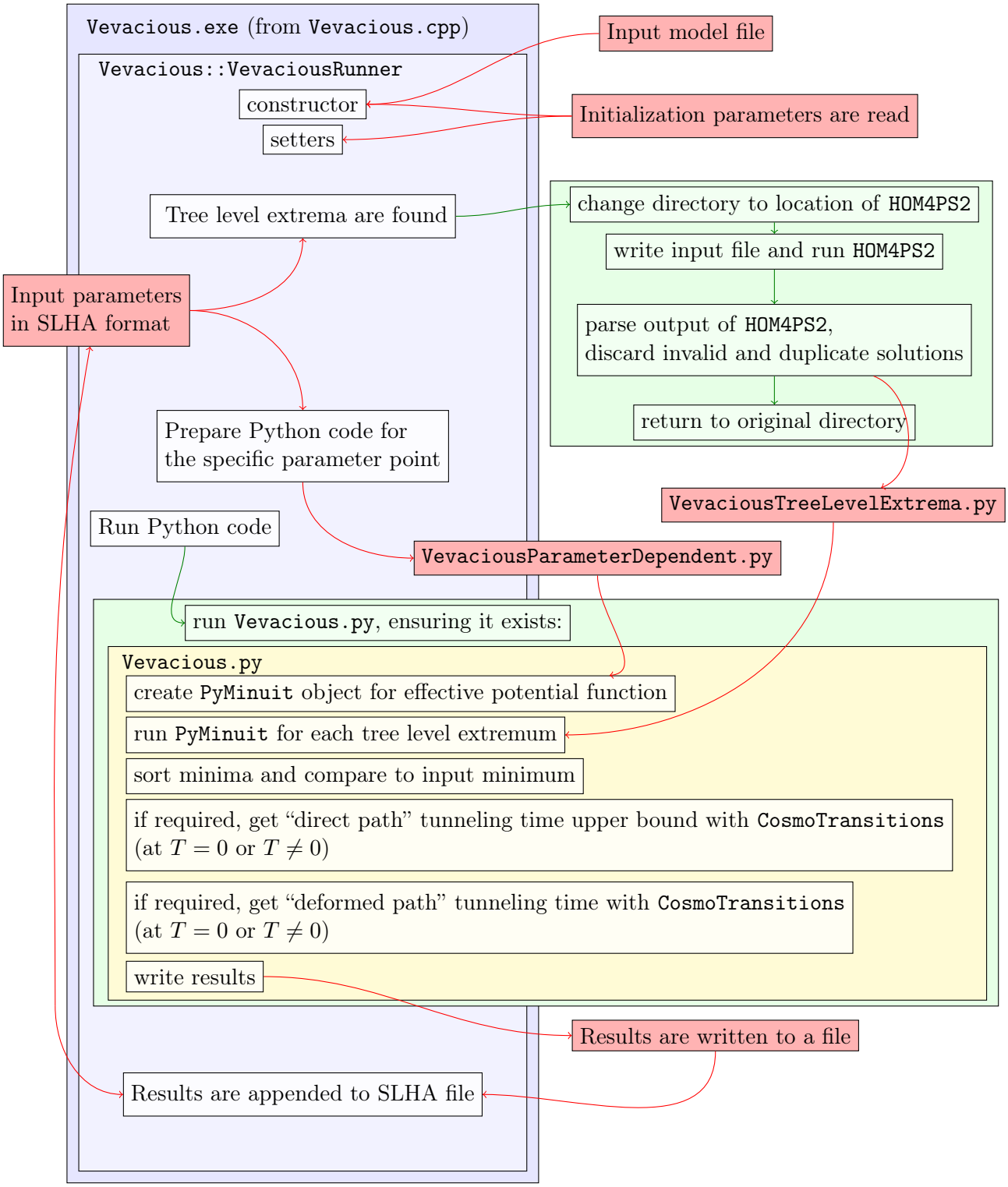

Figure 4.6.: Simplified `Vevacious` flow diagram. A complete version can be found in [89] for $T = 0$. The member functions of `VevaciousRunner` are shown from top to bottom in the order in which they are called by `Vevacious.exe`, as can be seen by looking into the `Vevacious.cpp` source file.

the code CosmoTransitions [88]. To save time, CosmoTransitions routines are called to calculate the bounce action with a straight path in field space from the DSB vacuum to the panic vacuum to get an upper bound on the tunneling time. If this upper bound is below the user-given threshold no refinement is pursued. If, however, the upper bound is above the threshold, the bounce action is calculated again allowing CosmoTransitions to deform the path in field configuration space. If the point is still reported to be long-lived, then the same procedure is carried out for the $T \neq 0$ case.

(5) The results are then given in a result file and also appended to the SLHA input file.

4.6.3. Features

Finds all tree level extrema. As discussed in section 4.13, the homotopy continuation method is guaranteed to find all the solutions of the system of minimization conditions up to the precision of the machine used to carry out the calculation [64]. One does not have to worry that there may be solutions just beyond the range of a scan looking for the solutions.

Rolls to one-loop minima. Vevacious rolls from the tree level extrema to the minima of the one-loop effective potential before comparing them, because in general the VEVs get shifted. In addition, the way the numerical minimization works allows us to catch extrema that change their nature at the one-loop level, such as the minimum with zero VEVs in the famous Coleman–Weinberg model of radiative spontaneous symmetry breaking [73], which is a minimum of the tree level potential but a local maximum of the one-loop effective potential.

Speed. An important aspect of the framework we propose, and therefore Vevacious, is that it is fast enough to be implemented as a systematic phenomenological constraint in parameter scans of interesting models. As an example, on a laptop with a 2.4 GHz processor, a parameter point for the MSSM allowing non-zero VEVs for both Higgs, two stau and two stop, it can report within 3.2 seconds that no deeper vacuum than the DSB vacuum was found. For a different parameter point it reports an upper bound on the tunneling time in 18 seconds. Although this is the case for typical parameter points, borderline cases which require a full calculation of the minimal bounce action can take up to 500 seconds. Reducing the number of degrees of freedom to four can improve the speed dramatically.

Flexible. Vevacious has been written in a way that should allow useful customizations with small changes to the source code. For example, one can change a single line in the code so that the tree level potential is used for the analysis rather than the one-loop effective potential and no further changes are necessary. The implementation allows non-trivial changes without forcing the user to go very deep into the code, though it does rely on the user learning some Python to be able to do so.

4.6.4. Limitations

Vevacious relies heavily in numerical procedures and their convergence. At the same time it does take a significant amount of assumptions to simplify the problem at hand. It is then important

to have a clear understanding of its limitations and what it does and does not do. In this section we discuss some of these issues and how to approach them.

May be excessively optimistic about the region of validity. By default, `Vevacious` allows VEVs to have values up to a hundred times the renormalization scale, and it is up to the user to decide whether any given set of results is meaningful and within the region of validity of the one-loop effective potential used. However, it is straightforward to change the allowed region to a smaller multiple of the renormalization scale.

Not guaranteed to find minima induced purely by radiative effects. While `Vevacious` does find all the extrema of the tree level effective potential, there is no guarantee that these correspond to all the minima of the effective potential at the one-loop level. The strategy adopted by `Vevacious` will find all the minima of the one-loop effective potential that are reachable with numerical minimization by rolling of the tree level minima. However any minima that develop which can't be reached in the same fashion will not be found. Although not typical, such potentials are not impossible. In the same example of the Coleman-Weinberg [73], if the quadratic coefficient of the potential is small but positive, the single tree level minimum can remain a minimum at the one-loop level while deeper minima induced by radiative corrections alone might appear.

Extreme slow-down with too many degrees of freedom. The running time for `Vevacious` increases worse than linearly with the number of fields that are allowed to have non-zero VEVs. Some typical running times for the `HOM4PS2` part on the same 2.4 GHz core mentioned before are:

- 3 fields allowed non zero VEVs: 0.03 seconds
- 5 fields allowed non zero VEVs: 0.28 seconds
- 7 fields allowed non zero VEVs: 5.1 seconds
- 10 fields allowed non zero VEVs: 20 minutes
- 15 fields allowed non zero VEVs: 10 days.

The `PyMinuit` minimization takes usually several seconds. The `CosmoTransitions` part is strongly dependent on the details of a particular potential and the path deformation procedure. Models with the same amount of allowed non-zero VEVs can vary wildly depending on the particular properties of the potential.

Homotopy continuation method: Discrete extrema and path tracking resolution. Although very powerful, the homotopy continuation method relies on tracking paths connecting discrete solutions. There is no guarantee that the method will work in systems with a continuous set of solutions. `Vevacious` does not check if there are redundant degrees of freedom, like for example the ones related to gauge transformations. The user is trusted to pick the appropriate degrees of freedom. There is also the danger that a finite-precision path-tracking algorithm will accidentally start following a path very close to the one it is following and get to a different solution. This might lead to one or more solutions not being found in extreme cases [64].

CHAPTER FIVE

RESULTS

We will now apply the developed framework through the use of `Vevacious` for three examples. We will first explore the vacuum structure of the CMSSM and see whether the existence of charge- and color- breaking minima might help constrain its parameter space. We will then explore what happens when thermal fluctuations come into play for the natural MSSM and learn from the trends observed in the CMSSM where to look for regions where vacuum stability can complement existing constraints. Lastly we will study the case of R-parity violation in the CBLSSM through sneutrinos getting VEVs. Along the way, we will compare our results with previous attempts at tackling the issue of deeper unphysical vacua and put them to test against our full numerical approach.

5.1. Charge- and color-breaking minima in the CMSSM at $T = 0$

As a first look onto the capabilities of vacuum stability as a phenomenological constraint, we will present the results of such analysis for a large parameter scan in the CMSSM. We will showcase our results in a twofold way, in a first step we will see what type of constraints in parameter space can be deduced when imposing stability constraints on the DSB minimum. Then we will compare how well previous attempts at including this type of constraints agree with our results.

5.1.1. Getting a feeling of the CMSSM parameter space

As we explained in section 3.9, the assumptions made regarding SUSY breaking for this model allow us to work with only a handful of parameters. This does not come for free and the unification of soft masses at the GUT scale induces relationships among the parameters at the SUSY scale (chosen as $\sqrt{m_{\tilde{t}_1} m_{\tilde{t}_2}}$).
The GUT scale constraints of the CMSSM broadly lead to fixed ratios of the gaugino masses at the SUSY scale, and groupings of the squark masses and slepton masses together respectively. The relationships between these masses and their groupings are controlled by $M_{1/2}$ for the gauginos and M_0 for the sfermions. We still have some freedom to change the spectrum through the tuning of A_0 and $\tan\beta$ which can allow us to separate out the third-generation sfermions from the other generations.

Surprisingly enough, the interplay between these few parameters is enough to explain a great deal of observations. The CMSSM offers several possibilities for dark matter and if we require that their relic density is within the uncertainties of the observed value, the viable CMSSM parameter space is significantly constrained [94]. However, by fixing one or two of the CMSSM parameters, there is always the possibility to find ranges of the other parameters which are consistent with the observations regarding this aspect [95]. For the so-called "stau coannihilation region" of parameter space, the stau is a little heavier than the lightest neutralino (the dark matter candidate) and freezes out only slightly earlier, making a fair amount of annihilation into SM particles before the neutralino freeze-out possible. This is convenient as in the CMSSM the relic density of the LSP tends to be higher than experimental results.
Another important phenomenological constraint is the consistency with the measured Higgs mass of ≈ 125 GeV. In the MSSM it is possible to be consistent with that value, although it certainly requires some degree of finetunning. In order to get the correct Higgs mass, we need at least one stop with a mass in the multi-TeV range [96–101]. An obvious way to force the CMSSM to comply with both constraints is through a sufficiently high M_0 (to get heavy enough stops) and a sufficiently high $M_{1/2}$ (to bring the mass of the lightest neutralino up to just below the lightest stau mass). This is of course not a bulletproof argument, as for sufficiently high masses, the stau coannihilation mechanism cannot reduce the relic density to the observed value, even for the case of degenerate stau and lightest neutralino masses [95, 102].
Although for high M_0 and $M_{1/2}$ we can accommodate some of the experimental results, that specific region of parameter space has a pretty bleak prospect for the discovery of SUSY particles at present experiments. The only other way that this can be achieved in the CMSSM is through large A_0. This induces a large splitting between the mass eigenstates of staus and stops. With this specific spectrum, the loop corrections to the Higgs mass can get large enough through the existence of a heavy stop and the large splitting between the stop mass eigenstates. Luckily such parameter points allow at least some potentially LHC-accessible sparticles [103].
As we have discussed along this work, the presence of many additional scalar partners for the SM fermions raises the question of whether they too could develop VEVs. We are interested in studying the specific case of stops and staus with non-zero VEVs. The existence of such vacuum will break spontaneously $SU(3)_c$ and $U(1)_{EM}$, and therefore color and electric charge.
Using `SPheno` [44, 45] as the spectrum generator and `Vevacious` as our tool to apply our proposed prescription we will show in the following how well the CMSSM does against charge- and color-breaking (CCB) minima. We will take the input values for the SM parameters to be used in `SPheno` as

$$\alpha^{-1}(M_Z) = 127.93,\ G_F = 1.166370 \cdot 10^{-5}\text{GeV}^{-2},\ \alpha_S = 0.1187,\ m_Z = 91.1887\text{ GeV},$$
$$m_b(m_b) = 4.18\text{ GeV},\ m_t = 173.5\text{ GeV},\ m_\tau = 1.7769\text{ GeV} \tag{5.1}$$

5.1.1.1. Dependence on which scalars are allowed non-zero VEVs

Most checks in literature for CCB minima allow for either stau or stop VEVs, but not both simultaneously. One of the first results coming from `Vevacious` is that it is not possible to treat them separately. In figure 5.1 we show the distribution of stable, long- and short-lived points in the (M_0, A_0)-plane for three cases: Only stau VEVs are allowed, only stop VEVs are allowed and both stop and stau VEVs are allowed. It is then very clear that overlaying cases with stop or stau VEVs does not reproduce the results of allowing both fields to get vacuum expectation values.

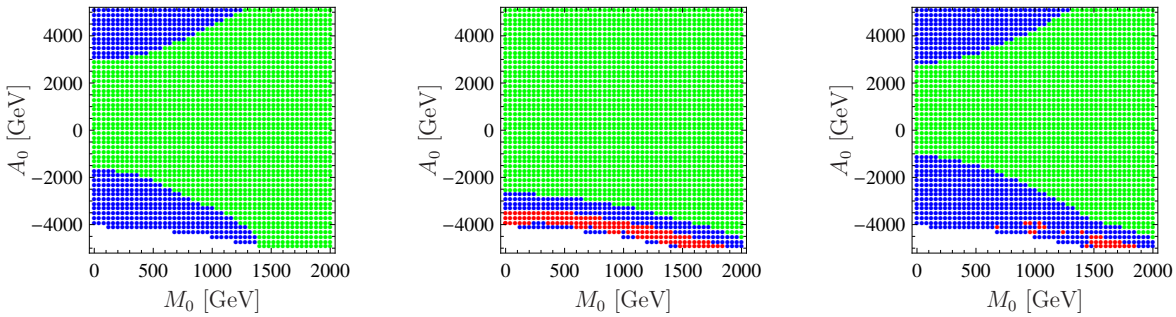

Figure 5.1.: Vacuum stability in the (M_0, A_0)-plane for input values of $\tan\beta = 10$, $M_{1/2} = 1$ TeV and $\mu > 0$. (Here and in the other figures, $\tan\beta$ is taken to mean the input parameter for the DSB vacuum.) On the left, we allow only for stau VEVs, in the middle only for stop VEVs and on the right for both stau and stop VEVs. Green indicates that no CCB minimum deeper than the DSB minimum was found, while blue and red indicate that the DSB minimum is only metastable, as there is at least one deeper CCB minimum. The red points are short-lived, while the blue points are long-lived, compared to a threshold of three gigayears. The lack of a smooth boundary between red and blue is a numerical artifact and is discussed in the text.

However, considering only the case with both stop and stau VEVs is not sufficient. Due to the fact that the path deformation step of our analysis depends strongly on the convergence of the deforming algorithm (which in turn depends on the structure of the potential), the optimal path calculated for the simpler single VEV cases produces shorter lifetimes for the DSB in some cases. In our particular analysis this is evident in the case of stop VEVs only, where more short-lived points are found than for the mixed case. Therefore in the CMSSM it is especially necessary to check carefully for all possible combinations for stau and stop VEVs. Just in the limit of large or small $\tan\beta$ checks for pure stau or stop VEV scenarios might be sufficient.

5.1.1.2. Scale and loop order dependence

Parameters like masses or cross-sections usually have a significant dependence on the scale when they are calculated at tree level. The dependence on the renormalization scale Q diminishes when higher order corrections are taken into account. As mentioned earlier, in our studies we will be taking $\sqrt{m_{\tilde{t}_1} m_{\tilde{t}_2}}$ as the renormalization scale. For vacuum stability analyses, Q dependence is also an important factor at tree level. We show this explicitly in the left column of figure 5.2, where we show results for $Q = \sqrt{m_{\tilde{t}_1} m_{\tilde{t}_2}}/2$, $Q = \sqrt{m_{\tilde{t}_1} m_{\tilde{t}_2}}$, and $Q = 2\sqrt{m_{\tilde{t}_1} m_{\tilde{t}_2}}$. If one then goes to the full one-loop effective potential, the sensitivity on the scale is significantly reduced as expected. In the same way, we show this explicitly in the right column of figure 5.2. In both cases we perform a scan in the (M_0, A_0) plane for fixed $M_{1/2} = 1$ TeV, $\mu > 0$ and $\tan\beta = 40$. We would like to note that this particular example shows that scale dependence would affect our conclusions significantly if we restrict ourselves to a tree level study. This result undermines arguments that radiative effects do not change tree level conclusions on the absolute stability of vacua such as in [104].

5.1.2. Constraining A_0 and $\tan\beta$

Let us get a closer look at the relationship between vacuum stability, A_0 and $\tan\beta$. We start with a check for regions in the CMSSM parameter space which don't have any CCB vacuum

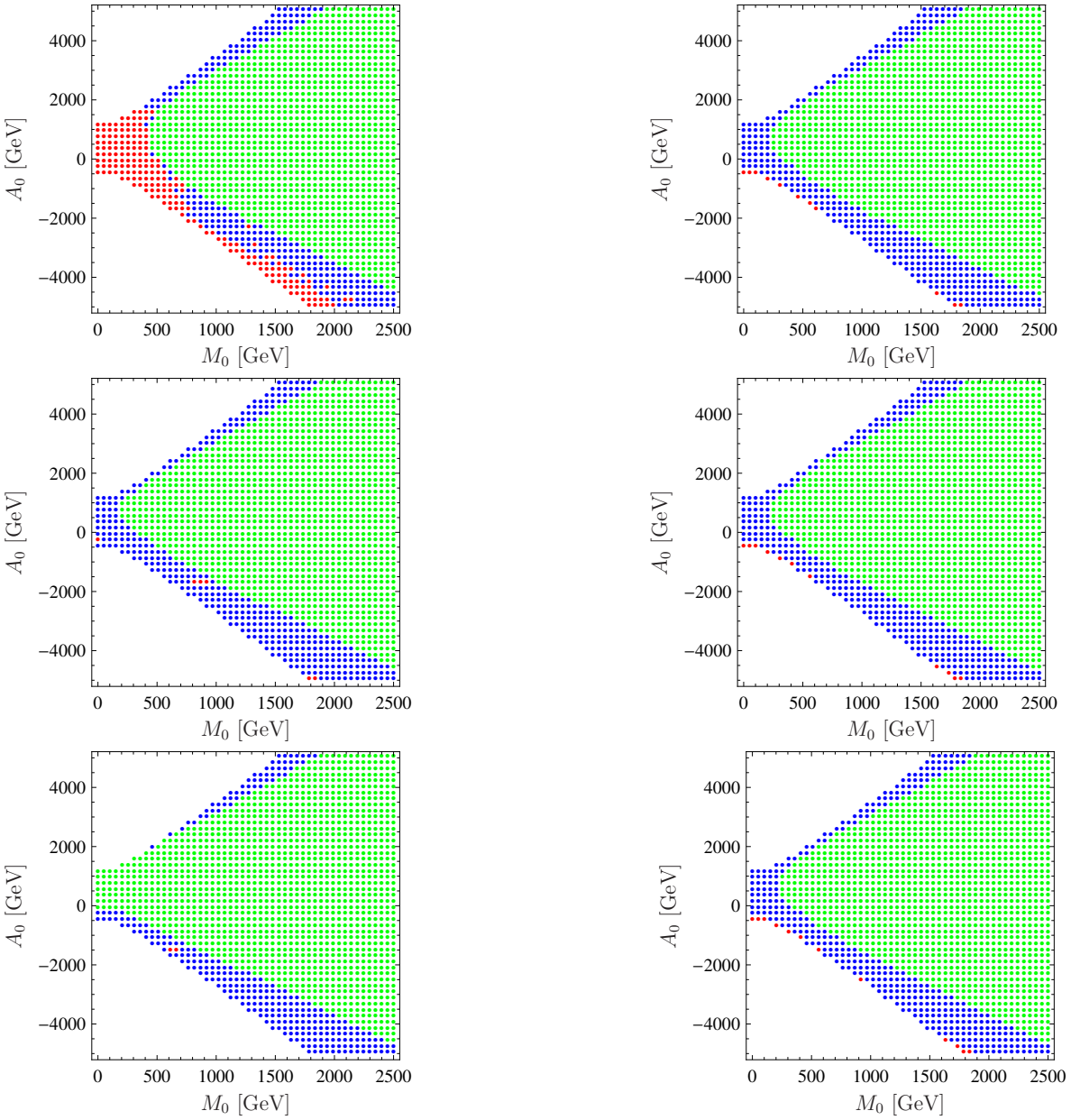

Figure 5.2.: Vacuum stability in the (M_0, A_0)-plane for fixed $M_{1/2} = 1$ TeV, $\mu > 0$ and $\tan\beta = 40$. On the left, only the tree level potential was considered. On the right, the full one-loop effective potential was taken into account. The renormalization scale was $Q = \sqrt{m_{\tilde{t}_1} m_{\tilde{t}_2}}/2$ (first row), $Q = \sqrt{m_{\tilde{t}_1} m_{\tilde{t}_2}}$ (second row), and $Q = 2\sqrt{m_{\tilde{t}_1} m_{\tilde{t}_2}}$ (last row). The color code is the same as in figure 5.1.

deeper than the DSB minimum. For this regions we have a stable DSB and can be thought as "safe". Regions where this is not the case and we have deeper CCB minima will require that we look into the probability of tunneling to the CCB minimum from the DSB one.
We look first for the maximal value of $|A_0|$ with a stable DSB vacuum for a given combination of M_0, $M_{1/2}$, $\tan\beta$ and $\text{sign}(\mu)$. We will concentrate on points for which $A_0 < 0$ as it has been showed to lead to better predictions for the Higgs mass [105]. The result is shown in figure 5.3. In this way it is easy to visualize not only the fact that for a large enough A_0 we will always be in the danger of CCB global minima but a quantitative estimation of how this happens.
We note that this will also restrict the allowed minimum mass for the lighter stau and stop. This condition gets even more unforgiving for large $\tan\beta$. The reason for this is that as $\tan\beta$ grows we get smaller $m^2_{\tilde{\tau}_R}$ for the rest of parameters fixed.
Let us now investigate the problem of CCB minima with more detail. In the following we take a relatively conservative threshold of 0.217 times the observed life time of the known Universe (corresponding to a one per-cent survival probability) to categorize parameter points as long-lived or short-lived. In other words, if the DSB minimum has less than 1% probability of having survived quantum tunneling since the Big Bang we will call it short-lived and long-lived otherwise. In figure 5.4 we show the distribution of stable (no deeper CCB), long-lived and short-lived DSB minima in the $(\tan\beta, A_0)$ plane for fixed values of $M_0 = M_{1/2} = 1$ TeV and $\mu > 0$. Here we will also start to compare our results with the regions excluded by the condition of section 4.1 by drawing lines for conditions (4.8) to (4.12).
The $\tan\beta$ dependence of vacuum stability is also a feature of the analytical limits, but their accuracy is not enough to treat them seriously. Note also that such conditions will of course not discriminate between long- and short-lived DSB minima, thus one has to compare them with the division between the stable (green) areas and the metastable (blue and red) areas. It is pretty clear then that even a combination of all the analytical conditions would fail to exclude about half the points of our scans with deeper CCB vacua.
It is worth mentioning that the CMSSM best-fit point after including $m_h = 126$ GeV of [103],

$$M_{1/2} = 1167.4^{+594.0}_{-513.0}\ \text{GeV}, M_0 = 1163.2^{+1185.3}_{-985.7}\ \text{GeV}, \tan\beta = 39.3^{+16.7}_{-32.7}, A_0 = -2969.1^{+6297.8}_{-1234.9},$$

is rather close in parameter space to the values $M_{1/2} = M_0 = 1$TeV that we have chosen in our study. If we look at the central values of $(\tan\beta)$ and A_0 for this point in figure 5.4, we will find ourselves in the long-lived region. Upon further consideration we find that this seems to be characteristic for models that relate the stau and stop masses, as required by the need to fit both the dark matter relic density (requiring light staus) and the correct Higgs mass (requiring heavy stops). This will force the allowed parameter region to have large A_0 and therefore move on the CCB minima "danger zone". This is also the case for models where the Higgs-masses are not unified at the GUT scale, as for example the so-called NUHM1"low" best-fit point of [106] also results in a CCB deeper vacuum. It is therefore interesting to perform a more detailed study of the light stau parameter space.

5.1.3. Constraining the light stau parameter space

As we mentioned in the previous section, one possibility to explain the observed dark matter relic density relies on light enough staus so that their mass is sufficiently close to that of a neutralino LSP. When this happens, both particles can co-annihilate and it is then possible to explain the measured value of the relic density [107–109]. The most recent measurement in the 3σ range of

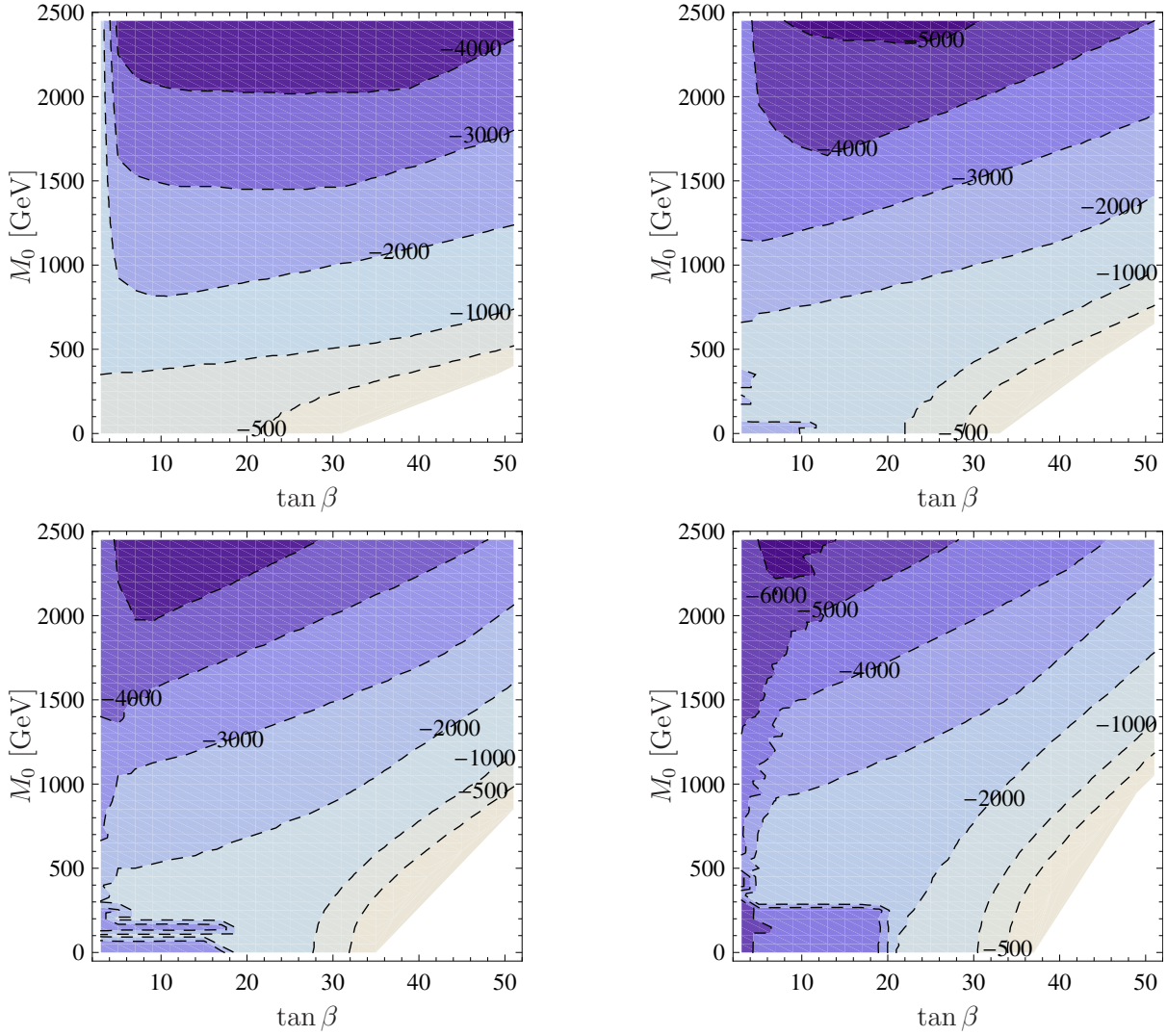

Figure 5.3.: Minimal value allowed for A_0 in the $(\tan\beta, M_0)$ plane to have a stable DSB vacuum. We used $\mu > 0$ and $M_{1/2} = 500$ GeV (upper left), $M_{1/2} = 1000$ GeV (upper right), $M_{1/2} = 1500$ GeV (lower left) and $M_{1/2} = 2000$ GeV (lower right).

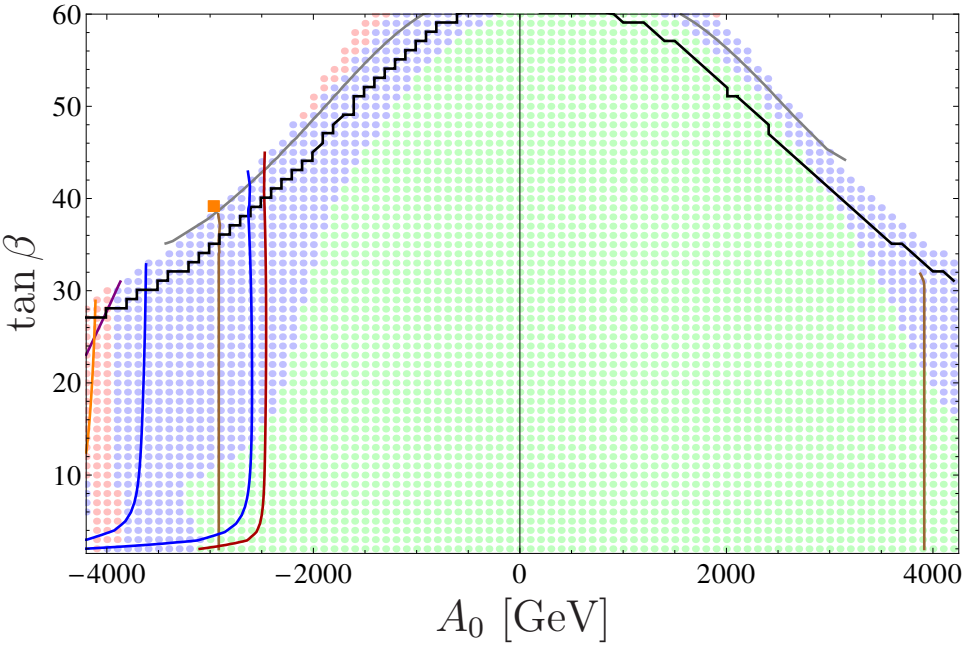

Figure 5.4.: Vacuum stability in the $(A_0, \tan\beta)$-plane for fixed values of $M_0 = M_{1/2} = 1$ TeV and $\mu > 0$. The color coding of parameter points is as in figure 5.1. In this and the following plots the solid colored lines correspond to the dividing lines between parameter points that satisfy or fail the conditions discussed in section 4.1 represented as:

- Condition (4.5) by purple,
- Condition (4.6) by orange,
- Condition (4.7) by dark red,
- Condition (4.8) by brown,
- Condition (4.10) by dark blue
- Condition (4.11) by pink,
- And condition (4.12) by gray.

Points on the other side of the solid lines from the $A_0 = 0$ axis fail the corresponding conditions and so would be identified as having CCB minima deeper than the DSB minima We do not plot any of these lines in white regions in our figures, where no spectra could be calculated for the DSB minimum anyway, due to the presence of negative squared masses. The left-most of the blue lines corresponds to taking 0.85^2 in condition (4.10), and the other to 0.65^2. The single orange square corresponds to a projection of the best-fit point of [103] for reference. Points below the dotted line have the lightest neutralino as the LSP.

the Planck collaboration is $\Omega h^2 = 0.1199 \pm 0.081$ [14]. This translates into a requirement for the masses of the lightest stau and neutralino to be at most a few GeV apart. For the CMSSM such spectra can be obtained for large values of A_0 and $\tan\beta$ which are precisely the parameter regions where we have shown vacuum stability constraints to be important.
To assess this in a more quantitative matter we will do the following: Taking the results shown in figure 5.3, where we see the maximal $|A_0|$ [1] consistent with a stable DSB we can then get a lower limit on the lightest stau mass for given parameter point. This is shown in figure 5.5. By looking at the results it is clear that for $M_{1/2} > 500$ GeV and stau masses below 500 GeV, deeper CCB vacua appear.
Now, CCB minima deeper than the DSB one are not necessarily a problem phenomenologically speaking. If the tunneling time is sufficiently long it is possible to allow a metastable DSB. We exemplify this in figure 5.6. There we plot (for the same parameter region studied in [109]) stable, short- and long-lived DSB vacua in the $(M_{1/2}, M_0)$ plane with $\tan\beta = 40$ and $A_0 = 3000$ GeV.
On the right-hand side of figure 5.6, we zoom into the area consistent with dark matter relic density constraints. For this we used `MicrOmegas 2.4.5` [110, 111] together with the `SUSY Toolbox` [112] to calculate the relic density. It is somewhat reassuring for advocates of the stau coannihilation mechanism that in this region the survival probability of the DSB vacua against tunneling to deeper CCB minima is reasonably high.
However, for the most conservative, the area is still in danger because of the existence of deeper CCB minima. Due to the limitations of any numerical analysis there still exists the chance that with better computers and more computing time, it could be possible to find a better optimal path with shorter tunneling time.
To complement this, in figure 5.7, we provide a similar example showcasing the fact that vacuum stability in the context of the stau coannihilation mechanism is a severe issue. Again in the (M_0, A_0)-plane, we show the region around the best-fit point found in [103]. In this region, the main part of the so-called stau coannihilation strip has deeper CCB vacua. However it would be allowed if one considers points for which `Vevacious` reports a lifetime of at least three gigayears stable.
The analytical conditions again perform poorly, with only condition (4.7) excluding some of the points with CCB minima while excluding a fair share of stable parameter points as well. It is curious to note that this particular condition is being applied to parameters where the assumption $Y_t \ll 1$ for its derivation is invalid (see section 4.1).
To finish our considerations regarding the light stau parameter space we would like to discuss another comparison between the results coming from `Vevacious` and the analytical approximations in section 4.1. In figure 5.8 we show vacuum stability and stau masses in the (M_0, A_0)-plane for $M_{1/2} = 1\,\text{TeV}$ with $\tan\beta = 40$ and 50. When $\tan\beta = 40$ is used, the analytical conditions fail completely with the exception of (4.7) which performs quite poorly. The rest of the conditions will lie in the white region which is excluded at the spectrum generator level (it shows tachyonic states for the DSB vacuum).
For $\tan\beta = 50$ the situation is slightly better with some regions within small M_0 areas being in conflict with condition (4.11). However, the main part of the region showing deeper CCB minima would also survive after applying the analytical constraints (with (4.7) performing less well).
This comparison shows that for large $\tan\beta$ and reasonable SUSY spectra above the current LHC exclusion limits, one can not rely at all on conditions (4.5), (4.6), (4.8), (4.11) or (4.12).

[1] As $A_0 < 0$ this also means its minimal value

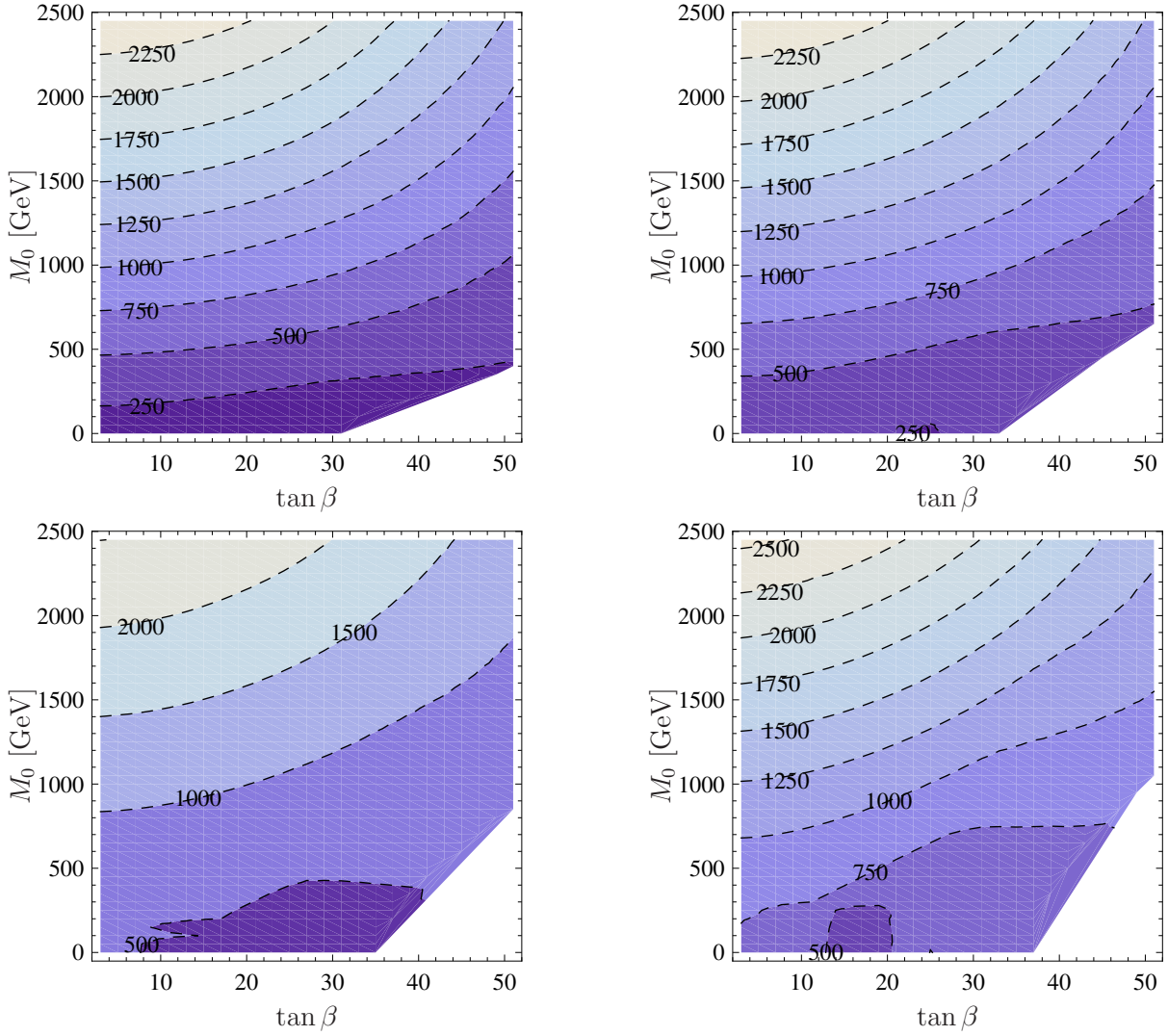

Figure 5.5.: Minimal stau mass in the $(\tan\beta, M_0)$ plane to have a stable DSB vacuum for $A_0 < 0$. We used $\mu > 0$ and $M_{1/2} = 500$ GeV (upper left), $M_{1/2} = 1000$ GeV (upper right), $M_{1/2} = 1500$ GeV (lower left) and $M_{1/2} = 2000$ GeV (lower right).

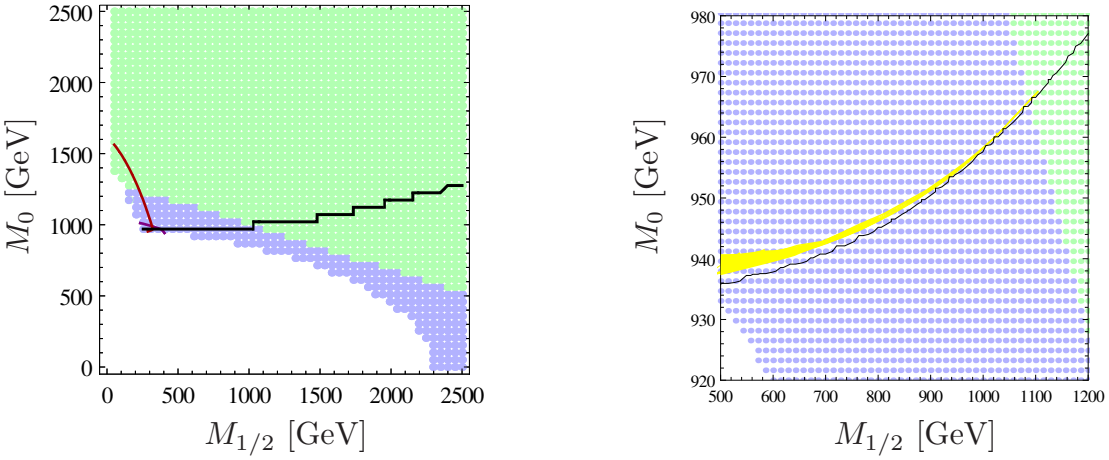

Figure 5.6.: Dark matter and vacuum stability in the $(M_{1/2}, M_0)$ plane with $A_0 = 3$ TeV, $\mu > 0$ and $\tan\beta = 40$. On the left, the dashed black line shows the transition between a neutralino and stau LSP (stau LSP beneath the line); on the right we zoom in on the interesting range for dark matter: the yellow bands show the region where $\Omega h^2 = 0.1199 \pm 0.081$. The constraints from vacuum stability allowing for stop and stau VEVs are indicated. The color coding is as in figure 5.4 : points to the left of the solid lines fail the corresponding conditions. Here and in subsequent figures, physical quantities such as the dark matter relic density and particles masses are taken to be evaluated at the DSB vacuum regardless of its stability.

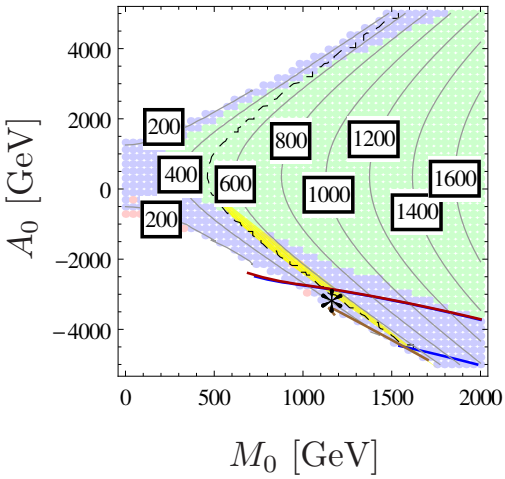

Figure 5.7.: Mass of the light stau and vacuum stability in the (M_0, A_0) plane with $M_{1/2} = 1167.4$ GeV, $\mu > 0$ and $\tan\beta = 39.3$. In the yellow region, the abundance of the LSP is in agreement with dark matter constraints, and the dashed line shows the transition to a charged LSP. The color coding is as in figure 5.4: points below the solid lines fail the corresponding conditions. The lower blue line corresponds to condition (4.10) taking 0.85^2, the upper, which is almost exactly degenerate with the dark red line of condition (4.7), corresponds to taking 0.65^2. The star indicates the best-fit point according to [103].

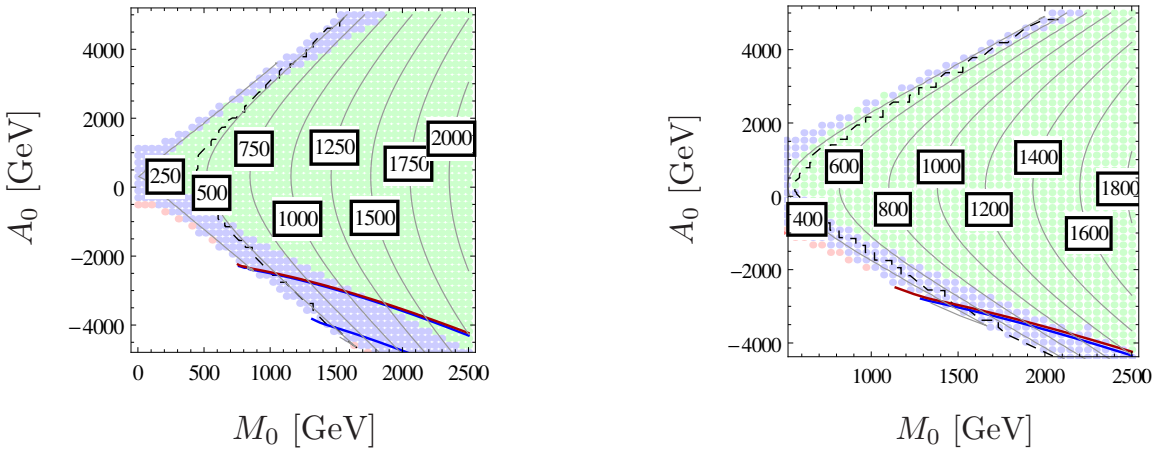

Figure 5.8.: Vacuum stability and stau masses in the (M_0, A_0) plane for fixed $M_{1/2} = 1$ TeV, $\mu > 0$ and $\tan\beta = 40$ (left) or $\tan\beta = 50$ (right). The dashed black line shows the transition to a charged LSP (neutralino LSP to the right of the line). The color coding is as in figure 5.4: points to the left of the solid lines fail the corresponding conditions. As in figure 5.7, the blue line for condition (4.10) with 0.65^2 is almost degenerate with the dark red line of condition (4.7) and the line for 0.85^2 only excludes points with even more negative A_0 (and is not visible on the right).

5.1.4. Constraining the light stop parameter space

As we discussed in the introduction, if we would like to be consistent with the measurements of the SM Higgs boson mass (corresponding to the light Higgs in the MSSM), we need the correct stop masses to push it to about 125 GeV via radiative corrections [96–100].
Achieving this requires rather heavy stops [98, 113], or conversely large enough $|A_t|$ to trigger the so-called maximal mixing scenario [96, 114, 115]. A very rough estimate is given by $A_t \simeq 0.2A_0 - 2M_{1/2}$ [116] by which we justify the observed preference for negative A_0 in our studies. Another estimate suggests that $|A_0| \simeq 2M_0$ [115] which following the conclusions of our previous observations clearly puts us in the dangerous region in the light of vacuum stability.
The information of figure 5.3 can be translated into a lower limit on the stop mass by demanding a stable DSB vacuum. We show the result in figure 5.9. We see that for small $M_{1/2}$, this condition excludes light stop masses in nice agreement with the results coming from direct searches ($m_{\tilde{t}} \gtrsim 600\,GeV$ [117]). For larger values of $M_{1/2}$ though, the lower mass limit is in the TeV range. Furthermore, our limits are independent of the mass splitting between the stop and the lightest neutralino or chargino.
As an alternative mechanism for the explanation of the dark matter relic density, a stop NLSP (next lightest SUSY particle) could also give the correct neutralino abundance through coannihilation much in the same way as the staus. The stop could then be accessible to the LHC, a fact also motivated by naturalness arguments (see [118, 119] and section 3.8). The mechanism of stop coannihilation usually works more efficiently for a larger mass splitting between the NSLP and LSP compared to the case for staus. However the stops still have to be sufficiently light [120]. Recent benchmark points for this scenario have been proposed in [121].
In this context, a scan around their benchmark point 5.1 ($M_0 = 2667$ GeV, $M_{1/2} = 933$ GeV, $\tan\beta = 8.52$, $\mu < 0$, $A_0 = -6444$ GeV) in the $(M_{1/2}, M_0)$ plane is shown in figure 5.10, where we give the contour lines of the stop mass as well as the vacuum stability. In the figure we show that the stop coannihilation region lies completely in the region suffering from CCB vacua.

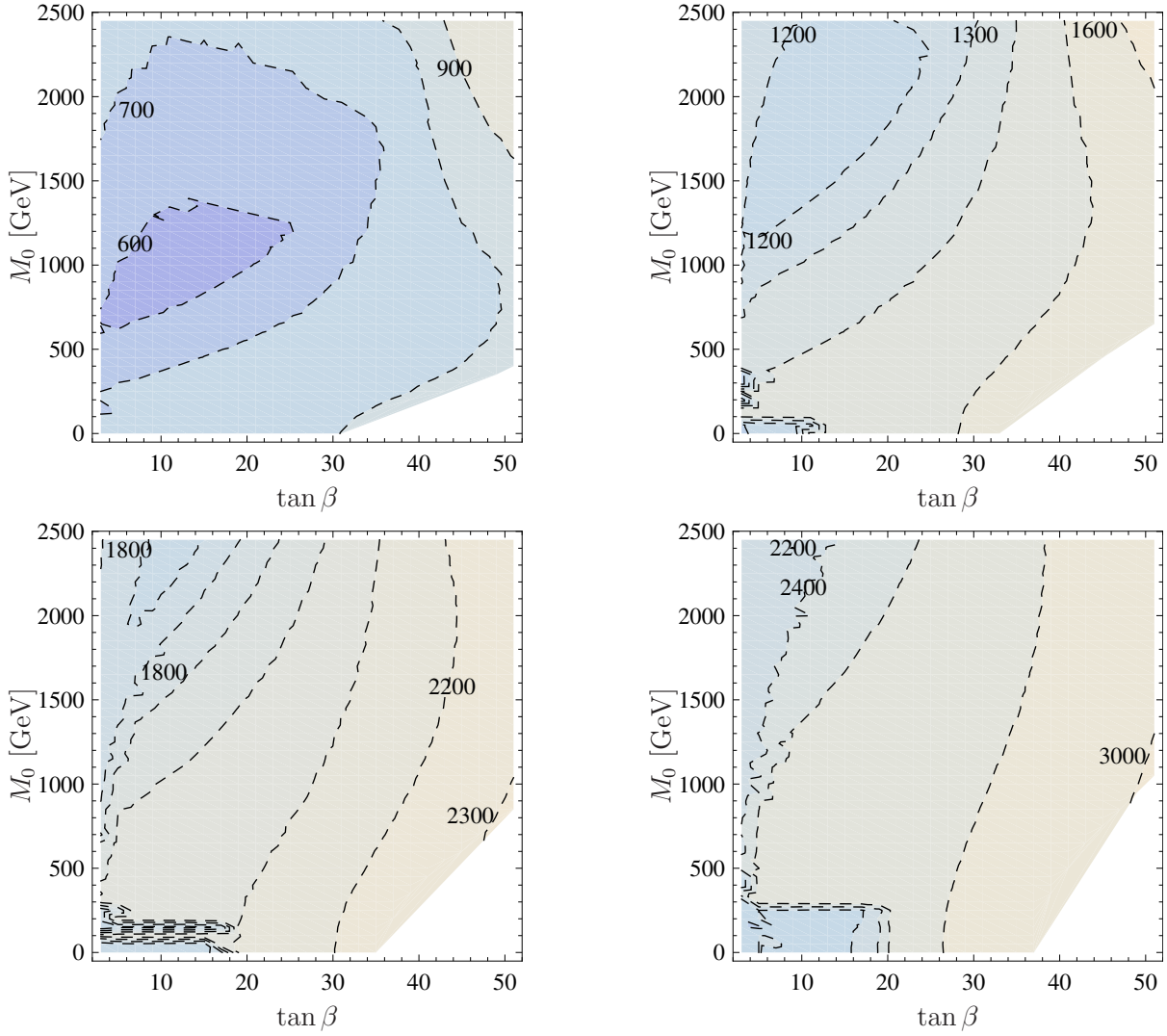

Figure 5.9.: Minimal stop mass in the $(\tan\beta, M_0)$ plane to have a stable DSB vacuum for $A_0 < 0$. We used $\mu > 0$ and $M_{1/2} = 500$ GeV (upper left), $M_{1/2} = 1000$ GeV (upper right), $M_{1/2} = 1500$ GeV (lower left) and $M_{1/2} = 2000$ GeV (lower right).

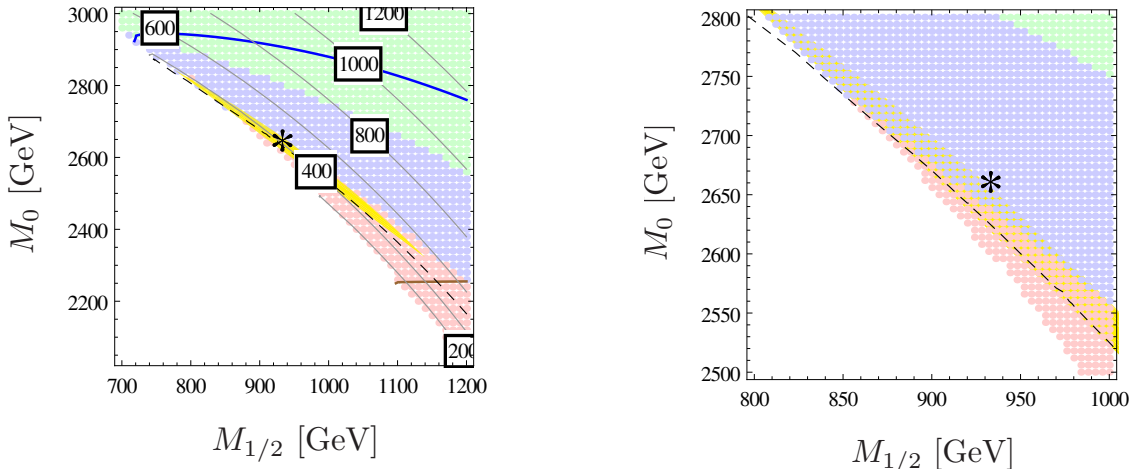

Figure 5.10.: Mass of the light stop and vacuum stability in the $(M_{1/2}, M_0)$ plane with $A_0 = -6444$ GeV, $\mu < 0$ and $\tan\beta = 8.52$. The dashed line shows the transition to a charged LSP (neutralino LSP to the right of the line). The color coding is as in figure 5.4: points below the solid lines fail the corresponding conditions. In the yellow region, Ωh^2 is in agreement with dark matter constraints (as in figure 5.7). The star indicates the benchmark point 5.1 of [121]. The reason that this point is not in the strip with the correct dark matter abundance is that different SM input parameters were used in [121] in comparison to eq. (5.1): $m_t = 174.3$ GeV, $\alpha_S = 0.1172$ and $m_b(m_b) = 4.25$ GeV. The line showing the division between passing and failing condition (4.10) using 0.65^2 does not appear on this plot, but over-zealously would exclude the entire region shown, while taking 0.65^2 would only exclude every point with $M_0 \lesssim 2900$ GeV.

Furthermore, at least half of the points exhibit very short lifetimes for the DSB, therefore being short-lived. We note that this can be a severe issue not only for stop coannihilation in the CMSSM, but also for natural MSSM benchmark scenarios such as those discussed in [122]. There is however one way to resurrect stop coannihilation: we need to consider much larger mass spectra. For this case we find that the BP 5.2 of [121] with $m_{\tilde{\chi}_1^0} = 1$ TeV seems to be stable against tunneling to CCB minima.

We conclude this section with another comparison between the results coming from our proposed framework and the thumb rules given in the literature. In figure 5.11 we show the mass of the light stop and the vacuum stability in the (M_0, A_0)-plane for $M_{1/2} = 1$ TeV and $\tan\beta = 2, 10$. By looking at the figure, it is clear that the conditions offer no help, except for the misused conditions (4.7) and (4.8) which have a limited success.

In conclusion, if we consider phenomenological constraints coming from deeper CCB minima (even when allowing long-lived DSB vacua) we can get strong limits on the mass of the light stop for the case of small $\tan\beta$ and negative A_0. Moreover we can safely say that vacuum stability can rule out light stops in the CMSSM depending on the values one takes for $M_{1/2}$.

5.1.5. Constraining the parameter space with $m_h \simeq 125$ GeV

The Higgs boson mass has been an important fact we kept in mind during our previous analysis. However we have not yet approached it directly. The measurement of $m_h \simeq 125.5$ GeV [123, 124] offers a powerful way to constrain the parameter space of SUSY models, in particular for the MSSM. To get loop contributions which are large enough to increase the tree level Higgs mass of $m_h^{(TL)} \leq m_Z$ up to 125 GeV without very heavy stops, a large mass splitting in the stop sector is necessary (see 3.8). This translates to the fact that $|A_0|$ must be large in comparison to M_0

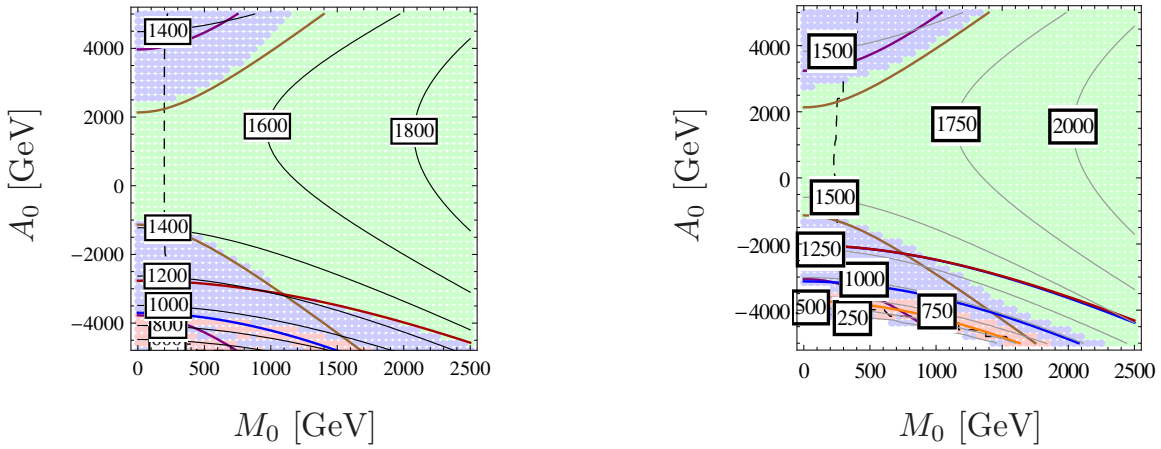

Figure 5.11.: Stop mass and vacuum stability in the (M_0, A_0) plane. We used $M_{1/2} = 1$ TeV, $\mu > 0$ and $\tan\beta = 2$ (left) or $\tan\beta = 10$ (right). The color coding is as in figure 5.4: points to the left of the solid lines fail the corresponding conditions. Again, there is a degeneracy between the more exclusive blue line of condition (4.10) with the dark red line of condition (4.7). Points to the left of the dashed line also have charged LSPs.

(for a detailed take on the subject we point the reader to [114, 125–128] and references therein).

At one-loop level, the corrections are maximal for $X_t = A_t - \mu/\tan\beta \simeq \sqrt{6}M_S$ where M_S is the average stop mass. If two-loop corrections are taken into account, the condition gets modified to $X_t \simeq 2M_S$ [115].

As we have shown in the last sections, these are precisely the regions typically suffering from a CCB minimum deeper than the DSB minimum for the CMSSM. We would like to show this fact more explicitly. For this we take the same parameter planes discussed previously and calculate the result for the predicted Higgs mass along parameter space using `SPheno`. These Higgs masses are based on a full diagrammatic one-loop calculation including the effects of the external momenta [129] together with the known two-loop corrections following the results of [130–134]. For completeness we will also show the result including only one-loop corrections.

One might wonder about whether two-loop effects are important for the analysis of the vacuum structure of SUSY models, given that they are critical for obtaining the experimental value of the Higgs mass in the CMSSM. However, given that the two-loop corrections to the Higgs mass-squared are small ($\sim 10\%$ of the one-loop value) compared to the one-loop corrections ($\sim 100\%$ of the tree level value), along with the indications from figure 5.2 that loop corrections play a sub-dominant role, it is reasonable to guess that the loop expansion converges well and the higher orders should not affect the results substantially.

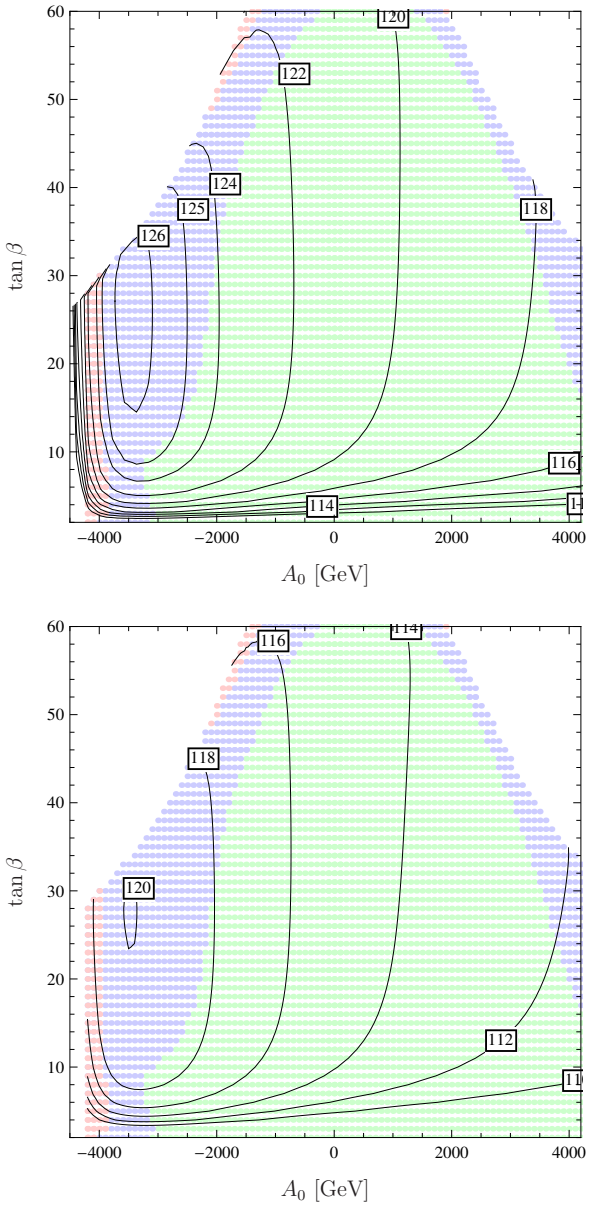

Figure 5.12.: Vacuum stability and the Higgs mass in the $(A_0, \tan\beta)$ plane for fixed $M_0 = M_{1/2} = 1$ TeV and $\mu > 0$. In the top picture, the leading two-loop corrections at the DSB minimum to m_h have been taken into account, while in the bottom picture only corrections at one-loop order are considered. The color code is the same as in figure 5.1.

To show the result of combining the Higgs mass constraint and vacuum stability, we will consider first moderate SUSY masses ($M_0 = M_{1/2} = 1$ TeV). The Higgs mass and the vacuum stability in the $(A_0, \tan\beta)$ plane is shown in figure 5.12. Quite remarkably we see that the entire region where $m_h = 125$ GeV lies in the area with charge- or color-breaking minima deeper than the DSB minima.

The question is now whether we can relax this tension when considering heavier SUSY spectra. To show this we consider in figure 5.13 the (M_0, A_0) plane with M_0 up to 2.5 TeV. The rest of parameters is set to $M_{1/2} = 1$ TeV, $\mu > 0$ and $\tan\beta = 10, 40$. As expected, for both values of

$\tan\beta$, the correct Higgs mass can only be reached for large negative values of A_0. In the case of small M_0, the ratio $|A_0/M_0|$ is forced to be very large to allow the correct value for the Higgs mass. As the reader might already guess, this means that all points with $m_h > 124$ GeV are in an area with CCB minima deeper than the DSB minima for $M_0 < 900$ GeV ($\tan\beta = 10$) and $M_0 < 1200$ GeV ($\tan\beta = 40$). Only for larger M_0 we find points with the Higgs mass in the correct range and a completely stable DSB. The lower bound on M_0 increases by about 300 GeV when taking $m_h \geqslant 125$ GeV. The results of this study have been reported in [135].

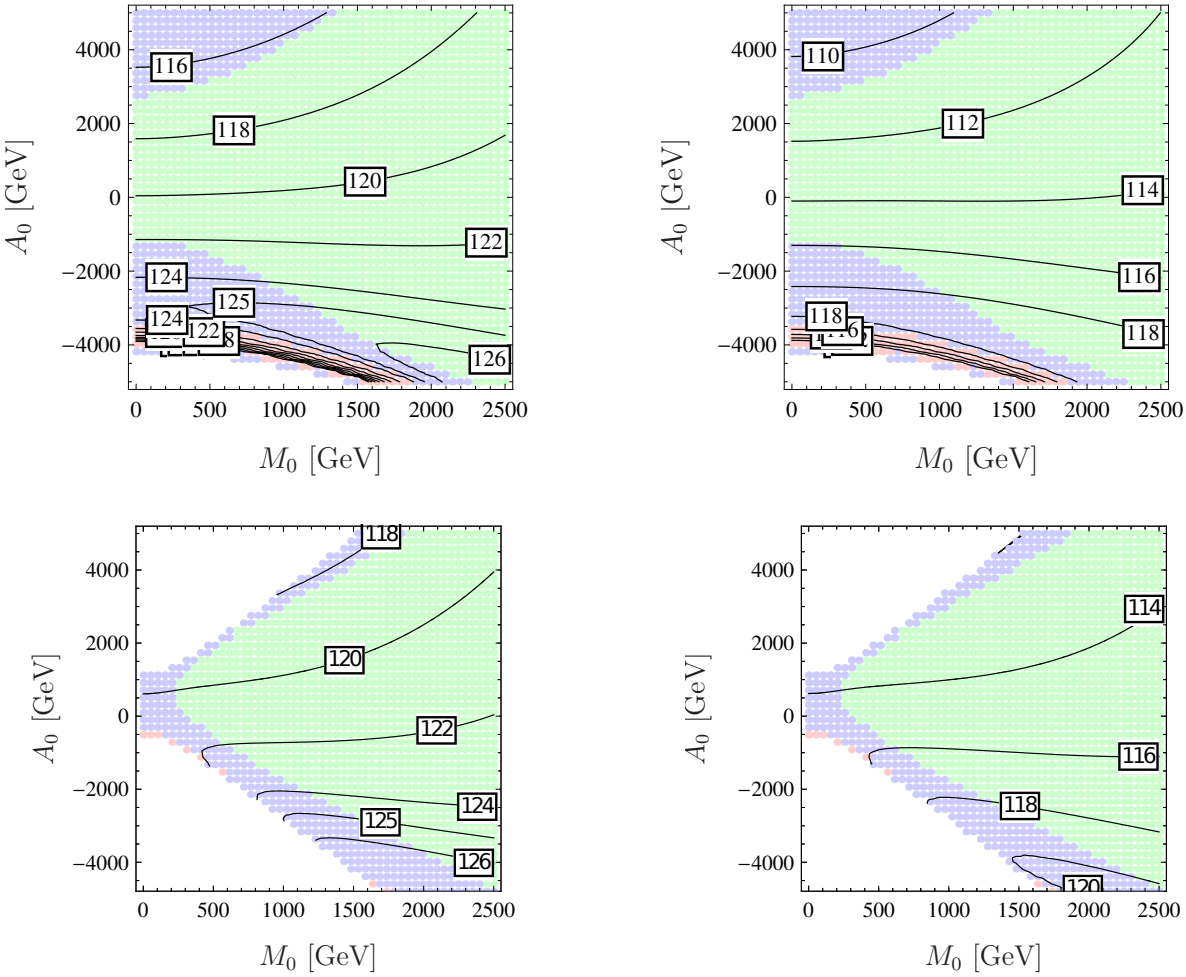

Figure 5.13.: Vacuum stability and the Higgs mass in the (M_0, A_0) plane for fixed $M_{1/2} = 1$ TeV, $\mu > 0$ and $\tan\beta = 10$ (upper) or $\tan\beta = 40$ (lower). On the left, the leading two-loop corrections to the mass of the lighter Higgs boson have been taken into account, on the right, only the mass at one-loop order is shown. The color coding is the same as in figure 5.1.

5.2. Charge- and color- breaking minima in the natural MSSM at $T \neq 0$

After our exploration of vacuum stability in the CMSSM, we were able to understand how constraints coming from the existence of deeper CCB vacua affect its parameter space. One of

the most interesting results was that the parameter space regions consistent with a lighter Higgs mass of 125 GeV is in strong tension with charge- and color- breaking minima.

It is then interesting to explore how this result would be modified when considering tunneling at non zero temperature. Although we showed the existence of deeper CCB vacua in these regions, it was still possible at zero temperature to find parameter points where the lifetime was reported by `Vevacious` to be much longer than the observed age of the universe. Under the effect of thermodynamic fluctuations, the lifetime of the DSB minimum might be significantly reduced, so the question remains as of what will happen with long-lived (at $T = 0$) points in the correct Higgs mass region.

Now that we have an idea about the interesting parameters to focus on in this type of analyses, it will also be interesting to depart from the CMSSM and study a more pragmatic version of the MSSM, the natural MSSM. We described this model in section 3.8.

As we will show in the following, if we consider the possibility of tunneling at non zero temperature a large proportion of the parameter space where the Higgs boson mass is even slightly compatible with the experimental measurement is ruled out. We performed a five-dimensional scan which then we projected onto a two-dimensional plane with the axes being the mass of the lightest Higgs scalar m_h and the ratio X_t/M_S, where $X_t = A_t - \mu \cot\beta$, and M_S is again the square root of the product of the tree level $\tilde{t}$ masses evaluated at the DSB minimum as this choice of scale keeps higher order corrections small [136].

As in the previous section, we calculate the Higgs mass through `SPheno` in a full diagrammatic one-loop approach including the effects of the external momenta [129] and the known two-loop corrections [130–134].

5.2.1. Range of validity

One should not trust a fixed-order loop expansion for VEVs very much larger than the renormalization scale Q as we run in the danger of leaving the convergent region of the perturbative expansion. In the same way thermal tunneling dominated at temperatures $T \gg Q$ might not be very accurate. One way of ameliorating this issue relies on a potential where the parameters are not calculated at a fixed scale but at the scale of the field values considered [83]. The implementation of such prescription is planned for new versions of `Vevacious`, thus the results presented here are based on the one-loop effective potential with parameters evaluated at a fixed Q. Given that for every single one of our parameter points, the VEVs of the CCB minima were within a factor of a few of Q and the thermal tunneling was dominated by $T \lesssim Q$, we consider this to be a reasonable approach.

It is also important to note that any conclusion made by considering thermal effects in tunneling probabilities depends on the thermal history of the Universe. Given a parameter point, if we consider a model where the optimal T for tunneling is never reached, such parameter point will still be valid. Our results are nonetheless important since in the most commonly hypothesized cosmologies, $T \sim 10^5$ GeV is already considered very low [137–142].

Finally, we do not address the question of additional CCB minima at large VEVs $\gtrsim 10^{16}$ GeV. This case can only be reliably calculated with current methods using running parameters and under very restricted circumstances [143]. We do not consider the effects of inflation and reheating either [137].

5.2.2. Parameter scan

In the familiar case of the SM, spontaneous symmetry breaking is triggered by a negative Higgs mass-squared term in the Lagrangian[2]. However this is neither a necessary nor sufficient condition for any scalar fields to develop a non-zero VEV in general. In particular, a positive mass-squared for the stop fields does not imply that a parameter point will have a stable DSB minimum, especially if the trilinear couplings $T_u^{3\,3} = Y_t A_t$ and $Y_t \mu$ for $H_u \tilde{t}_L \tilde{t}_R^*$ and $H_d \tilde{t}_L^* \tilde{t}_R$ respectively are large compared to the square roots of the soft SUSY-breaking mass-squareds $m^2_{\tilde{t}_L}$ and $m^2_{\tilde{t}_R}$.

We refer the reader to section 2.1 of [145] or section B of [146] for the explicit form of the relevant part of the tree level scalar potential

We will be restricting ourselves to the possibility of tunneling to minima with $\tilde{t}$ VEVs. Because of this and our previous discussion we will explore in detail the region in parameter space described by table 5.1. We would like to also restrict ourselves to the so-called decoupling limit, i.e. where the standard model can be thought of an effective theory once we decouple the MSSM particles. The chosen value of the pseudoscalar Higgs mass places the scan firmly in this limit [127]. To ensure that scalar SUSY particles other than the stops are not relevant to the analysis, we then choose large masses-squared for them and zero soft SUSY-breaking trilinear interactions. The gluino can have a non-negligible contribution to the mass of the lightest scalar Higgs, so we chose to keep it at 1000 GeV while taking masses for the other gauginos according to a typical hierarchy inspired in models with unification of the gauge forces at a GUT scale [19]. This choice largely overlaps with that of reference [146].

In order to study how well the Higgs mass constraint does together with vacuum stability, we run `Vevacious` in all of the points of our scan.

Parameter	**Range**
$\tan\beta$	5 – 60
$m^2_{\tilde{t}_L}$	500^2 GeV^2 – 1500^2 GeV^2
$m^2_{\tilde{t}_R}$	500^2 GeV^2 – 1500^2 GeV^2
μ	100 GeV – 500 GeV
$T_u^{3\,3}$	-3000 GeV – 3000 GeV

Table 5.1.: Parameter ranges used in the scan. All mass-squared matrices for the scalar partners of SM fermions were diagonal. All diagonal entries for SUSY particles but those shown above were set to 1500^2 GeV^2. The soft SUSY-breaking mass terms for the $U(1)_Y$, $SU(2)_L$, and $SU(3)_c$ gauginos were 100 GeV, 300 GeV, and 1000 GeV, respectively. Besides $T_u^{3\,3}$, all other soft SUSY-breaking trilinear terms were set to zero. Finally, the mass of the pseudoscalar Higgs boson was set to 1000 GeV. The renormalization scale for each parameter point was the mean of the physical $\tilde{t}$ masses at the DSB vacuum.

[2]The possibility that it is due to a massless Coleman-Weinberg model has been ruled out by measurements of the top mass, for example [144].

5.2.3. Natural MSSM, m_h and thermal effects

Now that we have laid out the specifics of the study performed for the natural MSSM, we can take a closer look at the results. In figure 5.14 we present the vacuum stability when considering stop VEVs in the natural MSSM for the $(X_t/M_S, m_h)$ plane. As found previously for the CMSSM, we find that the region in agreement with $m_h \approx 125$ GeV overlaps significantly with the region that has deeper CCB minima. At $T = 0$ we again find that a significant portion of the points with deeper CCB minima also have long-lived DSB minima, making them still viable if we do not consider thermal effects. The interesting result is that when allowing for thermal fluctuations at $T \neq 0$ (by using `Vevacious` with the implementation of the framework developed in section 4.5), most of the parameter points for which the DSB was long-lived at $T = 0$ will have very short lifetimes. This means that in the natural MSSM, a big amount of the parameter combinations providing a reasonable value for the Higgs mass, would have decayed long ago into minima that break charge and color thus excluding them from the allowed phenomenological region. It is clear from figure 5.14 that the constraint of correct Higgs mass is already quite stringent. By looking for deeper CCB minima and calculating tunneling times at $T \neq 0$ we find that vacuum stability constraints the parameter space even more. This is a clear sign that for any realistic phenomenological study of the natural MSSM vacuum stability has to be included.

5.2.4. Comparison to previous works on vacuum stability

As we did in our previous analyses we would like to compare the existing analytical conditions meant as safeguards against CCB minima. Even though it was derived under the assumption that the Yukawa coupling are much smaller than the gauge couplings and it has been known to be neither necessary nor sufficient [59, 147], the condition (4.9) has been used in place of a proper analysis as a check that parameter points have stable DSB vacua. As we showed in section 5.1 this is not meaningfully correlated with long-/short-lived metastable vacua, but for completeness we show how our results are if we exclude points which fail the condition in figure 5.15.
Curiously from all the conditions we investigated, this particular one happens to exclude all the points with DSB vacua that are short-lived at zero temperature, but it both unnecessarily excludes stable and long-lived metastable points at larger $|X_t|$ and it does not to exclude most of the points which we find decay quickly by thermal tunneling and show $m_h > 123$ GeV.
Let us compare our results with similar analyses of CCB minima. If we restrict ourselves to the case of $T = 0$, our results qualitatively agree with [145] and [146]. For [145] the regions of parameter space under study overlap poorly. However comparing both results we find an agreement with the ratios of X_t to M_S where the CCB minima become deeper than the DSB minima and where the tunneling time becomes unacceptably short.
From these results we can conclude that stability against thermal tunneling is a relevant constraint, especially in the parameter space of the MSSM where the mass of the lightest Higgs boson is consistent with experiments. While we also showed that exclusion based on zero-temperature tunneling can bring some insight into which regions of the parameter space are under danger of CCB minima, it is also true that points that have long-lived DSB at $T = 0$ might not be able to avoid tunneling to CCB minima at higher temperatures. Another important conclusion we can derive from our investigation is that due to the complicated dependence on the Lagrangian parameters, a full analysis of any given parameter point seems unavoidable, though straightforward given the framework we propose through `Vevacious`.
We have also showed that results on metastability based on previous tree level analyses can qualitatively agree with the zero temperature one-loop analysis, but are in disagreement with

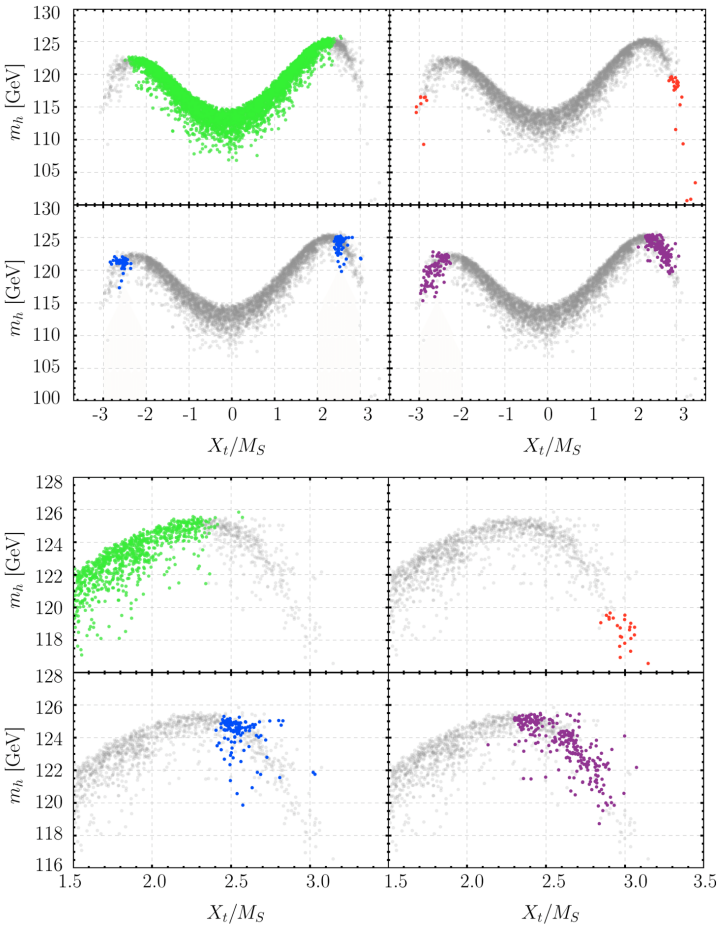

Figure 5.14.: Categorization of parameter points as to whether they are allowed or excluded by tunneling out of the DSB vacuum. Green (top left): no CCB minimum deeper than the DSB minimum was found. Blue (bottom left): the DSB minimum is a false vacuum, but the probability of surviving 13.8 Gy at zero temperature and surviving thermal fluctuations are both above one per-cent. Purple (bottom right): the probability of surviving tunneling out of the DSB false vacuum at non-zero temperature is less than one per-cent. Red (top right): the probability of the DSB false vacuum surviving 13.8 Gy at zero temperature is less than one per-cent. Below we zoom in on the region with $X_t/M_S \in [1.5, 3.5]$ and $m_h \in [116, 128]$ GeV.

the results once we include finite-temperature effects. The results from this study have been reported in [151].

5.3. Vacuum Stability in parameter fit studies

We have seen that the implemented framework in `Vevacious` can report results rather quickly. A great place to put this speed into test is by including it in fit studies. A parameter fit study relies on a wide set of observables to find the regions of parameter space in a model where the χ^2 parameter estimating the prediction accuracy for those observables is minimized. For this minimization a very large scan in parameter space ($O(10^8)$ points) is needed.
Including vacuum stability constraints into such type of studies requires the evaluation of such amount of points in a reasonable amount of time (O(seconds/point)). In particular the Fittino

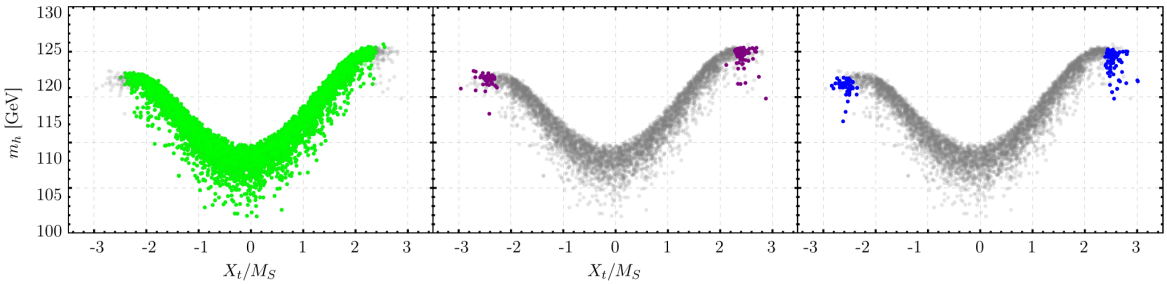

Figure 5.15.: Results without displaying those points which would be excluded by condition (4.9). The color coding is the same as in figure 5.14, with green points contrasted against the others on the left, purple in the middle, and blue on the right. We note that this condition excludes all points with short-lived DSB vacua at zero temperature.

collaboration [103] performs such studies using the Fittino code [152] for the CMSSM. We estimated `Vevacious` performance for different levels of accuracy and determined how to include vacuum stability in a future Fittino study.

It is possible to adapt our framework for such applications by running `Vevacious` for a large amount of points and storing M_0, $M_{1/2}$, A_0, $\tan\beta$, and , $\text{sign}(\mu)$ together with the result reported by `Vevacious`. Then a request can be made for each parameter point considered in the fit to obtain the vacuum stability of the closest parameter point in the vacuum stability analysis. As for our previous CMSSM analysis we observed grouping of regions with different stability results, this justifies our simplification as long as the initial scan for `Vevacious` analysis is sufficiently dense.

We note that this is a very conservative implementation of vacuum stability but it can give a clear hint to the regions in the fit that need to be looked at closely with a more stringent analysis. In order to incorporate such prescription in a future Fittino study, we performed a large scan in the parameter space of the CMSSM as shown in table 5.2. As time constraints are always important, we chose to limit `Vevacious` to straight paths between the DSB and panic vacua and allowed stop and stau VEVs. Even with these restrictions the scan took around 1 month using seven 3.4 GHz cores. A C++ class called `CheckVacuum` was written to use the data coming from the scan into parameter fit studies.

The results from the scan where parsed and stored so that the `CheckVacuum` class functions, given M_0, $M_{1/2}$, A_0, $\tan\beta$, and , $\text{sign}(\mu)$ as input, would output the stability of the closest parameter point in the `Vevacious` scan. By closest we mean the parameter point in the scan with the smallest normalized distance in parameter space to the input point. In this way it was easily implemented within the Fittino framework, where if necessary more detailed studies could be performed for dangerous regions of parameter space. The code used can be found in appendix C.

The results of this are to be reported in an upcoming publication of the author and the Fittino collaboration [153].

5.4. Spontaneous R-Parity violation in the CBLSSM

Undesired minima do not always have to be those breaking electric charge or color. As we saw in section 3.10, the BLSSM is a model constructed with R-parity conservation in mind. The introduction of the bilepton fields gives us particles that can break $U(1)_{B-L}$ (a symmetry we

Parameter	Range			Step size
m_0	0 GeV	–	3000 GeV	100 GeV
$M_{1/2}$	0 GeV	–	3000 GeV	100 GeV
A_0	−5000 GeV	–	5000 GeV	100 GeV
$\tan\beta$	2	–	60	2

Table 5.2.: Parameter range for the scan performed to implement vacuum stability for parameter fit studies of the CMSSM. `Vevacious` was then run in all the resulting spectra for stop and stau VEVs and straight path between minima. The sign of μ was fixed to +1.

want to break) but without breaking R-parity (a symmetry we might want to conserve).
A great deal of the phenomenology of a SUSY model relies on the conservation or violation of R-parity. Thus it is very important to be certain about the state of this symmetry for a given parameter point.
Although the bilepton fields get VEVs and might take the responsibility of breaking $U(1)_{B-L}$, sneutrinos are not exempt of doing so as well. However, sneutrino VEVs would generate R-parity-violating terms in the Lagrangian. It is therefore interesting to explore under which conditions this is possible.
So the question to answer will be what portion of the parameter points which have a phenomenologically acceptable, R-parity-conserving DSB minimum will have deeper minima and whether those will break R-parity or any other symmetry when allowing the possibility of sneutrino VEVs. In this case DSB minima will be those which only have expectation values for the Higgs doublet fields H_d, H_u and the bilepton fields $\eta, \bar{\eta}$ (leading to the correct values for m_W and m_Z).
To answer this question we performed a random scan over a range of input parameters constrained to having phenomenologically acceptable, R-parity-conserving DSB minima at expectation values for H_d, H_u, η, $\bar{\eta}$ given as input. We then applied our framework allowing non-zero sneutrino VEVs and calculating tunneling times at zero temperature.

5.4.1. Generation of parameter points

We used `SARAH` to create a `SPheno` executable specific to the CBLSSM, which was used with the `SSP` package [112] to perform random scans over two different parameter regions.
The first scan, in the following referred as the "democratic" scan, took random values for each diagonal entry of the R-sneutrino – bilepton Yukawa coupling Y_x independently over its range. The other scan, which we will refer to as the "hierarchical" scan, kept the $(1,1)$ and $(2,2)$ entries as 10^{-3} and 10^{-2} respectively. It was motivated by the hierarchy of the quark and charged lepton Yukawa couplings. We show the parameter ranges of each scan in Tab. 5.3.
We chose mass parameter ranges consistent with the lack of observed SUSY particles at LEP and LHC by requiring squarks and gluinos to be above one TeV. [3] [4] but still in ranges where effects

[3] In [36] the bounds on $m_{Z'}$ are shown to be about 300 GeV lower than claimed by the LHC experiments when gauge kinetic mixing is accounted for properly.
[4] The results reported here are a product of work done before updated bounds on SUSY searches were published. The latest relevant results by the ATLAS collaboration can be found in [154] where a lower limit of 1650 GeV

Parameter	Common to both
$M_{1/2}$	250 – 1000
M_0	100 – 3000
A_0	-3000 – 3000
$\tan\beta$	3 – 45
$m_{Z'}$	1500 – 3000
$\tan\beta'$	1.0 – 1.5

Parameter	Democratic	Hierarchical
Y_x^{11}	0.05 – 0.6	fixed 10^{-3}
Y_x^{22}	0.05 – 0.6	fixed 10^{-2}
Y_x^{33}	0.05 – 0.6	0.1 – 0.6

Table 5.3.: Ranges of parameters used in generating the samples. All dimensionful quantities are to be read as in units of GeV. The signs of μ and μ' were fixed to both be positive. The democratic scan consisted of 2330 points, the hierarchical of 1640 points.

Category	Description
"RPC"	$SU(2)_L$, $U(1)_{B-L}$ both broken, R-parity conserved.
"RPV"	$SU(2)_L$, $U(1)_{B-L}$ both broken, R-parity broken.
"unbroken"	Either $SU(2)_L$ or $U(1)_{B-L}$ broken but not both, R-parity conserved.

Table 5.4.: Categorization of parameter points according to the symmetries broken by their global minima in the BLSSM.

from the model might be observed in the close future. The couplings were chosen to cover the perturbative range. Using `SPheno` we then generated SUSY spectra for parameter points over the full described region where R-parity is possibly conserved.

As expected, each parameter point had several minima that both conserved and violated R-parity. We categorized the points by the nature of the lowest of their minima as shown in Tab. 5.4. The result of this categorization is shown in Tab. 5.5. Each parameter point of our scan fell into only one of the categories. In other words, there were no points which had a global minimum with no unbroken symmetries, and there were no points which broke R-parity without breaking both $SU(2)_L$ and $U(1)_{B-L}$. The points we label "RPC" did not have R-parity-violating vacua deeper than the DSB one and most of the "RPV" points broke R-parity by having deeper minima with sneutrino VEVs. There were six points in the hierarchical scan with panic vacua showing negative stop mass-squared. As we did not allow the possibility of stop VEVs for this study, we assume this is a sign of a direction along which stop VEVs will develop. We plot them together with other "RPV" points, as stop VEVs also imply R-parity violation (together with $SU(3)_c$ and $U(1)_{em}$ breaking).

The third category, "unbroken", appears when considering the one-loop effective potential. For specially pathological parameter points, it has been shown that the one-loop effective potential

for equal mass light-flavour squarks and gluinos is found for the scenario with a massless $\tilde{\chi}_1^0$.

Category	Hierarchical scan		Democratic scan	
total	1640		2330	
	tree level	one-loop level	tree level	one-loop level
"RPC"	1422	1275	2236	2167
"RPV"	218	212	94	86
"unbroken"	0	153	0	77

Table 5.5.: Number of parameter points in the various categories. All of the parameter points from both scans categorized as "unbroken" broke $SU(2)_L$ without breaking $U(1)_{B-L}$. Not all parameter points that are "RPC" at the one-loop level were "RPC" at tree level, and likewise for the "RPV" category.

might restore symmetries that are broken at tree level [155]. This is the case for such "unbroken" parameter points, where at the one-loop level there is a deeper minimum conserving either $U(1)_{B-L}$ or $SU(2)_L$. We note that all such points we found had zero sneutrino VEVs.

By looking at Figs. 5.16-5.19 it is clear that R-parity-violating points are scattered almost all over parameter space. If we restrict ourselves to a tree level analysis, it is easy to find regions of parameter space for which no deeper R-parity-violating minima exist. In tune with our developed intuition these regions lie where the R-sneutrino-bilepton Yukawa coupling Y_x is not so large, and the trilinear soft SUSY-breaking parameter A_0 is small compared to M_0. Analogously to the stop case discussed in the CMSSM, large A_0 can lead to large negative contributions to the potential energy but in this case for large values of v_R and $v_{\eta/\bar{\eta}}$. Conversely, high values of M_0 induce high values for $m^2_{\tilde{\nu}^c}$ which, if positive have a tendency to avoid minima with v_R values. This pattern is evident in both sets of scans as visible again in Figs. 5.16-5.19.

One of the main conclusions from our previous analyses is the fact that loop corrections to the potential are important for vacuum stability. In the case of the CBLSSM the regions where R-parity appears to be safe at tree level have $SU(2)_L$ and $U(1)_{B-L}$ breaking that does not survive loop corrections. Although parameter points often preserved R-parity at tree level, for many points all over parameter space, panic R-parity-violating vacua happened to lie lower than the DSB once one-loop effects where included.

For the CBLSSM it turns out that the additional new particles of the $B-L$ sector also play an important role in vacuum stability. Experimental bounds require the mass of the Z' boson to be in the multi-TeV range. This implies that the bilepton VEVs $v_\eta, v_{\bar{\eta}}$ have to also be in this range due to their contribution the the Z' mass. For $\tan\beta' \neq 1$ these VEVs give SUSY-breaking D-term contributions to the masses and, as they are much larger than the MSSM sector, the corresponding loop contributions to the potential are thus important. These contributions are also responsible for the observed restoration of $U(1)_{B-L}$ at the one-loop level for some parameter points as they lift the potential considerably for minima with bilepton VEVs.

This complements the discussions in [42, 43] where it is shown that at least one entry of Y_x has to be large to achieve the breaking of $U(1)_{B-L}$. From our results we conclude that one-loop contributions from the additional $B-L$ sector are more important for points in the hierarchical scan as in that case they drive a larger set of points from the global tree level R-parity-conserving minimum to the deeper R-parity-violating minimum at one-loop level. This is no surprise as for those points a single Y_x entry gives the most contribution to $\mathrm{Tr}[Y_x]$ and thus is correspondingly larger than the average of the democratic scan.

5.4.2. Comparison with previous results in the literature

The issue of R-parity breaking in the BLSSM parameter space has been previously studied in [42]. There the authors, following a close analogy with the Higgs sector, conclude that the condition of positive squared Soft SUSY breaking masses for the R-sneutrinos is a necessary and sufficient condition for no spontaneous breaking of R-parity.
By looking at Figs. 5.17 and 5.19 it is evident that although there is a general tendency, positive $m^2_{\tilde{\nu}^c}$ is not a necessary nor sufficient condition for R-parity conservation. By looking at these plots, one can see that there are points with negative $m^2_{\tilde{\nu}^c}$ that conserve R-parity and conversely points with positive $m^2_{\tilde{\nu}^c}$ that break R-parity spontaneously through sneutrino VEVs.
To understand R-parity conservation for $m^2_{\tilde{\nu}^c} < 0$, one has to remember that the relevant parameters to consider are the eigenvalues of the mass matrix. They can be all positive due to contributions of the F-terms, D-terms and other soft SUSY-breaking terms coming from non-zero bilepton VEVs despite negative $m^2_{\tilde{\nu}^c}$ entries. For example, in the case of only the third generation sneutrinos getting VEVs, the $(\tilde{\nu}^c_3, \tilde{\nu}^c_3)$ element of the tree level scalar mass-squared matrix is given by (we have suppressed the generation index for simplicity):

$$\begin{aligned} m^2_{(\tilde{\nu}^c_3,\tilde{\nu}^c_3)} &= m^2_{\tilde{\nu}^c} + \frac{1}{2}\left(v_L^2 + v_u^2\right)|Y_\nu|^2 - \sqrt{2}v_{\bar{\eta}}\Re\left(Y_x\mu'^*\right) + \sqrt{2}v_\eta\Re\left(T_x\right) + \left(2v_\eta^2 + 3v_R^2\right)|Y_x|^2 \\ &\quad + \frac{1}{8}\Big(\bar{g}g_{BL}\left(v_u^2 - v_d^2 - v_L^2\right) + g^2_{BL}\left(2\left(v_{\bar{\eta}}^2 - v_\eta^2\right) + 3v_R^2 - v_L^2\right)\Big). \end{aligned} \tag{5.2}$$

The case of R-parity violation with positive $m^2_{\tilde{\nu}^c}$ is easier to understand, as the presence of trilinear terms can lower the potential significantly for reasonably large values of sneutrino and bilepton VEVs. The full set of mass matrices for the BLSSM is given in appendix B.
In Ref. [42] starting by the fact that R-parity violation is driven by the sign of $m^2_{\tilde{\nu}^c}$, the authors conclude that a hierarchical Y_x would lead always to spontaneous R-parity breaking. They argue that because of the way Y_x enters the RGEs, hierarchical values would always drive $m^2_{\tilde{\nu}^c}$ negative before the bilepton mass-squared parameters. Both our previous discussion on $m^2_{\tilde{\nu}^c}$ and the subsequent large fraction of "RPC" points in our hierarchical scan refutes this claim. However, such points are harder to find (as shown by the smaller number of valid points found for the hierarchical scan compared to the democratic scan), and are in some sense finely tuned, as is evident from the large fraction of "unbroken" points. Nevertheless, around half of the hierarchical points conserve R-parity even at the one-loop level.
There is a subtle difference between our analysis and the one in Ref. [42]: We generated points that were naïvely R-parity-conserving, i.e. they were engineered to have a local minimum with the correct set of R-parity-conserving VEVs and explored whether they had deeper panic vacuum elsewhere. In contrast Ref. [42] explored various GUT-scale parameter configurations in the Yukawa sector for two points in the soft SUSY-breaking parameters to see whether RGE running would lead to a negative $m^2_{\tilde{\nu}^c}$. Since we started with a set of parameters engineered to have an R-parity-conserving local minimum it is no surprise that our results show a low tendency for R-parity violation. However, our conclusions are still valid in that they show that the statements about R-parity violation depending on the sign of $m^2_{\tilde{\nu}^c}$ are not valid even in a mostly R-parity-conserving region of the parameter space.
Finally, we examined whether the "RPC" minima of the "RPV" points were long-lived with respect to the age of the Universe. As can be deduced from looking at the difference between Figs. 5.16 and 5.19, there is no clear pattern to differentiate short and long-lived regions. This is again a sign that a full numerical study is unavoidable if one wants to get a definite answer about

spontaneous R-parity breaking in the BLSSM. The results of this study have been reported in [156].

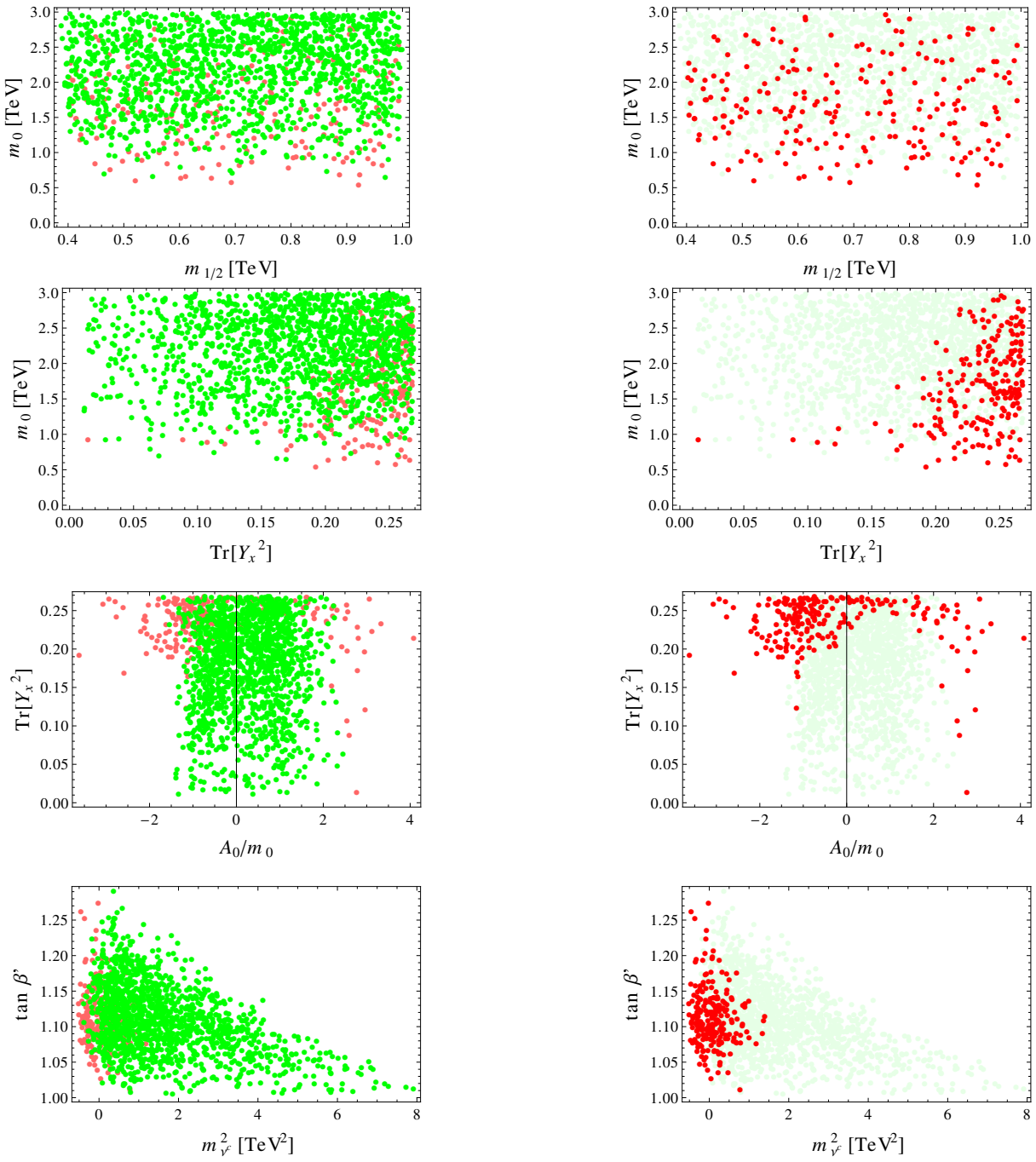

Figure 5.16.: Projections into various parameter planes of the 1640 hierarchical scan parameter points, categorized by the nature of their global minima (see Tab. 5.4) at tree level. "RPC" points are plotted in green, and "RPV" points are plotted in red. In the plots on the left, the "RPC" points are plotted on top of the "RPV" points, which are faded, while in the plots on the right the "RPV" points are plotted on top of the "RPC" points, which are faded. $m^2_{\tilde{\nu}^c}$ is the lowest or most negative of the three soft SUSY-breaking mass-squared parameters for the R-sneutrinos, evaluated at the SUSY scale.

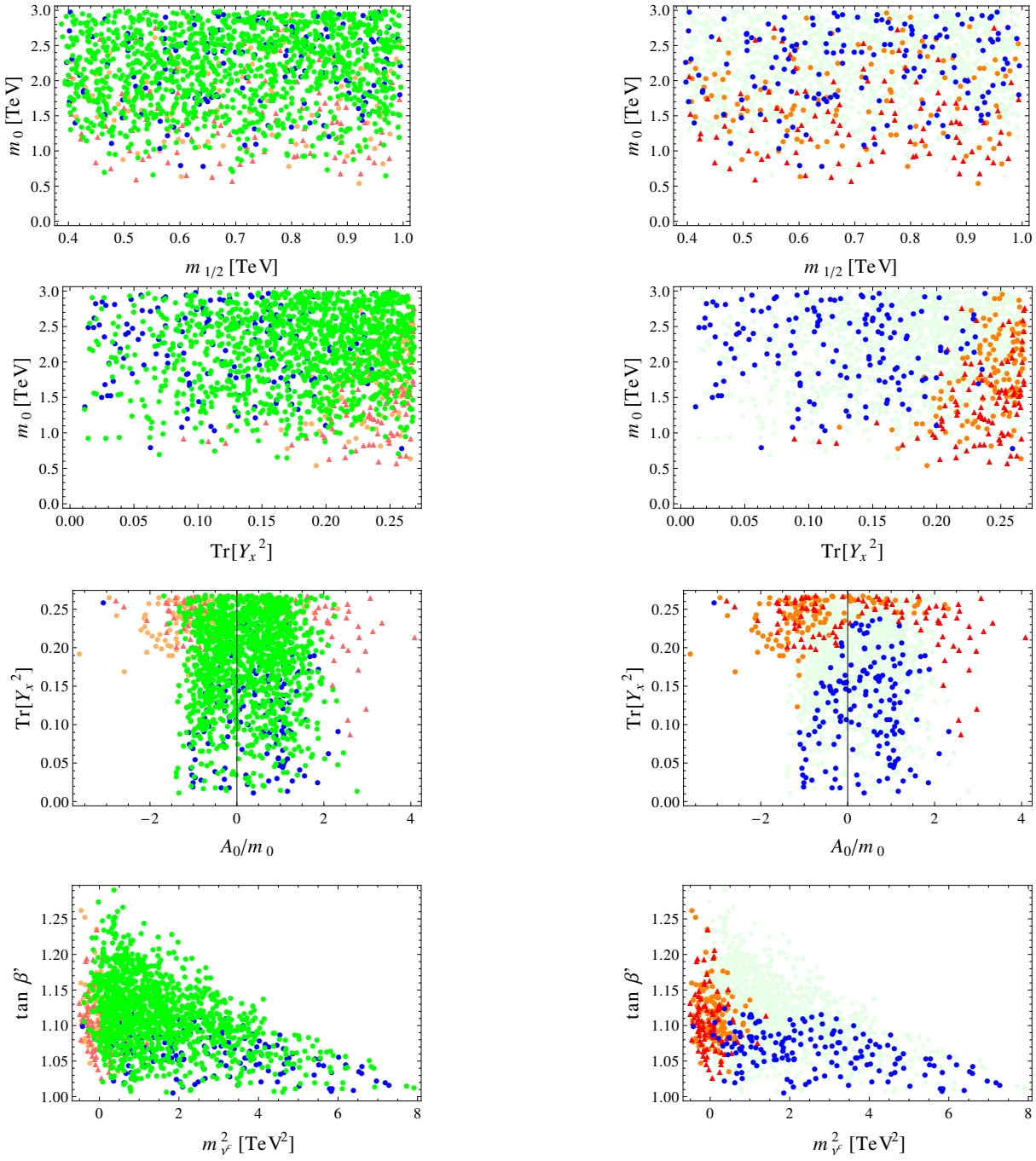

Figure 5.17.: Projections into various parameter planes of the 1640 hierarchical scan parameter points, categorized by the nature of their global minima (see Tab. 5.4) at one-loop level. As in Fig. 5.16 "RPC" points are plotted in green, but now the "RPV" points are in two groups based on the tunneling time from the "RPC" input minimum to the deeper "RPV" minimum: lower than one tenth of the age of the Universe as orange circles, greater than a tenth of the age of the Universe as red triangles. "Gauge conserving" points are in blue.

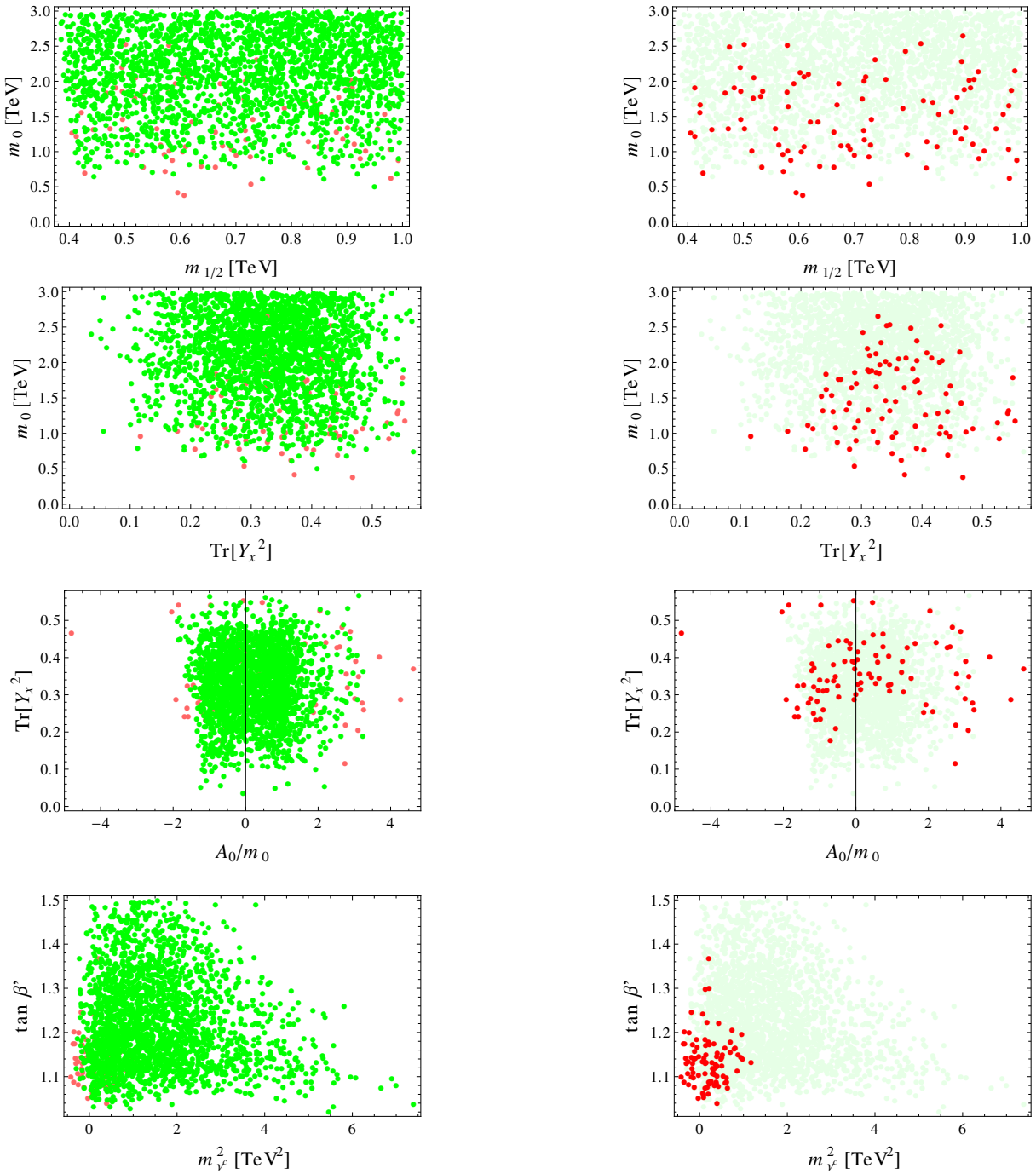

Figure 5.18.: Projections into various parameter planes of the 2330 democratic scan parameter points, categorized by the nature of their global minima (see Tab. 5.4) at tree level. The scheme is the same as in Fig. 5.16.

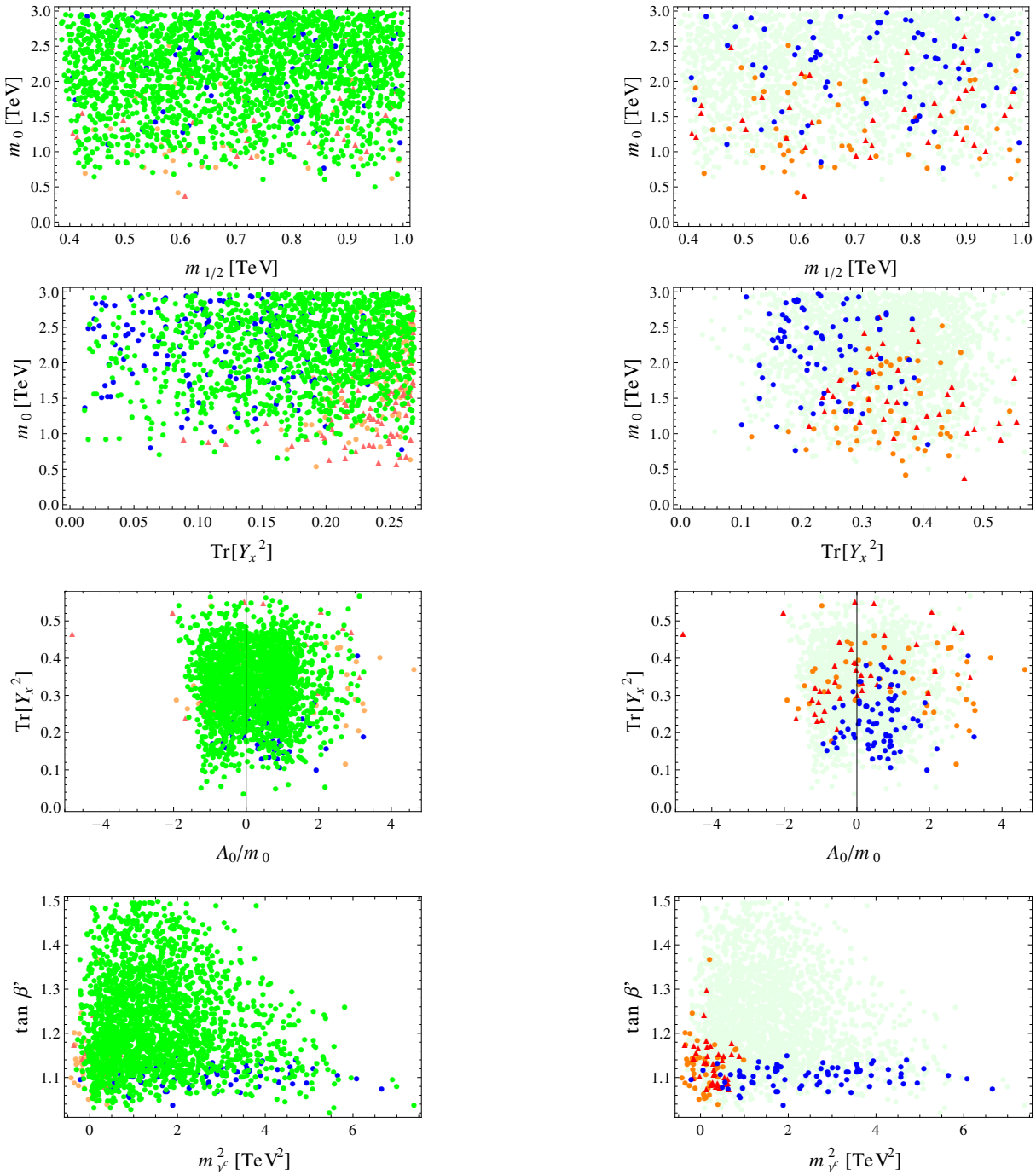

Figure 5.19.: Projections into various parameter planes of the 2330 democratic scan parameter points, categorized by the nature of their global minima (see Tab. 5.4) at one-loop level. The scheme is the same as in Fig. 5.17.

CHAPTER SIX

CONCLUSIONS

We have proposed a way to study the vacuum structure of a given model by combining the power of the Homotopy continuation method for finding the minima of the tree level potential, the minuit algorithm for numerical minimization of the one-loop effective potential and numerical methods to solve the problem of calculating the tunneling time between minima at zero and non-zero temperature.

The implementation of this framework resulted in the code `Vevacious`. Given a model and a parameter point with a reasonable candidate for a DSB minimum, it is then possible to use `Vevacious` to determine whether there exists a deeper panic vacuum at the one-loop level with VEVs that break symmetries we want to conserve and calculate the tunneling time from the DSB vacuum. With this information it is possible to exclude parameter points by requiring a stable or long-lived DSB minimum.

In general we found that a numerical study is inevitable in any serious phenomenological study. Previous attempts at including vacuum stability constraints through simple analytical rules do not hold well against any of our numerical studies. In most cases such naïve analytical conditions fail to meaningfully discriminate regions of parameter space with dangers of color-, charge- and R-parity breaking minima.

Specifically for the CMSSM we found that when stau and stop VEVs are allowed, regions otherwise favored by experiment are in direct conflict with vacuum stability constraints. By performing a conservative analysis at zero temperature we were able to pinpoint dangerous regions of parameter space.

In particular, regions consistent with the measured Higgs mass showed a high prevalence of deeper color- and charge- breaking minima with a fraction of such points having a short-lived DSB vacuum. We also showed there is an important overlap between the stop and stau coannihilation regions i.e. the regions that allow for the correct relic dark matter density, and regions with deeper CCB vacua. This puts the CMSSM parameter space in even more tension with experiments as demanding the correct relic density for dark matter is a very stringent constraint in itself.

However we stress that our framework always finds an upper bound on the lifetime of the DSB and it is possible that for points reported as long-lived the lifetime is much shorter. This will depend on the ability of the path deformation routine to find the optimal tunneling path. Nevertheless, reported short-lived DSB vacua are definitely so, and their existence shows the importance of

taking vacuum stability seriously.
We then studied the vacuum stability of the natural MSSM when allowing for stop VEVs. Inspired by the results found for the CMSSM we explored the region allowing the correct Higgs mass for this pragmatic incarnation of the MSSM. By accounting for thermal effects, the probability of tunneling out of the DSB minimum increases and therefore exploring the dangerous region found to be long-lived in the CMSSM was a natural next step.
We found that when thermal fluctuations come into play, the region consistent with a Higgs mass around 125 GeV overlaps quite significantly with regions suffering from short-lived CCB minima.
As a third example we applied our framework to explore spontaneous breaking of R-parity in the BLSSM. This model was proposed as an extension of the MSSM with an extra $U(1)_{B-L}$ gauge group with the possibility of breaking it without inducing R-parity violation. We explored whether this was the case by studying where in parameter space deeper minima with R-parity-violating sneutrino VEVs would arise. Our results showed that R-parity is broken for regions thought to be R-parity-conserving in previous analyses. In particular, the assumption of negative $m^2_{\tilde{\nu}^c}$ for sneutrinos as a definite discriminator for R-parity violation was shown not to hold.
We also adapted our proposed framework for use in parameter fit studies by limiting ourselves to stop and stau VEVs with straight tunneling paths. We performed a very large scan over the CMSSM parameter space and constructed a database together with a C++ class to check parameter points against vacuum stability. It is then possible to use it in CMSSM parameter fit studies and include vacuum stability together with fitting other experimental data.
In conclusion, our proposed framework implements vacuum stability as a useful constraint and shows the importance of such type of studies. We can get information about a particular model and its parameter space by using `Vevacious` and significant constraints can be extracted from the results.

APPENDIX ONE

EXPLICIT FORMULAS FOR ONE-LOOP EFFECTIVE POTENTIALS

We present explicit formulas for the One-loop effective potential of the models studied in this work. In both cases we start by the expression 4.30 and by following closely the results in [157] we can cast the effective potential in the $\overline{DR}$ scheme for the models at hand.

A.1. The one-loop effective potential of the MSSM

For the case of the MSSM the one-loop effective potential is given by

$$
\begin{aligned}
16\pi^2 V_{eff}^{MSSM} = & -3\left(\sum_{i=1}^{3}\left(\frac{m_{d_i}^4}{4}\left[ln\left(\frac{m_{d_i}^2}{Q^2}\right)-\frac{3}{2}\right]\right)+\sum_{i=1}^{3}\left(\frac{m_{u_i}^4}{4}\left[ln\left(\frac{m_{u_i}^2}{Q^2}\right)-\frac{3}{2}\right]\right)\right) \\
& +\frac{3}{2}\left(\sum_{i=1}^{6}\left(\frac{m_{\tilde{d}_i}^4}{4}\left[ln\left(\frac{m_{\tilde{d}_i}^2}{Q^2}\right)-\frac{3}{2}\right]\right)+\sum_{i=1}^{6}\left(\frac{m_{\tilde{u}_i}^4}{4}\left[ln\left(\frac{m_{\tilde{u}_i}^2}{Q^2}\right)-\frac{3}{2}\right]\right)\right) \\
& +\frac{3}{4}\left(\frac{m_W^4}{2}\left[ln\left(\frac{m_W^2}{Q^2}\right)+\frac{3}{2}\right]+\frac{m_Z^4}{4}\left[ln\left(\frac{m_Z^2}{Q^2}\right)-\frac{3}{2}\right]\right) \\
& -\sum_{i=1}^{2}\left(\frac{m_{\tilde{\chi}_i^\pm}^4}{4}\left[ln\left(\frac{m_{\tilde{\chi}_i^\pm}^2}{Q^2}\right)-\frac{3}{2}\right]\right)-\sum_{i=1}^{3}\left(\frac{m_{e_i}^4}{4}\left[ln\left(\frac{m_{e_i}^2}{Q^2}\right)-\frac{3}{2}\right]\right)-\frac{1}{2}\sum_{i=1}^{4}\left(\frac{m_{\tilde{\chi}_i^0}^4}{4}\left[ln\left(\frac{m_{\tilde{\chi}_i^0}^2}{Q^2}\right)-\frac{3}{2}\right]\right) \\
& +\frac{1}{4}\left(\sum_{i=1}^{2}\left(\frac{m_{h_i}^4}{4}\left[ln\left(\frac{m_{h_i}^2}{Q^2}\right)-\frac{3}{2}\right]\right)+\sum_{i=1}^{2}\left(\frac{m_{A_i^0}^4}{4}\left[ln\left(\frac{m_{A_i^0}^2}{Q^2}\right)-\frac{3}{2}\right]\right)\right) \\
& +\frac{1}{2}\sum_{i=1}^{6}\left(\frac{m_{\tilde{e}_i}^4}{4}\left[ln\left(\frac{m_{\tilde{e}_i}^2}{Q^2}\right)-\frac{3}{2}\right]\right)+\sum_{i=1}^{2}\frac{1}{2}\left(\frac{m_{H_i^\pm}^4}{4}\left[ln\left(\frac{m_{H_i^\pm}^2}{Q^2}\right)-\frac{3}{2}\right]\right). \qquad \text{(A.1)}
\end{aligned}
$$

We have included formally in the sums the would-be Goldstone-bosons to account for the fact that potentially the gauge group is broken only partially. This does not result in a double-counting because, in the Landau gauge, would-be Goldstone-bosons are massless and thus give a zero contribution to the one-loop effective potential.

The first two lines are the contributions from quarks and squarks. In the third line the loops including the gauge bosons are counted. The fourth line contains the contributions due to the chargino, lepton as well as neutralino states. The fifth and sixth lines show the contributions from charged slepton and Higgs states. As the gluino mass does not depend on the field values it can be thought as a constant shift and does not need to be taken into account.

A.2. The one-loop effective potential of the BLSSM

For the case of the BLSSM we have to extend the previous expression to accommodate the new particles added in this case. Explicitly we get:

$$\begin{aligned}
16\pi^2 V_{eff}^{BLSSM} = &-3\left(\sum_{i=1}^{3}\left(\frac{m_{d_i}^4}{4}\left[ln\left(\frac{m_{d_i}^2}{Q^2}\right)-\frac{3}{2}\right]\right)+\sum_{i=1}^{3}\left(\frac{m_{u_i}^4}{4}\left[ln\left(\frac{m_{u_i}^2}{Q^2}\right)-\frac{3}{2}\right]\right)\right)\\
&+\frac{3}{2}\left(\sum_{i=1}^{6}\left(\frac{m_{\tilde{d}_i}^4}{4}\left[ln\left(\frac{m_{\tilde{d}_i}^2}{Q^2}\right)-\frac{3}{2}\right]\right)+\sum_{i=1}^{6}\left(\frac{m_{\tilde{u}_i}^4}{4}\left[ln\left(\frac{m_{\tilde{u}_i}^2}{Q^2}\right)-\frac{3}{2}\right]\right)\right)\\
&+\frac{3}{4}\left(\frac{m_W^4}{2}\left[ln\left(\frac{m_W^2}{Q^2}\right)+\frac{3}{2}\right]+\frac{m_Z^4}{4}\left[ln\left(\frac{m_Z^2}{Q^2}\right)-\frac{3}{2}\right]+\frac{m_{Z'}^4}{4}\left[ln\left(\frac{m_{Z'}^2}{Q^2}\right)-\frac{3}{2}\right]\right)\\
&-\sum_{i=1}^{5}\left(\frac{m_{\tilde{\chi}_i^\pm}^4}{4}\left[ln\left(\frac{m_{\tilde{\chi}_i^\pm}^2}{Q^2}\right)-\frac{3}{2}\right]\right)-\frac{1}{2}\sum_{i=1}^{13}\left(\frac{m_{\tilde{\chi}_i^0}^4}{4}\left[ln\left(\frac{m_{\tilde{\chi}_i^0}^2}{Q^2}\right)-\frac{3}{2}\right]\right)\\
&+\frac{1}{4}\left(\sum_{i=1}^{10}\left(\frac{m_{h_i}^4}{4}\left[ln\left(\frac{m_{h_i}^2}{Q^2}\right)-\frac{3}{2}\right]\right)+\sum_{i=1}^{10}\left(\frac{m_{A_i^0}^4}{4}\left[ln\left(\frac{m_{A_i^0}^2}{Q^2}\right)-\frac{3}{2}\right]\right)\right)\\
&+\frac{1}{2}\sum_{i=1}^{8}\left(\frac{m_{\tilde{e}_i}^4}{4}\left[ln\left(\frac{m_{\tilde{e}_i}^2}{Q^2}\right)-\frac{3}{2}\right]\right). \qquad \text{(A.2)}
\end{aligned}$$

The first two lines are the contributions from quarks and squarks which are the same as for the MSSM. In the third line the loops including the three gauge bosons in the given model are counted. The fourth line contains the contributions due to the charged lepton-chargino as well as neutrino-neutralino mixed states. The fifth and sixth lines show the contributions from charged slepton-charged Higgs states as well as sneutrino-Higgs states. The tree-level mass matrices where R-parity violation induces a mixing between SM and SUSY particles are listed in appendix B. For completeness we note that in addition the sneutrino VEVs give contributions to the mass matrices of vector bosons and squarks.

APPENDIX TWO

MASS MATRICES OF THE BLSSM

Here we give the tree-level masses suppressing the generation indices of (s)neutrinos and (s)leptons.

- **Neutrino-Neutralino states**
  The mass matrix $m^2_{\tilde{\chi}^0}$ is given, in the basis

$$\left(\lambda_{\tilde{B}}, \tilde{W}^0, \tilde{H}^0_d, \tilde{H}^0_u, \nu_L, \nu^*_R, \tilde{\eta}, \tilde{\bar{\eta}}, \lambda_{\tilde{B}'}\right),$$

  by

$$\begin{pmatrix}
M_1 & 0 & -\frac{1}{2}g_1 v_d & \frac{1}{2}g_1 v_u & -\frac{1}{2}g_1 v_L & 0 & 0 & 0 & M_{BB'} \\
0 & M_2 & \frac{1}{2}g_2 v_d & -\frac{1}{2}g_2 v_u & \frac{1}{2}g_2 v_L & 0 & 0 & 0 & 0 \\
-\frac{1}{2}g_1 v_d & \frac{1}{2}g_2 v_d & 0 & -\mu & 0 & 0 & 0 & 0 & -\frac{1}{2}\bar{g} v_d \\
\frac{1}{2}g_1 v_u & -\frac{1}{2}g_2 v_u & -\mu & 0 & \frac{1}{\sqrt{2}} v_R Y_\nu & \frac{1}{\sqrt{2}} v_L Y_\nu & 0 & 0 & \frac{1}{2}\bar{g} v_u \\
-\frac{1}{2}g_1 v_L & \frac{1}{2}g_2 v_L & 0 & \frac{1}{\sqrt{2}} v_R Y_\nu & 0 & \frac{1}{\sqrt{2}} v_u Y_\nu & 0 & 0 & -\frac{1}{2}(\bar{g}+g_B) v_L \\
0 & 0 & 0 & \frac{1}{\sqrt{2}} v_L Y_\nu & \frac{1}{\sqrt{2}} v_u Y_\nu & \sqrt{2} v_\eta Y_x & \sqrt{2} v_R Y_x & 0 & \frac{1}{2} g_B v_R \\
0 & 0 & 0 & 0 & 0 & \sqrt{2} v_R Y_x & 0 & -\mu' & -g_B v_\eta \\
0 & 0 & 0 & 0 & 0 & 0 & -\mu' & 0 & g_B v_{\bar{\eta}} \\
M_{BB'} & 0 & -\frac{1}{2}\bar{g} v_d & \frac{1}{2}\bar{g} v_u & -\frac{1}{2}(\bar{g}+g_B) v_L & \frac{1}{2} g_B v_R & -g_B v_\eta & g_B v_{\bar{\eta}} & M_{B'}
\end{pmatrix}. \tag{B.1}$$

- **Charged lepton-Charginos**
  The mass matrix is given, in the basis

$$\left(e_L, \tilde{W}^-, \tilde{H}^-_d\right); \left(e^*_R, \tilde{W}^+, \tilde{H}^+_u\right)^T,$$

by

$$m^2_{\bar{\chi}^-} = \begin{pmatrix} \frac{1}{\sqrt{2}}v_d Y_e & \frac{1}{\sqrt{2}}g_2 v_L & -\frac{1}{\sqrt{2}}v_R Y_\nu \\ 0 & M_2 & \frac{1}{\sqrt{2}}g_2 v_u \\ -\frac{1}{\sqrt{2}}v_L Y_e & \frac{1}{\sqrt{2}}g_2 v_d & \mu \end{pmatrix}. \tag{B.2}$$

- **CP even sneutrino-Higgs**
  In the basis

$$(\sigma_d, \sigma_u, \sigma_L, \sigma_R, \sigma_\eta, \sigma_{\bar{\eta}}),$$

the entries of the mass matrix read:

$$m_{\sigma_d\sigma_d} = \frac{1}{8}\Big(\bar{g}g_{BL}\Big(2v_\eta^2 - 2v_{\bar{\eta}}^2 - v_R^2 + v_L^2\Big) + \Big(g_1^2 + \bar{g}^2 + g_2^2\Big)\Big(3v_d^2 - v_u^2 + v_L^2\Big)\Big) + m_{H_d}^2 + \mu^2 \tag{B.3}$$

$$m_{\sigma_d\sigma_u} = -B_\mu - \frac{1}{4}\Big(g_1^2 + \bar{g}^2 + g_2^2\Big)v_d v_u \tag{B.4}$$

$$\begin{aligned} m_{\sigma_u\sigma_u} = {} & m_{H_u}^2 + \frac{1}{8}\Big(\Big(-\bar{g}^2 - g_1^2 - g_2^2\Big)\Big(v_d^2 - 3v_u^2 + v_L^2\Big) + \bar{g}g_{BL}\Big(2v_{\bar{\eta}}^2 - 2v_\eta^2 - v_L^2 + v_R^2\Big)\Big) \\ & + \frac{1}{2}\Big(v_L^2 + v_R^2\Big)Y_\nu^2 + \mu^2 \end{aligned} \tag{B.5}$$

$$m_{\sigma_d\sigma_L} = \frac{1}{4}\Big(\bar{g}\Big(\bar{g} + g_{BL}\Big) + g_1^2 + g_2^2\Big)v_d v_L - \frac{1}{\sqrt{2}}v_R Y_\nu \mu \tag{B.6}$$

$$m_{\sigma_u\sigma_L} = -\frac{1}{4}\Big(\bar{g}\Big(\bar{g} + g_{BL}\Big) + g_1^2 + g_2^2\Big)v_L v_u + \frac{1}{\sqrt{2}}v_R T_\nu + Y_\nu\Big(v_L v_u Y_\nu + v_R v_\eta Y_x\Big) \tag{B.7}$$

$$\begin{aligned} m_{\sigma_L\sigma_L} = {} & m_L^2 + \frac{1}{8}\Big(\Big(g_1^2 + \bar{g}^2 + g_2^2\Big)\Big(3v_L^2 - v_u^2 + v_d^2\Big) + g_{BL}^2\Big(-2v_{\bar{\eta}}^2 + 2v_\eta^2 + 3v_L^2 - v_R^2\Big) \\ & + \bar{g}g_{BL}\Big(-2v_{\bar{\eta}}^2 + 2v_\eta^2 + 6v_L^2 - v_R^2 - v_u^2 + v_d^2\Big)\Big) + \frac{1}{2}\Big(v_R^2 + v_u^2\Big)Y_\nu^2 \end{aligned} \tag{B.8}$$

$$m_{\sigma_d\sigma_R} = -\frac{1}{4}\bar{g}g_{BL}v_d v_R - \frac{1}{\sqrt{2}}v_L Y_\nu \mu \tag{B.9}$$

$$m_{\sigma_u\sigma_R} = \frac{1}{4}\bar{g}g_{BL}v_R v_u + \frac{1}{\sqrt{2}}v_L T_\nu + Y_\nu\Big(v_L v_\eta Y_x + v_R v_u Y_\nu\Big) \tag{B.10}$$

$$m_{\sigma_L\sigma_R} = -\frac{1}{4}g_{BL}\Big(\bar{g} + g_{BL}\Big)v_L v_R + \frac{1}{\sqrt{2}}v_u T_\nu + v_L v_R Y_\nu^2 + Y_\nu\Big(-\frac{1}{\sqrt{2}}v_d\mu + v_u v_\eta Y_x\Big) \tag{B.11}$$

$$\begin{aligned} m_{\sigma_R\sigma_R} = {} & m_{\bar{\nu}^c}^2 - \frac{1}{8}g_{BL}\Big(\bar{g}\Big(-v_u^2 + v_d^2 + v_L^2\Big) + g_{BL}\Big(-2v_{\bar{\eta}}^2 + 2v_\eta^2 - 3v_R^2 + v_L^2\Big)\Big) \\ & + \frac{1}{2}\Big(2\Big(\sqrt{2}v_\eta T_x + Y_x\Big(\Big(2v_\eta^2 + 3v_R^2\Big)Y_x - \sqrt{2}\mu' v_{\bar{\eta}}\Big)\Big) + \Big(v_L^2 + v_u^2\Big)Y_\nu^2\Big) \end{aligned} \tag{B.12}$$

$$m_{\sigma_d\sigma_\eta} = \frac{1}{2}\bar{g}g_{BL}v_d v_\eta \tag{B.13}$$

$$m_{\sigma_u\sigma_\eta} = -\frac{1}{2}\bar{g}g_{BL}v_u v_\eta + v_L v_R Y_x Y_\nu \tag{B.14}$$

$$m_{\sigma_L\sigma_\eta} = \frac{1}{2}g_{BL}\Big(\bar{g} + g_{BL}\Big)v_L v_\eta + v_R v_u Y_x Y_\nu \tag{B.15}$$

$$m_{\sigma_R\sigma_\eta} = -\frac{1}{2}g_{BL}^2 v_R v_\eta + \sqrt{2}v_R T_x + Y_x\Big(4v_R v_\eta Y_x + v_L v_u Y_\nu\Big) \tag{B.16}$$

$$m_{\sigma_\eta\sigma_\eta} = 2v_R^2 Y_x^2 + \frac{1}{4}g_{BL}\Big(\bar{g}\Big(v_d^2 - v_u^2 + v_L^2\Big) + g_{BL}\Big(6v_\eta^2 - 2v_{\bar{\eta}}^2 - v_R^2 + v_L^2\Big)\Big) + m_\eta^2 + \mu'^2 \tag{B.17}$$

$$m_{\sigma_d\sigma_{\bar{\eta}}} = -\frac{1}{2}\bar{g}g_{BL}v_d v_{\bar{\eta}} \tag{B.18}$$

$$m_{\sigma_u\sigma_{\bar{\eta}}} = \frac{1}{2}\bar{g}g_{BL}v_u v_{\bar{\eta}} \tag{B.19}$$

$$m_{\sigma_L\sigma_{\bar{\eta}}} = -\frac{1}{2}g_{BL}\Big(\bar{g} + g_{BL}\Big)v_L v_{\bar{\eta}} \tag{B.20}$$

$$m_{\sigma_R\sigma_{\bar{\eta}}} = \frac{1}{2}g_{BL}^2 v_R v_{\bar{\eta}} - \sqrt{2}\mu' v_R Y_x \tag{B.21}$$

$$m_{\sigma_\eta\sigma_{\bar{\eta}}} = -B_{\mu'} - g_{BL}^2 v_\eta v_{\bar{\eta}} \tag{B.22}$$

$$m_{\sigma_{\bar{\eta}}\sigma_{\bar{\eta}}} = -\frac{1}{4}g_{BL}\Big(\bar{g}\Big(-v_u^2 + v_d^2 + v_L^2\Big) + g_{BL}\Big(2v_\eta^2 - 6v_{\bar{\eta}}^2 - v_R^2 + v_L^2\Big)\Big) + m_{\bar{\eta}}^2 + \mu'^2 \tag{B.23}$$

- **CP odd sneutrino-Higgs**
  In the basis $(\phi_d, \phi_u, \phi_L, \phi_R, \phi_\eta, \phi_{\bar{\eta}})$ and using Landau gauge, the nonzero entries of the mass matrix read:

$$m_{\phi_d\phi_d} = \frac{1}{8}\Big(\bar{g}g_{BL}\Big(2\Big(v_\eta^2 - v_{\bar{\eta}}^2\Big) - v_R^2 + v_L^2\Big) + \Big(g_1^2 + \bar{g}^2 + g_2^2\Big)\Big(v_d^2 - v_u^2 + v_L^2\Big)\Big) + m_{H_d}^2 + \mu^2 \tag{B.24}$$

$$m_{\phi_d\phi_u} = B_\mu \tag{B.25}$$

$$\begin{aligned} m_{\phi_u\phi_u} = {} & m_{H_u}^2 + \frac{1}{8}\Big(\Big(-\bar{g}^2 - g_1^2 - g_2^2\Big)\Big(-v_u^2 + v_d^2 + v_L^2\Big) + \bar{g}g_{BL}\Big(2v_{\bar{\eta}}^2 - 2v_\eta^2 - v_L^2 + v_R^2\Big)\Big) \\ & + \frac{1}{2}\Big(v_L^2 + v_R^2\Big)Y_\nu^2 + \mu^2 \end{aligned} \tag{B.26}$$

$$m_{\phi_d\phi_L} = -\frac{1}{\sqrt{2}}v_R Y_\nu \mu \tag{B.27}$$

$$m_{\phi_u\phi_L} = -\frac{1}{2}v_R\Big(2v_\eta Y_x Y_\nu + \sqrt{2}T_\nu\Big) \tag{B.28}$$

$$\begin{aligned} m_{\phi_L\phi_L} = {} & m_L^2 + \frac{1}{8}\Big(\Big(g_1^2 + \bar{g}^2 + g_2^2\Big)\Big(v_d^2 - v_u^2 + v_L^2\Big) + \bar{g}g_{BL}\Big(2\Big(v_L^2 + v_\eta^2 - v_{\bar{\eta}}^2\Big) - v_R^2 - v_u^2 + v_d^2\Big) \\ & + g_{BL}^2\Big(2\Big(-v_{\bar{\eta}}^2 + v_\eta^2\Big) - v_R^2 + v_L^2\Big)\Big) + \frac{1}{2}\Big(v_R^2 + v_u^2\Big)Y_\nu^2 \end{aligned} \tag{B.29}$$

$$m_{\phi_d\phi_R} = -\frac{1}{\sqrt{2}}v_L Y_\nu \mu \tag{B.30}$$

$$m_{\phi_u\phi_R} = v_L\Big(\frac{1}{\sqrt{2}}T_\nu - v_\eta Y_x Y_\nu\Big) \tag{B.31}$$

$$m_{\phi_L\phi_R} = \frac{1}{\sqrt{2}}v_u T_\nu + Y_\nu\Big(-\frac{1}{\sqrt{2}}v_d\mu - v_u v_\eta Y_x\Big) \tag{B.32}$$

$$\begin{aligned} m_{\phi_R\phi_R} = {} & m_{\tilde{\nu}^c}^2 + \frac{1}{8}g_{BL}\Big(-\bar{g}\Big(-v_u^2 + v_d^2 + v_L^2\Big) + g_{BL}\Big(2v_{\bar{\eta}}^2 - 2v_\eta^2 - v_L^2 + v_R^2\Big)\Big) \\ & + \frac{1}{2}\Big(-2\sqrt{2}v_\eta T_x + 2Y_x\Big(\Big(2v_\eta^2 + v_R^2\Big)Y_x + \sqrt{2}\mu' v_{\bar{\eta}}\Big) + \Big(v_L^2 + v_u^2\Big)Y_\nu^2\Big) \end{aligned} \tag{B.33}$$

$$m_{\phi_u\phi_\eta} = v_L v_R Y_x Y_\nu \tag{B.34}$$

$$m_{\phi_L\phi_\eta} = v_R v_u Y_x Y_\nu \tag{B.35}$$

$$m_{\phi_R\phi_\eta} = \sqrt{2} v_R T_x + v_L v_u Y_x Y_\nu \tag{B.36}$$

$$m_{\phi_R\phi_{\bar{\eta}}} = \sqrt{2}\mu' v_R Y_x \tag{B.37}$$

$$m_{\phi_\eta\phi_\eta} = 2v_R^2 Y_x^2 + \frac{1}{4} g_{BL}\Big(\bar{g}\Big(v_d^2 - v_u^2 + v_L^2\Big) + g_{BL}\Big(2\Big(v_\eta^2 - v_{\bar{\eta}}^2\Big) - v_R^2 + v_L^2\Big)\Big) + m_\eta^2 + \mu'^2 \tag{B.38}$$

$$m_{\phi_{\bar{\eta}}\phi_{\bar{\eta}}} = \frac{1}{4} g_{BL}\Big(- \bar{g}\Big(- v_u^2 + v_d^2 + v_L^2\Big) + g_{BL}\Big(2v_{\bar{\eta}}^2 - 2v_\eta^2 - v_L^2 + v_R^2\Big)\Big) + m_{\bar{\eta}}^2 + \mu'^2 \tag{B.39}$$

- **Charged slepton - charged Higgs**
  In the basis

$$\left(H_d^-, H_u^{+,*}, \tilde{e}_L, \tilde{e}_R\right),$$

the entries of the mass matrix read:

$$\begin{aligned} m_{H_d^- H_d^{-,*}} = {} & m_{H_d}^2 + \frac{1}{8}\Big(\bar{g} g_{BL}\Big(2\Big(- v_{\bar{\eta}}^2 + v_\eta^2\Big) - v_R^2 + v_L^2\Big) + \Big(g_1^2 + \bar{g}^2\Big)\Big(- v_u^2 + v_d^2 + v_L^2\Big) \\ & + g_2^2\Big(- v_L^2 + v_d^2 + v_u^2\Big)\Big) + \frac{1}{2} v_L^2 Y_e^2 + \mu^2 \end{aligned} \tag{B.40}$$

$$m_{H_d^{-\,b} H_u^+} = \frac{1}{4} g_2^2 v_d v_u + B_\mu \tag{B.41}$$

$$\begin{aligned} m_{H_u^{+,*} H_u^+} = {} & m_{H_u}^2 + \frac{1}{8}\Big(\Big(- \bar{g}^2 - g_1^2\Big)\Big(- v_u^2 + v_d^2 + v_L^2\Big) + \bar{g} g_{BL}\Big(2v_{\bar{\eta}}^2 - 2v_\eta^2 - v_L^2 + v_R^2\Big) \\ & + g_2^2\Big(v_d^2 + v_L^2 + v_u^2\Big)\Big) + \frac{1}{2} v_R^2 Y_\nu^2 + \mu^2 \end{aligned} \tag{B.42}$$

$$m_{H_d^- \tilde{e}_L^*} = -\frac{1}{2} v_d v_L Y_e^2 + \frac{1}{4} g_2^2 v_d v_L - \frac{1}{\sqrt{2}} v_R Y_\nu \mu \tag{B.43}$$

$$m_{H_u^{+,*} \tilde{e}_L^*} = -\frac{1}{2} Y_\nu\Big(2 v_R v_\eta Y_x + v_L v_u Y_\nu\Big) + \frac{1}{4} g_2^2 v_L v_u - \frac{1}{\sqrt{2}} v_R T_\nu \tag{B.44}$$

$$\begin{aligned} m_{\tilde{e}_L \tilde{e}_L^*} = {} & m_L^2 + \frac{1}{8}\Big(\Big(g_1^2 + \bar{g}^2\Big)\Big(v_d^2 - v_u^2 + v_L^2\Big) + g_2^2\Big(v_L^2 - v_d^2 + v_u^2\Big) + \frac{1}{2}\Big(v_d^2 Y_e^2 + v_R^2 Y_\nu^2\Big) \\ & + \bar{g} g_{BL}\Big(- 2v_{\bar{\eta}}^2 + 2\Big(v_L^2 + v_\eta^2\Big) - v_R^2 - v_u^2 + v_d^2\Big) + g_{BL}^2\Big(2\Big(- v_{\bar{\eta}}^2 + v_\eta^2\Big) - v_R^2 + v_L^2\Big)\Big) \end{aligned} \tag{B.45}$$

$$m_{H_d^- \tilde{e}_R^*} = -\frac{1}{2} v_R v_u Y_e Y_\nu - \frac{1}{\sqrt{2}} v_L T_e \tag{B.46}$$

$$m_{H_u^{+,*} \tilde{e}_R^*} = -\frac{1}{2} Y_e\Big(\sqrt{2} v_L \mu + v_d v_R Y_\nu\Big) \tag{B.47}$$

$$m_{\tilde{e}_L \tilde{e}_R^*} = \frac{1}{\sqrt{2}}\Big(v_d T_e - v_u Y_e \mu\Big) \tag{B.48}$$

$$\begin{aligned} m_{\tilde{e}_R \tilde{e}_R^*} = {} & m_E^2 + \frac{1}{8}\Big(- \Big(2\bar{g} + g_{BL}\Big)\Big(\bar{g}\Big(- v_u^2 + v_d^2 + v_L^2\Big) + g_{BL}\Big(- 2v_{\bar{\eta}}^2 + 2v_\eta^2 - v_R^2 + v_L^2\Big)\Big) \\ & - 2g_1^2\Big(- v_u^2 + v_d^2 + v_L^2\Big)\Big) + \frac{1}{2}\Big(v_d^2 + v_L^2\Big) Y_e^2 \end{aligned} \tag{B.49}$$

We write only independent entries as the matrix is Hermitian thus $m_{ij}^2 = (m_{ji}^2)^*$.

APPENDIX THREE

C++ CODE FOR IMPLEMENTING `VEVACIOUS` IN PARAMETER FIT STUDIES

The following code was written in order to implement results coming from `Vevacious` into a C++ class that can be easily added to any existing code. It is assumed that a large parameter space scan and `Vevacious` analysis has been performed and the results have been parsed and written to a file where each line has the format

$$m_0,\, m_{1/2},\, \tan\beta,\, sign(\mu),\, A_0,\, s,\, l \tag{C.1}$$

where $s \in \{-1, 0, 1\}$ is the stability result with a threshold of 1% survival probability (1 for stable, 0 for long-lived and -1 for short-lived points) and l is -1 for stable points, 10^6 for long-lived points and the lifetime of the DSB minimum in universe ages for short-lived points. In this way the user can always implement more stringent thresholds regarding the survival probability. The data file has to be read only once which speeds up the process considerably. A large scan for the CMSSM has already been performed by the author as referred in section 5.3.
The code then uses that information and provides two functions, `Check.Lifetime` and `Check.Stability`. Given input values for a CMSSM point, both functions calculate the closest point in parameter space that is in the scan. `Check.Lifetime` will then report l and `Check.Stability` will report s.

C.1. `CheckVacuum` C++ class

```
/* file CheckVacuum.h
* Header containing class CheckVacuum. This class reads in a data file
* containing vacuum stability information from Vevacious and gives
* a result for a given parameter point.
* In essence it takes the data file and given the 5 parameters m_0 m_1/2
* tan(beta) sign(mu) and A_0 it gives you the lifetime/stability of the
* desired phenomenological minimum.
*
*     Author: Jose Eliel Camargo-Molina (Elielx AT gmail.com)
*     Copyright 2014 J. E. Camargo-Molina
```

```
 */

#include <cstdio>
#include <cstdlib>
#include <stdexcept>
#include <vector>
#include <iostream>
#include <fstream>
#include <cmath>
#include <algorithm>


class CheckVacuum

  {
    //Matrix containing data from grid.
    std::vector < std::vector < double > > DataMatrix;
    //Ranges of parameters in the grid, determined automatically from data.
    double mzeroRange, mhalfRange, TanBRange, AzeroRange;
    double Entry (double mzero_in, double mhalf_in, double TanB_in, double SignMu_in
    , double Azero_in, int index );


    public:
      // Constructor where the filename of the data file is given.
      CheckVacuum (std::string);

      //function that outputs lifetime data for given parameter point
      double Lifetime (double mzero_in, double mhalf_in, double TanB_in, double
          SignMu_in
      , double Azero_in)
      { return Entry( mzero_in, mhalf_in, TanB_in, SignMu_in , Azero_in, 6); }
      //function that outputs stability data for given parameter point
      int Stability (double mzero_in, double mhalf_in, double TanB_in, double SignMu_in
      , double Azero_in)
      { return Entry( mzero_in, mhalf_in, TanB_in, SignMu_in , Azero_in, 5); }


  };

inline CheckVacuum::CheckVacuum (std::string Datafile)

    {

   std::ifstream StabilityDataFile(Datafile.c_str());// Opening and reading data file
       from grid.

   if(!StabilityDataFile) // Check if file is opened.
     {
              std::cout<<"Error opening stability data file"<<std::endl;
              exit(EXIT_FAILURE); //abort program
     }
```

```
while( StabilityDataFile.good() )
{
  std::vector<double> Parpoint; // Vector to hold MINPAR + Stability + lifetime

  double mzero, mhalf, TanB, SignMu, Azero, StableQ, Lifetime; // MINPAR
      parameters, Stability and lifetime
       // Reading from data file into variables
  StabilityDataFile >> mzero >> mhalf >> TanB >> SignMu >> Azero >> StableQ >>
      Lifetime;
  Parpoint.push_back(mzero); // saving variables into vector Parpoint
  Parpoint.push_back(mhalf);
  Parpoint.push_back(TanB);
  Parpoint.push_back(SignMu);
  Parpoint.push_back(Azero);
  Parpoint.push_back(StableQ);
  Parpoint.push_back(Lifetime);

  DataMatrix.push_back(Parpoint); // Storing Vector into DataMatrix



}


    //Finding range of parameters from data for weighted distance.

  std::vector<double> mzeroData, mhalfData, TanBData, AzeroData;

  for(int k=0;k< DataMatrix.size();k++)
  {
    mzeroData.push_back(DataMatrix[k][0]);
    mhalfData.push_back(DataMatrix[k][1]);
      TanBData.push_back(DataMatrix[k][2]);
      AzeroData.push_back(DataMatrix[k][4]);
  }

  mzeroRange = *max_element(mzeroData.begin(),mzeroData.end());
  mhalfRange = *max_element(mhalfData.begin(),mhalfData.end());
  TanBRange = *max_element(TanBData.begin(),TanBData.end());
  AzeroRange = *max_element(AzeroData.begin(),AzeroData.end());


   }


   inline double CheckVacuum::Entry (double mzero_in, double mhalf_in, double
   TanB_in, double SignMu_in , double Azero_in, int index)
    // Finding the closest points in the .dat file to the input point to check
  {
```

```
   std::vector<double> Distances;

   for (int j=0;j< DataMatrix.size();j++)
   {
   double Distance=0;
   double SignMuCondition=DataMatrix[j][3]- SignMu_in;
   //Checks if input point and data have the same sign(mu)
   if(SignMuCondition == 0) // if they do, calculate normalized distance.
   {
   Distance = std::pow(DataMatrix[j][0]-mzero_in,2)/mzeroRange +
   std::pow(DataMatrix[j][1]-mhalf_in,2)/std::pow(mhalfRange,2) +
   std::pow(DataMatrix[j][2]-TanB_in,2)/std::pow(TanBRange,2) +
   std::pow(DataMatrix[j][4]- Azero_in,2)/std::pow(AzeroRange,2);
   }
   else
   {
   Distance= 130000000;
   }

   Distances.push_back(Distance);
   }

   int minDistance = std::distance( Distances.begin(), std::min_element(
       Distances.begin(), Distances.end() ) );

   return DataMatrix[minDistance][index];// Outputs the lifetime for the closest point
       in the grid.

     }
```

C.2. Example use of `CheckVacuum` class

```
/* file main.cpp
 * Example use of CheckVacuum class. This class reads in a data file
 * containing vacuum stability information from Vevacious and gives
 * a result for a given parameter point.
 *
 *      Author: Jose Eliel Camargo-Molina (Elielx AT gmail.com)
 *      Copyright 2014 J. E. Camargo-Molina
 */


#include "CheckVacuum.h"
#include <ctime>

int main()

{
```

```
    //First read in data file with information from grid. This has to be done once
        only as it
    // is an expensive task. No need to call it again.

    CheckVacuum Check ("../CMSSM(TEST).dat");

    clock_t startTime = std::clock(); // Timing

    // The Stability function takes in m_0, m_1/2, Tan(beta), sign(mu) and A_0.
    // It outputs 1 , 0 or -1 for stable, long-lived and short-lived

    std::cout<< Check.Stability(0, 1000, 10, 1, -4000)<<std::endl;

    // The Lifetime function takes in m_0, m_1/2, Tan(beta), sign(mu) and A_0.
    // If the input point is short-lived it outputs the lifetime in universe ages
    // If the input point is long-lived it outputs 1e+6
    // If the input point is stable it outputs -1

    std::cout<< Check.Lifetime(0, 1000, 10, 1, -4000)<<std::endl;


    std::cout << double( std::clock() - startTime ) / (double)CLOCKS_PER_SEC<< "
        seconds." << std::endl; // Timing


}
```

LIST OF FIGURES

LIST OF TABLES

REFERENCES

[1] A. M. Guénault, *Basic superfluids.* Taylor & Francis, London, 2003. ISBN 0748408924.

[2] G. Savvidy, *Infrared instability of the vacuum state of gauge theories and asymptotic freedom*, *Phys. Lett. B* **71** (Nov., 1977) 133–134.

[3] A. Pich, *The Standard model of electroweak interactions*, `arXiv:0705.4264`.

[4] P. Binetruy, *Supersymmetry theory, experiment, and cosmology.* Oxford University Press, Oxford New York, 2006. ISBN 9780198509547.

[5] M. Böhm, A. Denner, and H. Joos, *Gauge theories of strong and electroweak interactions; 3rd ed.* B. G. Teubner, Stuttgart, 2001. ISBN 3322801624.

[6] F. Englert and R. Brout, *Broken symmetry and the mass of gauge vector mesons*, *Phys. Rev. Lett.* **13** (Aug., 1964) 321–323.

[7] P. W. Higgs, *Broken symmetries and the masses of gauge bosons*, *Phys. Rev. Lett.* **13** (Oct., 1964) 508–509.

[8] S. Weinberg, *A Model of Leptons*, *Phys.Rev.Lett.* **19** (1967) 1264–1266.

[9] A. Mazumdar, *The origin of dark matter, matter-anti-matter asymmetry, and inflation*, `arXiv:1106.5408`.

[10] A. Sakharov, *Violation of CP Invariance, c Asymmetry, and Baryon Asymmetry of the Universe*, *Pisma Zh.Eksp.Teor.Fiz.* **5** (1967) 32–35.

[11] A. G. Cohen, D. B. Kaplan, and A. E. Nelson, *Weak scale baryogenesis*, *Phys.Lett.* **B245** (1990) 561–564.

[12] M. Fukugita and T. Yanagida, *Barygenesis without grand unification*, *Phys. Lett. B* **174** (June, 1986) 45–47.

[13] G. Bertone, D. Hooper, and J. Silk, *Particle dark matter: Evidence, candidates and constraints*, *Phys.Rept.* **405** (2005) 279–390, [`hep-ph/0404175`].

[14] **Planck Collaboration** Collaboration, P. Ade *et. al.*, *Planck 2013 results. I. Overview of products and scientific results*, *Astron.Astrophys.* **571** (2014) A1, [`arXiv:1303.5062`].

[15] P. Cushman *et. al.*, *Working Group Report: WIMP Dark Matter Direct Detection*, arXiv:1310.8327.

[16] J. Conrad, *Indirect Detection of WIMP Dark Matter: a compact review*, arXiv:1411.1925.

[17] G. Karagiorgi *et. al.*, *Leptonic CP violation studies at MiniBooNE in the (3+2) sterile neutrino oscillation hypothesis*, *Phys.Rev.* **D75** (2007) 013011, [hep-ph/0609177].

[18] A. Strumia and F. Vissani, *Neutrino masses and mixings and...*, hep-ph/0606054.

[19] S. P. Martin, *A Supersymmetry primer*, hep-ph/9709356.

[20] S. Coleman and J. Mandula, *All Possible Symmetries of the S Matrix*, *Phys. Rev.* **159** (July, 1967) 1251–1256.

[21] R. Haag, J. T. Łopuszański, and M. Sohnius, *All possible generators of supersymmetries of the S-matrix*, *Nucl. Phys. B* **88** (Mar., 1975) 257–274.

[22] Y. Shirman, *TASI 2008 Lectures: Introduction to Supersymmetry and Supersymmetry Breaking*, arXiv:0907.0039.

[23] L. Girardello and M. Grisaru, *Soft breaking of supersymmetry*, *Nucl. Phys. B* **194** (Jan., 1982) 65–76.

[24] P. Nath and R. Arnowitt, *Generalized super-gauge symmetry as a new framework for unified gauge theories*, *Physics Letters B* **56** (1975), no. 2 177 – 180.

[25] J. Wess and B. Zumino, *Superspace formulation of supergravity*, *Physics Letters B* **66** (1977), no. 4 361 – 364.

[26] P. Van Nieuwenhuizen, *Supergravity*, *Phys.Rept.* **68** (1981) 189–398.

[27] H. P. Nilles, *Dynamically Broken Supergravity and the Hierarchy Problem*, *Phys.Lett.* **B115** (1982) 193.

[28] R. Barbieri, S. Ferrara, and C. A. Savoy, *Gauge Models with Spontaneously Broken Local Supersymmetry*, *Phys.Lett.* **B119** (1982) 343.

[29] G. 't Hooft, *Symmetry breaking through bell-jackiw anomalies*, *Phys. Rev. Lett.* **37** (July, 1976) 8–11.

[30] M. Papucci, J. T. Ruderman, and A. Weiler, *Natural SUSY Endures*, *JHEP* **1209** (2012) 035, [arXiv:1110.6926].

[31] K. Kowalska and E. M. Sessolo, *Natural MSSM after the LHC 8 TeV run*, *Phys.Rev.* **D88** (2013) 075001, [arXiv:1307.5790].

[32] J. R. Ellis, K. Enqvist, D. V. Nanopoulos, and F. Zwirner, *Observables in Low-Energy Superstring Models*, *Mod.Phys.Lett.* **A1** (1986) 57.

[33] L. J. Hall, D. Pinner, and J. T. Ruderman, *A Natural SUSY Higgs Near 126 GeV*, *JHEP* **1204** (2012) 131, [arXiv:1112.2703].

[34] D. Ghosh, M. Guchait, S. Raychaudhuri, and D. Sengupta, *How Constrained is the cMSSM?*, *Phys.Rev.* **D86** (2012) 055007, [arXiv:1205.2283].

[35] B. Fuks, *Supersymmetry - When Theory Inspires Experimental Searches*, arXiv:1401.6277.

[36] M. E. Krauss, B. O'Leary, W. Porod, and F. Staub, *Implications of gauge kinetic mixing on Z' and slepton production at the LHC*, *Phys.Rev.* **D86** (2012) 055017, [arXiv:1206.3513].

[37] L. Basso, B. O'Leary, W. Porod, and F. Staub, *Dark matter scenarios in the minimal SUSY B-L model*, *JHEP* **1209** (2012) 054, [arXiv:1207.0507].

[38] L. Basso and F. Staub, *Enhancing $h \to \gamma\gamma$ with staus in SUSY models with extended gauge sector*, *Phys.Rev.* **D87** (2013) 015011, [arXiv:1210.7946].

[39] P. Fileviez Perez, S. Spinner, and M. K. Trenkel, *The LSP Stability and New Higgs Signals at the LHC*, *Phys.Rev.* **D84** (2011) 095028, [arXiv:1103.5504].

[40] P. Fileviez Perez and S. Spinner, *The Minimal Theory for R-parity Violation at the LHC*, *JHEP* **1204** (2012) 118, [arXiv:1201.5923].

[41] R. M. Fonseca, M. Malinsky, W. Porod, and F. Staub, *Running soft parameters in SUSY models with multiple U(1) gauge factors*, *Nucl. Phys.* **B854** (2012) 28–53, [arXiv:1107.2670].

[42] P. Fileviez Perez and S. Spinner, *The Fate of R-Parity*, *Phys. Rev.* **D83** (2011) 035004, [arXiv:1005.4930].

[43] B. O'Leary, W. Porod, and F. Staub, *Mass spectrum of the minimal SUSY B-L model*, *JHEP* **1205** (2012) 042, [arXiv:1112.4600].

[44] W. Porod, *SPheno, a program for calculating supersymmetric spectra, SUSY particle decays and SUSY particle production at e+ e- colliders*, *Comput. Phys. Commun.* **153** (2003) 275–315, [hep-ph/0301101].

[45] W. Porod and F. Staub, *SPheno 3.1: Extensions including flavour, CP-phases and models beyond the MSSM*, *Comput.Phys.Commun.* **183** (2012) 2458–2469, [arXiv:1104.1573].

[46] F. E. Paige, S. D. Protopopescu, H. Baer, and X. Tata, *ISAJET 7.69: A Monte Carlo event generator for pp, anti-p p, and e+e- reactions*, hep-ph/0312045.

[47] B. Allanach, *SOFTSUSY: a program for calculating supersymmetric spectra*, *Comput.Phys.Commun.* **143** (2002) 305–331, [hep-ph/0104145].

[48] A. Djouadi, J.-L. Kneur, and G. Moultaka, *SuSpect: A Fortran code for the supersymmetric and Higgs particle spectrum in the MSSM*, *Comput.Phys.Commun.* **176** (2007) 426–455, [hep-ph/0211331].

[49] H. P. Nilles, M. Srednicki, and D. Wyler, *Weak Interaction Breakdown Induced by Supergravity*, *Phys.Lett.* **B120** (1983) 346.

[50] L. Alvarez-Gaume, J. Polchinski, and M. B. Wise, *Minimal Low-Energy Supergravity*, *Nucl.Phys.* **B221** (1983) 495.

[51] J. Derendinger and C. A. Savoy, *Quantum Effects and SU(2) x U(1) Breaking in Supergravity Gauge Theories*, *Nucl.Phys.* **B237** (1984) 307.

[52] M. Claudson, L. J. Hall, and I. Hinchliffe, *Low-Energy Supergravity: False Vacua and Vacuous Predictions*, *Nucl.Phys.* **B228** (1983) 501.

[53] J. Casas, A. Lleyda, and C. Muñoz, *Strong constraints on the parameter space of the MSSM from charge and color breaking minima*, *Nucl.Phys.* **B471** (1996) 3–58, [hep-ph/9507294].

[54] C. Kounnas, A. Lahanas, D. V. Nanopoulos, and M. Quiros, *Low-Energy Behavior of Realistic Locally Supersymmetric Grand Unified Theories*, *Nucl.Phys.* **B236** (1984) 438.

[55] J. Hisano and S. Sugiyama, *Charge-breaking constraints on left-right mixing of stau's*, *Phys.Lett.* **B696** (2011) 92–96, [arXiv:1011.0260].

[56] T. Kitahara and T. Yoshinaga, *Stau with Large Mass Difference and Enhancement of the Higgs to Diphoton Decay Rate in the MSSM*, *JHEP* **1305** (2013) 035, [arXiv:1303.0461].

[57] U. Ellwanger and C. Hugonie, *Constraints from charge and color breaking minima in the (M+1)SSM*, *Phys.Lett.* **B457** (1999) 299–306, [hep-ph/9902401].

[58] C. Le Mouel, *Charge and color breaking conditions associated to the top quark Yukawa coupling*, *Phys.Rev.* **D64** (2001) 075009, [hep-ph/0103341].

[59] J. Gunion, H. Haber, and M. Sher, *Charge / Color Breaking Minima and a-Parameter Bounds in Supersymmetric Models*, *Nucl.Phys.* **B306** (1988) 1.

[60] P. Ferreira, *A Full one loop charge and color breaking effective potential*, *Phys.Lett.* **B509** (2001) 120–130, [hep-ph/0008115].

[61] M. Carena *et. al.*, *Light Stau Phenomenology and the Higgs $\gamma\gamma$ Rate*, *JHEP* **1207** (2012) 175, [arXiv:1205.5842].

[62] M. Carena *et. al.*, *Vacuum Stability and Higgs Diphoton Decays in the MSSM*, arXiv:1211.6136.

[63] G. Degrassi *et. al.*, *Higgs mass and vacuum stability in the Standard Model at NNLO*, *JHEP* **1208** (2012) 098, [arXiv:1205.6497].

[64] A. Sommese, *The numerical solution of systems of polynomials arising in engineering and science*. World Scientific, Hackensack, NJ, 2005. ISBN 9789812561848.

[65] T. Li, *Numerical solution of polynomial systems by homotopy continuation methods*, *Handbook of numerical analysis* **11** (2003) 209–304.

[66] D. Mehta, A. Sternbeck, L. von Smekal, and A. G. Williams, *Lattice Landau Gauge and Algebraic Geometry*, *PoS* **QCD-TNT09** (2009) 025, [arXiv:0912.0450].

[67] D. Mehta, *Finding All the Stationary Points of a Potential Energy Landscape via Numerical Polynomial Homotopy Continuation Method*, *Phys.Rev.* **E84** (2011) 025702, [arXiv:1104.5497].

[68] D. Mehta, J. D. Hauenstein, and M. Kastner, *Energy landscape analysis of the two-dimensional nearest-neighbor ϕ^4 model*, *Phys.Rev.* **E85** (2012) 061103, [arXiv:1202.3320].

[69] D. Mehta, *Numerical Polynomial Homotopy Continuation Method and String Vacua*, *Adv.High Energy Phys.* **2011** (2011) 263937, [arXiv:1108.1201].

[70] D. Mehta, Y.-H. He, and J. D. Hauenstein, *Numerical Algebraic Geometry: A New Perspective on String and Gauge Theories*, *JHEP* **1207** (2012) 018, [arXiv:1203.4235].

[71] M. Maniatis and D. Mehta, *Minimizing Higgs Potentials via Numerical Polynomial Homotopy Continuation*, *Eur.Phys.J.Plus* **127** (2012) 91, [arXiv:1203.0409].

[72] T. Lee, T. Li, and C. Tsai, *Hom4PS-2.0: a software package for solving polynomial systems by the polyhedral homotopy continuation method*, *Computing* **83** (2008), no. 2 109–133.

[73] S. R. Coleman and E. J. Weinberg, *Radiative Corrections as the Origin of Spontaneous Symmetry Breaking*, *Phys.Rev.* **D7** (1973) 1888–1910.

[74] S. R. Coleman, *The Fate of the False Vacuum. 1. Semiclassical Theory*, *Phys.Rev.* **D15** (1977) 2929–2936.

[75] J. Callan, Curtis G. and S. R. Coleman, *The Fate of the False Vacuum. 2. First Quantum Corrections*, *Phys.Rev.* **D16** (1977) 1762–1768.

[76] T. Banks, C. Bender, and T. Wu, *Coupled anharmonic oscillators. i. equal-mass case*, *Phys. Rev. D* **8** (Nov., 1973) 3346–3366.

[77] S. R. Coleman, V. Glaser, and A. Martin, *Action Minima Among Solutions to a Class of Euclidean Scalar Field Equations*, *Commun.Math.Phys.* **58** (1978) 211.

[78] D. Metaxas and E. J. Weinberg, *Gauge independence of the bubble nucleation rate in theories with radiative symmetry breaking*, *Phys.Rev.* **D53** (1996) 836–843, [hep-ph/9507381].

[79] W. Fischler and R. Brout, *Gauge invariance in spontaneously broken symmetry*, *Phys. Rev. D* **11** (Feb., 1975) 905–908.

[80] M. Garny and T. Konstandin, *On the gauge dependence of vacuum transitions at finite temperature*, *JHEP* **1207** (2012) 189, [arXiv:1205.3392].

[81] C. L. Wainwright, S. Profumo, and M. J. Ramsey-Musolf, *Phase Transitions and Gauge Artifacts in an Abelian Higgs Plus Singlet Model*, *Phys.Rev.* **D86** (2012) 083537, [arXiv:1204.5464].

[82] A. Linde, *Fate of the false vacuum at finite temperature: Theory and applications*, *Phys. Lett. B* **100** (1981), no. 1 37–40.

[83] A. Brignole, J. Espinosa, M. Quiros, and F. Zwirner, *Aspects of the electroweak phase transition in the minimal supersymmetric standard model*, *Phys.Lett.* **B324** (1994) 181–191, [hep-ph/9312296].

[84] D. Gorbunov, *Introduction to the theory of the early universe cosmological perturbations and inflationary theory*. World Scientific, Singapore Hackensack, N.J, 2011. ISBN 9789814322225.

[85] A. D. Linde, *Decay of the False Vacuum at Finite Temperature*, *Nucl.Phys.* **B216** (1983) 421.

[86] M. Laine, "Basics of thermal field theory." http://www.laine.itp.unibe.ch/basics.pdf, 2013. lecture notes.

[87] T. L. Lee, T. Y. Li, and C. H. Tsai, *HOM4PS2.0: a software package for solving polynomial systems by the polyhedral homotopy continuation method*, *Computing* **83** (2008) 109–133.

[88] C. L. Wainwright, *CosmoTransitions: Computing Cosmological Phase Transition Temperatures and Bubble Profiles with Multiple Fields*, *Comput.Phys.Commun.* **183** (2012) 2006–2013, [arXiv:1109.4189].

[89] J. E. Camargo-Molina, B. O'Leary, W. Porod, and F. Staub, **Vevacious***: A Tool For Finding The Global Minima Of One-Loop Effective Potentials With Many Scalars*, *Eur.Phys.J.* **C73** (2013), no. 10 2588, [arXiv:1307.1477].

[90] P. Z. Skands *et. al.*, *SUSY Les Houches accord: Interfacing SUSY spectrum calculators, decay packages, and event generators*, *JHEP* **0407** (2004) 036, [hep-ph/0311123].

[91] B. Allanach *et. al.*, *SUSY Les Houches Accord 2*, *Comput.Phys.Commun.* **180** (2009) 8–25, [arXiv:0801.0045].

[92] F. James and M. Roos, *Minuit: A System for Function Minimization and Analysis of the Parameter Errors and Correlations*, *Comput.Phys.Commun.* **10** (1975) 343–367.

[93] J. Pivarski, "Pyminuit." https://code.google.com/p/pyminuit/, 2014.

[94] K. A. Olive and M. Srednicki, *New Limits on Parameters of the Supersymmetric Standard Model from Cosmology*, *Phys.Lett.* **B230** (1989) 78.

[95] J. R. Ellis, T. Falk, and K. A. Olive, *Neutralino - Stau coannihilation and the cosmological upper limit on the mass of the lightest supersymmetric particle*, *Phys.Lett.* **B444** (1998) 367–372, [hep-ph/9810360].

[96] P. Draper, P. Meade, M. Reece, and D. Shih, *Implications of a 125 GeV Higgs for the MSSM and Low-Scale SUSY Breaking*, *Phys.Rev.* **D85** (2012) 095007, [arXiv:1112.3068].

[97] S. Heinemeyer, O. Stal, and G. Weiglein, *Interpreting the LHC Higgs Search Results in the MSSM*, *Phys.Lett.* **B710** (2012) 201–206, [arXiv:1112.3026].

[98] F. Brümmer, S. Kraml, and S. Kulkarni, *Anatomy of maximal stop mixing in the MSSM*, *JHEP* **1208** (2012) 089, [arXiv:1204.5977].

[99] A. Djouadi and J. Quevillon, *The MSSM Higgs sector at a high M_{SUSY}: reopening the low tanβ regime and heavy Higgs searches*, arXiv:1304.1787.

[100] A. Arbey, M. Battaglia, A. Djouadi, and F. Mahmoudi, *An update on the constraints on the phenomenological MSSM from the new LHC Higgs results*, *Phys.Lett.* **B720** (2013) 153–160, [arXiv:1211.4004].

[101] E. Arganda, J. L. Diaz-Cruz, and A. Szynkman, *Decays of H^0/A^0 in supersymmetric scenarios with heavy sfermions*, *Eur.Phys.J.* **C73** (2013) 2384, [arXiv:1211.0163].

[102] M. Citron *et. al.*, *The End of the CMSSM Coannihilation Strip is Nigh*, *Phys.Rev.* **D87** (2013) 036012, [arXiv:1212.2886].

[103] P. Bechtle *et. al.*, *Constrained Supersymmetry after two years of LHC data: a global view with Fittino*, *JHEP* **1206** (2012) 098, [arXiv:1204.4199].

[104] R. Kuchimanchi and R. N. Mohapatra, *No parity violation without r-parity violation*, *Phys. Rev. D* **48** (Nov., 1993) 4352–4360.

[105] A. Arbey *et. al.*, *Implications of a 125 GeV Higgs for supersymmetric models*, *Phys.Lett.* **B708** (2012) 162–169, [arXiv:1112.3028].

[106] O. Buchmueller *et. al.*, *The CMSSM and NUHM1 in Light of 7 TeV LHC, B_s to mu+mu- and XENON100 Data*, *Eur.Phys.J.* **C72** (2012) 2243, [arXiv:1207.7315].

[107] J. R. Ellis and K. A. Olive, *How finely tuned is supersymmetric dark matter?*, *Phys.Lett.* **B514** (2001) 114–122, [hep-ph/0105004].

[108] J. R. Ellis, K. A. Olive, Y. Santoso, and V. C. Spanos, *Supersymmetric Dark Matter in Light of WMAP*, *Phys. Lett.* **B565** (2003) 176–182, [hep-ph/0303043].

[109] J. Ellis and K. A. Olive, *Revisiting the Higgs Mass and Dark Matter in the CMSSM*, *Eur.Phys.J.* **C72** (2012) 2005, [arXiv:1202.3262].

[110] G. Belanger, F. Boudjema, A. Pukhov, and A. Semenov, *MicrOMEGAs 2.0: A Program to calculate the relic density of dark matter in a generic model*, *Comput.Phys.Commun.* **176** (2007) 367–382, [hep-ph/0607059].

[111] G. Belanger, F. Boudjema, A. Pukhov, and A. Semenov, *MicrOMEGAs: A Program for calculating the relic density in the MSSM*, *Comput.Phys.Commun.* **149** (2002) 103–120, [hep-ph/0112278].

[112] F. Staub, T. Ohl, W. Porod, and C. Speckner, *A Tool Box for Implementing Supersymmetric Models*, *Comput.Phys.Commun.* **183** (2012) 2165–2206, [arXiv:1109.5147].

[113] M. A. Ajaib, I. Gogoladze, F. Nasir, and Q. Shafi, *Revisiting mGMSB in Light of a 125 GeV Higgs*, *Phys.Lett.* **B713** (2012) 462–468, [arXiv:1204.2856].

[114] H. E. Haber, R. Hempfling, and A. H. Hoang, *Approximating the radiatively corrected Higgs mass in the minimal supersymmetric model*, *Z.Phys.* **C75** (1997) 539–554, [hep-ph/9609331].

[115] M. Carena *et. al.*, *Reconciling the two loop diagrammatic and effective field theory computations of the mass of the lightest CP - even Higgs boson in the MSSM*, *Nucl.Phys.* **B580** (2000) 29–57, [hep-ph/0001002].

[116] A. Bartl *et. al.*, *General flavor blind MSSM and CP violation*, *Phys.Rev.* **D64** (2001) 076009, [hep-ph/0103324].

[117] **ATLAS collaboration** Collaboration, A. collaboration, *Search for direct third generation squark pair production in final states with missing transverse momentum and two b-jets in $\sqrt{s}$ = 8 TeV pp collisions with the atlas detector.*, Tech. Rep. ATLAS-CONF-2013-053, CERN, Geneva, May, 2013.

[118] R. Barbieri and G. Giudice, *Upper Bounds on Supersymmetric Particle Masses*, *Nucl.Phys.* **B306** (1988) 63.

[119] R. Kitano and Y. Nomura, *Supersymmetry, naturalness, and signatures at the LHC*, *Phys.Rev.* **D73** (2006) 095004, [hep-ph/0602096].

[120] J. R. Ellis, K. A. Olive, and Y. Santoso, *Calculations of neutralino stop coannihilation in the CMSSM*, *Astropart.Phys.* **18** (2003) 395–432, [hep-ph/0112113].

[121] T. Cohen and J. G. Wacker, *Here be Dragons: The Unexplored Continents of the CMSSM*, arXiv:1305.2914.

[122] J. Harz *et. al.*, *Neutralino-stop co-annihilation into electroweak gauge and Higgs bosons at one loop*, *Phys.Rev.* **D87** (2013) 054031, [arXiv:1212.5241].

[123] **ATLAS Collaboration** Collaboration, G. Aad *et. al.*, *Observation of a new particle in the search for the Standard Model Higgs boson with the ATLAS detector at the LHC*, *Phys.Lett.* **B716** (2012) 1–29, [arXiv:1207.7214].

[124] **CMS Collaboration** Collaboration, S. Chatrchyan *et. al.*, *Observation of a new boson at a mass of 125 GeV with the CMS experiment at the LHC*, *Phys.Lett.* **B716** (2012) 30–61, [arXiv:1207.7235].

[125] H. E. Haber and R. Hempfling, *Can the mass of the lightest Higgs boson of the minimal supersymmetric model be larger than m(Z)?*, *Phys.Rev.Lett.* **66** (1991) 1815–1818.

[126] M. S. Carena and H. E. Haber, *Higgs boson theory and phenomenology*, *Prog.Part.Nucl.Phys.* **50** (2003) 63–152, [hep-ph/0208209].

[127] A. Djouadi, *The Anatomy of electro-weak symmetry breaking. II. The Higgs bosons in the minimal supersymmetric model*, *Phys.Rept.* **459** (2008) 1–241, [hep-ph/0503173].

[128] M. Frank *et. al.*, *The Higgs Boson Masses and Mixings of the Complex MSSM in the Feynman-Diagrammatic Approach*, *JHEP* **0702** (2007) 047, [hep-ph/0611326].

[129] D. M. Pierce, J. A. Bagger, K. T. Matchev, and R.-j. Zhang, *Precision corrections in the minimal supersymmetric standard model*, *Nucl. Phys.* **B491** (1997) 3–67, [hep-ph/9606211].

[130] G. Degrassi, P. Slavich, and F. Zwirner, *On the neutral Higgs boson masses in the MSSM for arbitrary stop mixing*, *Nucl.Phys.* **B611** (2001) 403–422, [hep-ph/0105096].

[131] A. Brignole, G. Degrassi, P. Slavich, and F. Zwirner, *On the two loop sbottom corrections to the neutral Higgs boson masses in the MSSM*, *Nucl.Phys.* **B643** (2002) 79–92, [hep-ph/0206101].

[132] A. Brignole, G. Degrassi, P. Slavich, and F. Zwirner, *On the O(alpha(t)**2) two loop corrections to the neutral Higgs boson masses in the MSSM*, *Nucl.Phys.* **B631** (2002) 195–218, [hep-ph/0112177].

[133] A. Dedes and P. Slavich, *Two loop corrections to radiative electroweak symmetry breaking in the MSSM*, *Nucl.Phys.* **B657** (2003) 333–354, [hep-ph/0212132].

[134] B. Allanach *et. al.*, *Precise determination of the neutral Higgs boson masses in the MSSM*, *JHEP* **0409** (2004) 044, [hep-ph/0406166].

[135] J. E. Camargo-Molina, B. O'Leary, W. Porod, and F. Staub, *Stability of the CMSSM against sfermion VEVs*, *JHEP* **1312** (2013) 103, [arXiv:1309.7212].

[136] G. Gamberini, G. Ridolfi, and F. Zwirner, *On Radiative Gauge Symmetry Breaking in the Minimal Supersymmetric Model*, *Nucl.Phys.* **B331** (1990) 331–349.

[137] T. Falk *et. al.*, *Constraints from inflation and reheating on superpartner masses*, *Phys.Lett.* **B396** (1997) 50–57, [hep-ph/9611325].

[138] S. Davidson and A. Ibarra, *A Lower bound on the right-handed neutrino mass from leptogenesis*, *Phys.Lett.* **B535** (2002) 25–32, [hep-ph/0202239].

[139] J. L. Feng, *Supersymmetry and cosmology*, *eConf* **C0307282** (2003) L11, [hep-ph/0405215].

[140] J. Pradler and F. D. Steffen, *Thermal gravitino production and collider tests of leptogenesis*, *Phys.Rev.* **D75** (2007) 023509, [hep-ph/0608344].

[141] W. Buchmuller *et. al.*, *Gravitino Dark Matter in R-Parity Breaking Vacua*, *JHEP* **0703** (2007) 037, [hep-ph/0702184].

[142] M. Olechowski, S. Pokorski, K. Turzynski, and J. D. Wells, *Reheating Temperature and Gauge Mediation Models of Supersymmetry Breaking*, *JHEP* **0912** (2009) 026, [arXiv:0908.2502].

[143] J. R. Ellis *et. al.*, *Against Tachyophobia*, *Phys.Rev.* **D78** (2008) 075006, [arXiv:0806.3648].

[144] M. Sher, *Electroweak Higgs Potentials and Vacuum Stability*, *Phys.Rept.* **179** (1989) 273–418.

[145] N. Blinov and D. E. Morrissey, *Vacuum Stability and the MSSM Higgs Mass*, *JHEP* **1403** (2014) 106, [arXiv:1310.4174].

[146] D. Chowdhury, R. M. Godbole, K. A. Mohan, and S. K. Vempati, *Charge and Color Breaking Constraints in MSSM after the Higgs Discovery at LHC*, *JHEP* **1402** (2014) 110, [arXiv:1310.1932].

[147] P. Langacker and N. Polonsky, *Implications of Yukawa unification for the Higgs sector in supersymmetric grand unified models*, *Phys.Rev.* **D50** (1994) 2199–2217, [hep-ph/9403306].

[148] R. Garani, S. Vempati, and D. Chowdhury *private communication.*

[149] S. Heinemeyer, W. Hollik, and G. Weiglein, *FeynHiggs: A Program for the calculation of the masses of the neutral CP even Higgs bosons in the MSSM*, *Comput.Phys.Commun.* **124** (2000) 76–89, [hep-ph/9812320].

[150] T. Hahn *et. al.*, *FeynHiggs: A program for the calculation of MSSM Higgs-boson observables - Version 2.6.5*, *Comput.Phys.Commun.* **180** (2009) 1426–1427.

[151] J. E. Camargo-Molina, B. Garbrecht, B. O'Leary, W. Porod, and F. Staub, *Constraining the Natural MSSM through tunneling to color-breaking vacua at zero and non-zero temperature*, *Phys.Lett.* **B737** (2014) 156–161, [arXiv:1405.7376].

[152] P. Bechtle, K. Desch, and P. Wienemann, *Fittino, a program for determining MSSM parameters from collider observables using an iterative method*, *Comput.Phys.Commun.* **174** (2006) 47–70, [hep-ph/0412012].

[153] P. Bechtle *et. al.*, *Studying, Killing and Burying the CMSSM (In Preparation)*, .

[154] **ATLAS Collaboration** Collaboration, G. Aad *et. al.*, *Search for squarks and gluinos with the ATLAS detector in final states with jets and missing transverse momentum using* $\sqrt{s} = 8$ *TeV proton–proton collision data*, *JHEP* **1409** (2014) 176, [arXiv:1405.7875].

[155] B. de Carlos and J. Casas, *One-loop analysis of the electroweak breaking in supersymmetric models and the fine-tuning problem*, *Phys. Lett. B* **309** (1993), no. 314 320–328.

[156] J. E. Camargo-Molina, B. O'Leary, W. Porod, and F. Staub, *The Stability Of R-Parity In Supersymmetric Models Extended By* $U(1)_{B-L}$, *Phys.Rev.* **D88** (2013) 015033, [arXiv:1212.4146].

[157] S. P. Martin, *Two-loop effective potential for a general renormalizable theory and softly broken supersymmetry*, *Phys. Rev. D* **65** (2002) 116003.